(NASA-CR-142553) [RESEARCH ON FLUORESCENCE FROM PHOTOIONIZATION, PHOTODISSOCIATION, AND VACUUM, ALONG WITH BENDING QUANTRUM STUDY] Progress Reports, 1 Nov. 1971 - 31 Oct. 1974 (University of Southern Calif.) 108 p HC G3/72 18041

N75-21091

Unclas

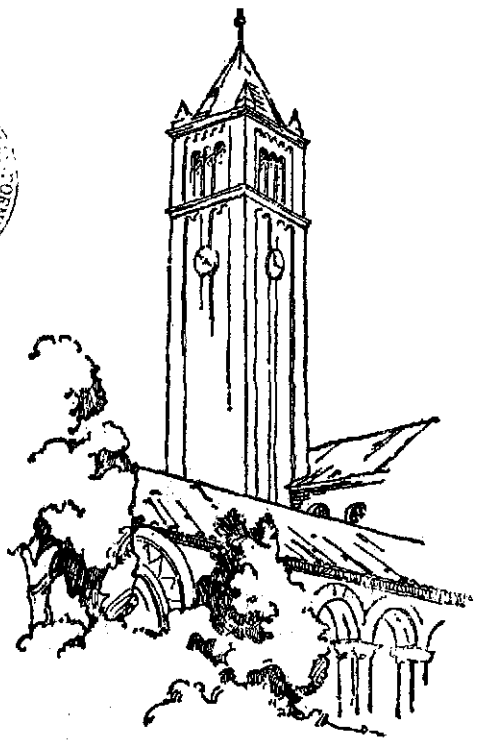

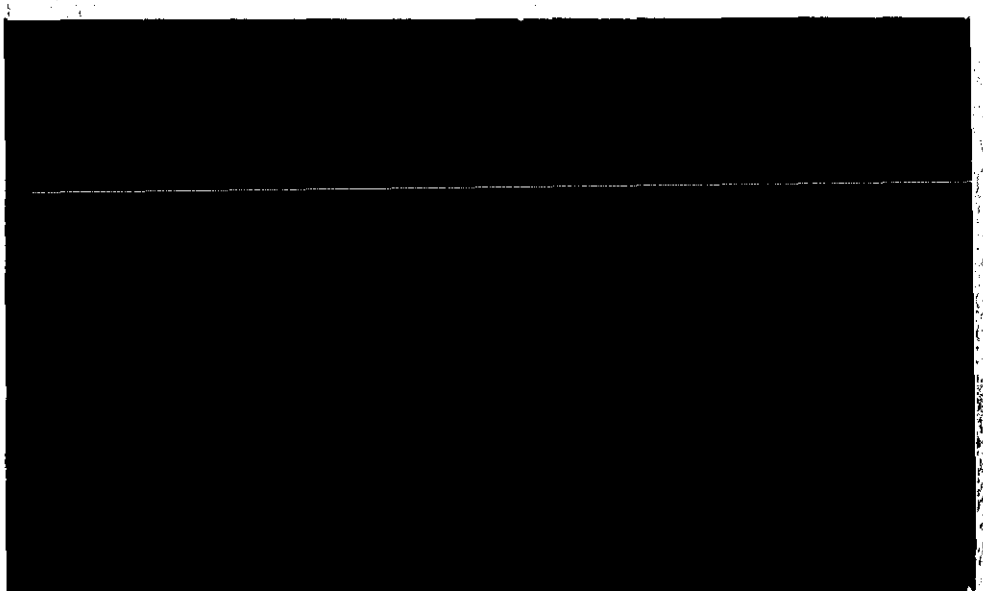

DEPARTMENT OF PHYSICS
University of Southern California
Los Angeles, California 90007

Progress Report No.:	Period Covered:
4 and 5	11/1/71-10/31/72
6 and 7	11/1/72-10/31/73
8 and 9	11/1/73-10/31/74

PROGRESS REPORTS NO. 4, 5, 6, 7, 8 AND 9 FOR THE PERIOD ENDING OCTOBER 31, 1974

Grant # NGR 05-018-180

Darrell L. Judge
Principal Investigator
University of Southern California
Los Angeles, California 90007

1 April 1975

/

TABLE OF CONTENTS

I. Introductory Comments

REPORT NO. 4 and 5

* II. "Absolute Specific Photodissociation Cross Sections of CH_4 in the Extreme Ultraviolet," J. Chem. Phys. 57, 286 (1972).

* III. "Electronic Transition Moments for the A→X, B→X, and B→A Transitions in CO^+ and the A←X and B←X Moments for the CO→CO^+ Systems; Absolute Cross Sections for the Absorption Processes," J. Chem. Phys. 57, 455 (1972).

* IV. "Cross Sections for the Production of $CO_2^+[A^2\Pi_u, B^2\Sigma_u^+ \rightarrow X^2\Pi_g]$ Fluorescence by Vacuum Ultraviolet Radiation," J. Chem. Phys. 57, 4443 (1972).

* V. "Cross Sections for the Production of $CO(a'^3\Sigma^+, d^3\Delta_i$, and $e^3\Sigma^- \rightarrow a^3\Pi)$ Fluorescence through Photodissociation of CO_2," J. Chem. Phys. 58, 104 (1973).

* VI. "Population Distribution of Triplet Vibrational Levels of CO Produced by Photodissociation of CO_2," Can. J. Phys. 51, 378 (1973).

REPORT NO. 6 and 7

* VII. "The Electronic Transition Moment of the $N_2^+(B^2\Sigma_u^+ \rightarrow X^2\Sigma_g^+)$ System," J. Phys. B. 6, L121 (1973).

* VIII. "Band Strengths for the $CO_2^+(A^2\Pi_u \rightarrow X^2\Pi_g)$ System Produced Through Photoionization Excitation of CO_2," J. Phys. B. 6, 2150 (1973).

* IX. "Cross Sections and Band Strengths for the $N_2O^+(A^2\Sigma^+ \rightarrow X^2\Pi)$ System Produced by Vacuum Ultraviolet Radiation," J. Phys. B. 7, 626 (1974).

* X. "Identification of the $N_2O^+[A^2\Sigma^+(0,0,0) \rightarrow X^2\Pi(n_1,n_2,n_3)]$ Vibrational Bands," J. Molec. Spectroscopy 53, 317 (1974).

REPORT NO. 8 and 9

XI. "Fluorescence from the Fragment of CS_2 Vapor Produced by Vacuum Ultraviolet Radiation," Second Int. Conf. on Spectral Lines, Eugene, Oregon, August 1974. Abstract only.

XII. "$CS_2^+(B^2\Sigma_u^+, A^2\Pi_u \rightarrow X^2\Pi_g)$ Fluorescence from Photoionization of CS_2 Vapor," accepted for publication in Can. J. Phys. 1975.

* Reprints intentionally Omitted

XIII. "$CS(A^1\Pi \rightarrow X^1\Sigma^+)$ Fluorescence from Photodissociation of CS_2 and OCS," submitted to J. Chem. Phys. 1974.

XIV. "$OCS^+(A^2\Pi \rightarrow X^2\Pi)$ Fluorescence from Photoionization of OCS," accepted for publication in Int. J. Mass Spectrometry Ion Phys. 1975.

XV. "Reevaluation of the $CO_2^+(X^2\Pi_g)$ Bending Quantum," accepted for publication in Can. J. Phys. 1975.

APPENDIX A

Continuation Proposal, April 26, 1972.

APPENDIX B

Continuation Proposal, July 10, 1973

SECOND INTERNATIONAL

CONFERENCE

ON

SPECTRAL LINES

Sponsored by the
Division of Electron and Atomic Physics
of the American Physical Society

M.7 Fluorescence from the Fragment of CS_2 Vapor Produced by Vacuum Ultraviolet Radiation, L.C. LEE and D.L. JUDGE, Univ. of So. Calif.--The fluorescence from the photo-fragments of CS_2 produced by line emission sources at wavelengths between 462 and 1239 Å has been studied. The fluorescence emitted from the transitions of $CS_2^+(B^2\Sigma_u^+ \rightarrow X^2\Pi_g)$, $CS_2^+(A^2\Pi_u \rightarrow X^2\Pi_g)$ and $CS(A^1\Pi \rightarrow X^1\Sigma)$ has been observed and the corresponding emission band strengths and production cross sections measured. From the $CS(A^1\Pi \rightarrow X^1\Sigma)$ emission spectrum the populations of vibrational levels of CS photo-fragments in the $A^1\Pi$ electronic state have been obtained. The vibrational population of the $v' = 0$-4 levels are well represented by a Poisson distribution, in agreement with a theoretical argument.

$CS_2^+(B^2\Sigma_u^+, A^2\Pi_u \rightarrow X^2\Pi_g)$ FLUORESCENCE FROM PHOTOIONIZATION EXCITATION OF CS_2 VAPOR

L. C. Lee, D. L. Judge and M. Ogawa

Department of Physics
University of Southern California
Los Angeles, California 90007

Index classification: 5.447

Abstract

$CS_2^+(B^2\Sigma_u^+, A^2\Pi_u \rightarrow X^2\Pi_g)$ fluorescence bands produced by irradiation of CS_2 vapor with emission lines from λλ462-977 Å were analyzed and their production cross sections measured. The emission bands of the bending transitions, $B^2\Sigma_u^+(0v0) \rightarrow X^2\Pi_g(0v0)$, were tentatively assigned and ν_2 of the $B^2\Sigma_u^+$ state is accordingly found to be 338.8 cm^{-1}. Using the tentatively assigned positions of the band heads for the $A^2\Pi_u(v00) \rightarrow X^2\Pi_g(000)$ transitons the ionization potentials for the $A^2\Pi_u(v00)$ vibrational levels were obtained and are in a good agreement with the photoelectron data. The splitting constant of the spin-orbit interaction for the $A^2\Pi_u$ state thereby determined to be 169 cm^{-1}. The $CS_2^+(A^2\Pi_u^+, B^2\Sigma_u \rightarrow X^2\Pi_g)$ fluorescence has exceptionally high production cross sections at the absorption bands associated with the n=3 member of the Rydberg series III and V, respectively.

I. Introduction

Fluorescence emission from CS_2^+ was observed by Cook and Ogawa (1969) following irradiation of the CS_2 molecule by photons of the wavelengths shorter than λ976.5 Å. Such fluorescence produced by λ955 Å photons has been dispersed and reported by Weissler et al. (1971), the fluorescence being identified as the CS_2^+ ($A^2\Pi_u \rightarrow X^2\Pi_g$) system. However, due to the spectral resolution limitation the most interesting features of the spectrum were not revealed.

Using various techniques the ionization potentials of the CS_2^+ ions in the $B^2\Sigma^+_u$, $A^2\Pi_u(i)$, and $X^2\Pi_g(i)$ electronic states have been studied by several authors: Price and Simpson (1932), Tanaka et al. (1960), and Ogawa and Chang (1970) have investigated the Rydberg series and obtained the ionization potentials from the series limits; Callomon (1958) studied the emission spectrum of the $CS_2^+(B^2\Sigma^+_u \rightarrow X^2\Pi_g)$ system; Diebeler and Walker (1967) and Momigny and Delwiche (1968) have investigated the mass spectra of the CS_2^+ ions ionized by photoabsorption; Turner and May (1967), Eland and Dunby (1968), Collin and Natalis (1968), and Brundle and Turner (1969) have studied the photoelectron spectra resulting from the photoionization of CS_2 by the λ584 Å helium resonance line. Through such observations the nature of the CS_2^+ electronic states is reasonably well understood. However, due to the lack of high resolution rotational analysis of the $B^2\Sigma^+_u \rightarrow X^2\Pi_g$ and

$A^2\Pi_u \rightarrow X^2\Pi_g$ emission systems, the precise positions of the vibrational levels of those states are still not established, and further study of these systems is required.

Carbon disulfide is one of the molecules of astrophysical and aeronomic interest (Hudson, 1970). Measurement of the production cross sections for the $CS_2^+(B^2\Sigma_u^+, A^2\Pi_u \rightarrow X^2\Pi_g)$ fluorescence, produced by vacuum ultraviolet radiation is thus of considerable interest. Such data will provide basic information for an understanding of the role CS_2 plays in planetary atmospheres.

II. Experiment

The experimental set-up has been described in a previous paper (Judge and Lee, 1972). In brief, the light source is a condensed spark discharge through a boron nitride capillary containing either N_2 or Ar. The emission lines of interest were isolated with a 1-m normal incidence monochromator (McPh. 225). The fluorescence was dispersed by a 0.3-m monochromator (McPh. 218), with the bandwidth set at 5 Å or less.

The source line intensities were measured with a nickel film detector for which the quantum efficiency was known (Walker et al., 1955). For the absolute intensity measurement of fluorescence the response of the combination of a grating blazed at 5000 Å and a cooled photomultiplier (EMI 9558 QB) in the wavelength region λλ3000-7000 Å was calibrated with an EG&G tungsten halogen lamp.

The response curve is similar to that published in a previous paper (Lee and Judge, 1972). The second order spectrum of the $B^2\Sigma_u^+ \rightarrow X^2\Pi_g$ emission in the region $\lambda\lambda$2750-2950 Å was observed. The response in this region was calibrated against sodium salicylate, for which the quantum efficiency is known (Slavin et al., 1961). The system response was found to be reasonably constant.

CS_2 vapor was obtained from an analytical-reagent-grade liquid CS_2. The vapor was purified by fractional distillation so that the fluorescence from the possible impurities, especially N_2, produced by irradiation of λ555 Å was not detectable. The vapor pressure inside the sample cell was monitored with a Baratron Capacitance manometer and was limited to 15 mTorr or less so that the fluorescence intensity was linearly proportional to the pressure.

III. Result and Discussion

A. $B^2\Sigma_u^+ \rightarrow X^2\Pi_g$ System

The $B^2\Sigma_u^+ \rightarrow X^2\Pi_g$ fluorescence spectra produced by irradiation of photons with wavelengths λ555, 827, 835, and 851 Å are shown in Figure 1. The spectrum produced by λ555 Å radiation is characteristic of all observed spectra produced by photons with wavelengths not longer than λ827 Å. The observed positions of band heads, the wave numbers, and the relative production cross sections for the various emission bands are listed in Table I.

The bands a to y shown in Figure 2 have been observed by

Callomon (1958) who obtained the emission spectrum from the negative flow of a d.c. discharge through CS_2 vapor. The rotational spectrum of the a and b bands has been analyzed by Callomon (1958) and assigned respectively to the $B^2\Sigma_u^+(000) \rightarrow X^2\Pi_{g,3/2}(000)$ and $X^2\Sigma_{g,1/2}(000)$ transitions. The p band has a rotational spectrum similar to the a band and is thus assigned to the $B^2\Sigma_u^+(000) \rightarrow X^2\Pi_{g,3/2}(020)$ transition. Callomon (1958) also suggested that the e and f bands correspond to the $B^2\Sigma_u^+(000) \rightarrow X^2\Pi_{g,3/2}(100)$ and $X^2\Pi_{g,1/2}(100)$ transitions. The correctness of this suggestion is corroborated by the presently observed spectra. Because the a, b, e, and f bands are emitted from the same upper level, $B^2\Pi_u^+(000)$, their relative emission cross sections will be independent of the incident photon energy. This independence is apparently consistent with the present spectra shown in Figure 1 and listed in Table I.

As shown in Figure 2, the spearations of the α-β and the c-d bands are the same as that of the a-b bands. And, the intensity distribution of the α, c, and a bands is similar to that of the β, d, and b bands. Considering the uniformity of the band separations these bands may thus be vibrational progressions. As shown in Figure 1 the α, c, β, and d bands are not produced by primary photons having wavelengths shorter than $\lambda 835$ Å; their production is strongly dependent on the primary photon energies. This may imply that these bands are emitted from the various vibrational levels of the upper $B^2\Sigma_u^+$ state, of which the formation is dependent

on the primary photon energy.

The bending vibration transition, $B^2\Sigma_u^+(010) \rightarrow X^2\Pi_g(010)$ has been observed in the BO_2 molecule by Johns (1961). Since the CS_2^+ ion is isoelectronic (Callomon, 1958, Johns, 1961) to the BO_2 molecule, the $CS_2^+[B^2\Sigma_u^+(0v'0) \rightarrow X^2\Pi_g(0v''0)]$ transitions are thus to be expected. In fact, in considering the combination of the vibrational frequencies for the $B^2\Sigma_u^+ \rightarrow X^2\Pi_g$ transitions, only the $(0v'0) \rightarrow (0v''0)$ transitions can possibly explain the separations of the c-a and d-b bands which are given by Callomon (1958) as 134.04 and 137.27 cm^{-1}, respectively. The ν_1 vibrational frequency of the $B^2\Sigma_u^+$ has been determined by photoelectron spectroscopy (Eland and Danby, 1968, Brundle and Turner, 1969) to be 605 cm^{-1}, which is comparable to ν_1(= 623.94 cm^{-1}) of the $X^2\Pi_g$ state given by Callomon (1958). The ν_3 vibrational frequencies are still unknown for both the $B^2\Sigma_u^+$ and $X^2\Pi_g$ state. However, according to the data ν_1 = 1070 cm^{-1} and ν_3 = 1322 cm^{-1} for the $BO_2(X^2\Pi_g)$ state, ν_3 for the $CS_2^+(X^2\Pi_g)$ state is expected to be of the order of ν_1. From these considerations the possibility that the α, c, β, and d bands are emitted from the most likely populated levels, $B^2\Sigma_u^+(v00)$, is ruled out. The Frank-Condon factors for the productions of the $CS_2^+(B^2\Sigma_u^+)$ ions in the (000), (100), and (200) levels have been determined by λ584 Å photoelectron spectroscopy (Brundle and Turner, 1969) to be 0.89, 0.10, and 0.01, respectively.

According to the vibrational selection rules for electronic

transition (Herzberg, 1966) $\Delta V_2 = 0, \pm 2, \pm 4, ---$, the bending vibrational levels of the $CS_2^+(B^2\Sigma_u^+)$ electronic state can only be populated by excitation of the neutral molecules in the bending vibrational levels of the ground electronic state. Since the $\Delta V_2 = 0$ are usually the strongest transitions (Herzberg, 1966), the populations in the bending vibrational levels of the upper electronic state will approximately have the same distribution as that of the ground electronic state, whenever the electronic transition moment is assumed constant. In fact, as indicated in Table I, the relative production cross sections for the a: c: α or b: d: β bands (= 1.0: 0.16: 0.03), which are in turn proportional to the populations of the vibrational elevels, do indeed agree with the population distribution of the bending vibrational levels in the ground electronic state. THe bending vibrational frequency ν_2 for the $CS_2(X^1\Sigma_g^+)$ ground state (Herzberg, 1966) is 396.7 cm^{-1}, which results in a calculated Boltzman population distribution for the vibrational levels, (000): (010): (020) of 1: 0.14: 0.02, respectively. This fact also suggests that the c and α or the d and β bands may be emitted, respectively, from the bending vibrational levels, (010) and (020) of the $B^2\Sigma_u^+$ state. And the corresponding lower levels for these bands will be the (010) and (020) levels of the $X^2\Pi_g$ state whichare again determined by the selection rules, $\Delta V_2 = 0, \pm 2$, ---. The result for the suggested assignment is listed in Table I and also indicated in Figure 2. From this tentative assignment

and the ν_2 bending vibrational frequency (Callomon, 1958) (=204.8 cm^{-1}) of the $X^2\Pi_{g,3/2}$ state, ν_2 of the $B^2\Sigma_u^+$ state is thus 338.8 cm^{-1}. Similarly, ν_2 for the $B^2\Sigma_u^+$ state is larger than that for the $X^2\Pi_g$ state in the BO_2 molecule (Johns 1961), for which ν_2 values are, respectively, 505 and 464 cm^{-1}.

Production of the α, c, β, and d bands is strongly dependent on the incident wavelengths near λ835 Å. These wavelengths are in a region (λλ820-840 Å) where a strong and rather broad absorption feature is observed (Cook and Ogawa, 1969). This coincidence suggests that the $CS_2^+(B^2\Sigma_u^+)$ ions in the bending vibrational levels may not be produced by direct photoionization.

B. $A^2\Pi_u \rightarrow X^2\Pi_g$ System

The fluorescence spectrum in the wavelength region λλ4300-5800 Å produced by irradiating CS_2 vapor with photons of wavelength λ923 Å is shown in Figure 3. This spectrum is characteristic of all the observed spectra produced by photons of wavelengths not longer than λ955 Å.

The present spectrum has been identified as the $CS_2^+(A^2\Pi_u \rightarrow X^2\Pi_g)$ system (Weissler, 1971). However, this emission system is relatively unknown, in contrast to the isoelectronic systems, $CO_2^+(A^2\Pi_u \rightarrow X^2\Pi_g)$ and $BO_2(A^2\Pi_u \rightarrow X^2\Pi_g)$, which have been rotationally analyzed by Mrozowski (1941, 1942, 1947a,b) and Johns (1961), respectively. From the analysis of the $CS_2^+(B^2\Sigma_u^+ \rightarrow X^2\Pi_g)$ system Callomon (1958)

has determined that the vibrational levels of $X^2\Pi_{g,1/2}(000)$ and $X^2\Pi_{g,3/2}(000)$ are inverted, with a splitting of 440.71 cm^{-1}. On the other hand, the splitting in the vibrational levels of the $CS_2^+(A^2\Pi_u)$ state is not yet known. Although the ionization potentials for each vibrational level are well determined by photoelectron spectroscopy (Eland and Danby, 1968, Brundle and Turner, 1969), the splitting is not resolved.

In the $CO_2^+(A^2\Pi_u \rightarrow X^2\Pi_g)$ fluorescence spectra (Lee and Judge, 1972, Judge et al., 1969), the strong emission bands are grouped into sequences, $A^2\Pi_u(v00) \rightarrow X^2\Pi_g(v + m00)$, where $v + m \geq 0$, $v = 0$, 1, 2, --- and m is a fixed integer for each sequence. The band at the shorter wavelength side of each sequence is an $A^2\Pi_u(v00) \rightarrow X^2\Pi_g(000)$ transition. In analogy with the isoelectronic CO_2^+, the wavelengths for the $CS_2^+[A^2\Pi_u(v00) \rightarrow X^2\Pi_g(000)]$ transitions have been determined from the band head positions at the shorter wavelength side of each sequence and are listed in Table II. Combining the emission photon energies of these transitions with the ionization potentials of the $X^2\Pi_{g,1/2}(000)$ and $X^2\Pi_{g,3/2}(000)$ levels, which are respectively 81735 and 81299 cm^{-1} according to Tanaka et al. (1960), the ionization potentials for the vibrational levels of $A^2\Pi_u(v00)$ are obtained and listed in Table II. The ionization potentials given by other authors (Eland and Danby, 1968, Brundle and Turner, 1969, Ogawa and Chang, 1970) are also listed in the Table for comparison. The average value for the $\Omega = 1/2$ and $3/2$

components of each vibrational level agrees very well with the value given by Eland and Danby (1968). The splitting averaged over all vibrational levels is 0.021 eV (169 cm^{-1}). The uncertainty of the band head position is estimated to be ±5 Å resulting in an energy level uncertainty of 0.0025 eV.

It is interesting to compare the splittings of the Ω = 1/2 and 3/2 components of the isoelectronic molecules, CS_2^+, CO_2^+, and BO_2. The splittings for the $A^2\Pi_u(i)$ and $X^2\Pi_g(i)$ states are respectively 169 and 441 cm^{-1} (Callomon, 1958) for CS_2^+, 95 (Mrozowski, 1941, 1942, Tanaka and Ogawa, 1962) and 160 cm^{-1} (Bueso-Sanllehf, 1941) for CO_2^+, and 101 and 149 cm^{-1} for BO_2 (Johns, 1961).

Adopting the ν_1 values of the $CS_2^+(X^2\Pi_{g,1/2}$ and $X^2\Pi_{g,3/2})$ states from Callomon (1958), which are given, respectively, 631.06 and 616.82 cm^{-1}, and the ionization potentials of the $X^2\Pi_g$ states from Tanaka et al. (1960), the ionization potentials for the $X^2\Pi_g(v00)$ states may be obtained. Combining these ionization potentials with the presently obtained ionization potentials for the $A^2\Pi_u(v00)$ levels, the wavelengths for the vibrational transitions, $A^2\Pi_u(v'00) \rightarrow X^2\Pi_g(v''00)$ are calculated and listed in Table IV. As shown in Figure 3 the calculated wavelengths fit the fluorescence spectrum quite well.

C. Production Cross Sections

At a constant primary photon intensity and a constant gas

pressure, the fluorescence cross section, $\sigma_f(\lambda,\lambda_f)$, for a band at wavelength λ_f produced by a primary photon of wavelength λ, is proportional to the fluorescence radiation rate (Lee and Judge, 1972). The relative production cross sections for the various emission wavelengths produced by various incident photon wavelengths are given in Tables I and IV for the $CS_2^+(B^2\Sigma_u^+ \rightarrow X^2\Pi_g)$ and the $CS_2^+(A^2\Pi_u \rightarrow X^2\Pi_g)$ systems, respectively.

The absolute production cross section is obtained by comparing the presently observed fluorescence radiation rates with those of the N_2^+ or CO_2^+ fluorescence, for which the production cross sections are known (Lee and Judge, 1972, Judge and Weissler, 1968). The total production cross sections, $\Sigma_f\sigma_f(\lambda,\lambda_f)$, of the $CS_2^+(A^2\Pi_u, B^2\Sigma_u^+ \rightarrow X^2\Pi_g)$ fluorescence bands produced by incident wavelengths from $\lambda\lambda$462-977 Å are listed in Table V and shown in Figure 4. The absorption cross sections, σ_T, given by Cook and Ogawa (1969) are adopted for the calculation of the production yields, $\eta_f = \sigma_f/\sigma_T$, and are also listed in Table V. The cross sections are in units of Mb ($= 10^{-18}$ cm^2) and the yields in %. The uncertainty for the production cross sections is estimated to be ±15% of the given value.

As shown in Figure 4 the production cross section of the $A^2\Pi_u \rightarrow X^2\Pi_g$ fluorescence at the incident wavelength λ955 Å is exceptionally high. This wavelength is within the strong absorption band (Cook and Ogawa, 1969) associated with the n = 3 member of the Rydberg series III (Tanaka et al., 1960), where a high relative photoionization

cross section is also seen in the ion mass spectrum observed by Dibeler and Walker (1967). Similarly, the large production cross section of the $B^2\Sigma_u^+ \rightarrow X^2\Pi_g$ fluorescence at wavelength λ827 Å is correlated with the strong absorption and ionization (Cook and Ogawa, 1969, Dibeler and Walker, 1967) bands associated with the n = 3 member of the Rydberg series V (Tanaka et al., 1960). For wavelengths shorter than λ800 Å the ion mass spectra (Dibeler and Walker, 1967) show that both the dissociative ionization processes, $CS_2 + h\nu \rightarrow S^+ + CS + e$ and $CS^+ + S + e$, have appreciable efficiencies. Since these dissociative ionization processes will reduce the production of CS_2^+ ions, the cross sections for the production of fluorescence from excited CS_2^+ ions may be expected to decrease at the shorter primary photon wavelengths which are shown in Figure 4.

Acknowledgment

This work was supported by the National Aeronautics and Space Administration under Grant No. NGR 05-018-180.

REFERENCES

Brundle, C. R. and Turner, D. W. 1969. Int. J. Mass Spect. Ion Phys. 2, 195.

Bueso-Sanllehf, Facundo. 1941. Phys. Rev. 60, 556.

Callomon, J. H. 1958. Proc. Roy. Soc. (London). A244, 220.

Collin, J. E. and Natalis, Paul. 1968. Int. J. Mass Spect. Ion Phys. 1, 121.

Cook, G. R. and Ogawa, M. 1969. J. Chem. Phys. 51, 2419.

Diebeler, V. H. and Walker, J. A. 1967. J. Opt. Soc. Am. 57, 1007.

Eland, J.H.D. and Danby, C. J. 1968. Int. J. Mass. Spect. Ion Phys. 1, 111.

Herzberg, G. (Editor). 1966. Electronic spectra of polyatomic molecules (Van Nostrand, N.Y.), p. 150, 601.

Hudson, R. D. 1970. Rev. Geophys. Space Phys. 9, 305.

Johns, J.W.C. 1961. Can. J. Phys. 39, 1738.

Judge, D. L., Bloom, G. S., and Morse, A. L. 1969. Can. J. Phys. 47, 489.

Judge, D. L. and Lee, L. C. 1972. J. Chem. Phys. 57, 455.

Judge, D. L. and Weissler, G. L. 1968. J. Chem. Phys. 48, 4590.

Lee, L. C. and Judge, D. L. 1972. J. Chem. Phys. 57, 4443.

Momigny, J. and Delwiche, J. 1968. J. Chem. Phys. 65, 1213.

Mrozowski, S. 1941. Phys. Rev. 60, 730.

_____ 1942. Phys. Rev. 62, 270.

_____ 1947a. Phys. Rev. 72, 682.

_____ 1947b. Phys. Rev. 72, 691.

Ogawa, M. and Chang, H. C. 1970. Can. J. Phys. 48, 2455.

Price, W. C. and Simpson, D. M. 1932. Proc. Roy Soc. (London). A165, 272.

Slavin, W., Mooney, R. W., and Palumbo, D. T. 1961. J. Opt. Soc. Am. 51, 93.

Tanaka, Y., Jursa, A. S., and LeBlanc, F. J. 1960. J. Chem. Phys. 32, 1205.

Tanaka, Y. and Ogawa, M. 1962. Can. J. Phys. 40, 879.

Turner, D. W. and May, D. P. 1967. J. Chem. Phys. 46, 1156.

Walker, W. C., Wainfan, N., and Weissler, G. L. 1955. J. Appl. Phys. 26, 1366.

Weissler, G. L., Ogawa, M., and Judge, D. L. 1971. J. de Physique Suppl. 32, C4-154.

Table I

The band head positions, the wave numbers, and the relative production cross sections for the various bands of the $CS_2^+(B^2\Sigma_u^+ \rightarrow X^2\Pi_g)$ system produced by photons at various incident wavelengths. The assigned transitions are also given.

band head λ(Å)	Incident λ(Å) / cm^{-1}	835	555 I 827	Transitions $B^2\Sigma_u^+ \rightarrow X^2\Pi_g(\Omega)$
2798	α 35740 *	0.030		(020) → (020) (3/2)
2809	c 35594.83*	0.16		(010) → (010) (3/2)
2820	a 35460.77	1.00	1.00	(000) → (000) (3/2)
2826	35386	0.016		
2834	β 35286 *	0.026		(020) → (020) (1/2)
2844	d 35157.33*	0.13		(010) → (010) (1/2)
2855.5	b 35020.06	0.91	0.86	(000) → (000) (1/2)
2863	34928 *	0.017		
2870	e 34843.95	0.021	0.023	(000) → (100) (3/2)
2874	34795*	0.052	0.055	
2908	f 34389	0.020	0.021	(000) → (100) (1/2)
2914	34317	0.014	0.015	

*The wave numbers are adopted from Callomon

Table II

The ionization potentials for the $A^2\Pi_{u,\Omega}(v00)$ vibrational levels obtained from the presently observed sequence bandheads. The values given by other authors are also given for comparison.

Sequence Band heads $\lambda(\mathring{A})$	Vibrational Levels $^2\Pi_u(V00)(\Omega)$		Ionization Potentials (ev) This Work	Eland and Danby	Bundle and Turner	Ogawa and Chang
4880	0	3/2	12.620	12.634		12.563
4940		1/2	12.643			12.586
4740	1	3/2	12.695	12.704	12.69	12.638
4803		1/2	12.714			12.661
4607	2	3/2	12.770	12.772	12.77	12.711
4671		1/2	12.787			12.735
4497	3	3/2	12.836	12.845	12.84	12.784
4542		1/2	12.863			12.808
4380	4	3/2	12.910	12.917	12.91	12.856
4437		1/2	12.927			12.879

Table III

The wavelengths for the vibrational transitions of the $CS_2^+[A^2\Pi_{u,\Omega}(v'00) \rightarrow X^2\Pi_{g,\Omega}(v''00)]$ system

v' \ v''		0	1	2	3
0	Ω=3/2	4880 Å	5031 Å	5193 Å	5365
	1/2	4940	5099	5268	5450
1	3/2	4740	4883	5035	5196
	1/2	4803	4953	5113	5283
2	3/2	4607	4742	4885	5037
	1/2	4671	4813	4964	5124
3	3/2	4497	4625	4761	4905
	1/2	4542	4676	4818	4969
4	3/2	4380	4500	4630	4766
	1/2	4437	4565	4700	4844

Table IV

The relative cross sections for the $CS_2^+(A^2\Pi_u \rightarrow X^2\Pi_g)$ system in various emission wavelength regions. The $CS_2^+(A^2\Pi_u)$ ions are produced by incident wavelengths of λ923 or 955 Å.

$\Delta\lambda$(Å)	4380 | 4430	4430 | 4475	4475 | 4535	4535 | 4600	4600 | 4650	4650 | 4730	4730 | 4790	4790 | 4875	4875 | 4930	4930 | 5025
σ_f	0.17	0.15	0.43	0.43	0.63	0.75	1.00	0.93	1.07	1.41

λ(Å)	5025 | 5080	5080 | 5180	5180 | 5265	5265 | 5360	5360 | 5570	5570 | 5770
σ_f	1.02	1.44	1.33	1.69	2.32	1.52

Table V

The production cross sections, σ_{Af} and σ_{Bf}, and the yields, η_{Af} and η_{Bf}, respectively for the $CS_2^+(A^2\Pi_u, B^2\Sigma_u^+ \rightarrow X^2\Pi_g)$ fluorescence produced by primary photon wavelengths from λλ462-977Å. The absorption cross sections, σ_T, were given by Cook and Ogawa. The cross sections are in units of Mb(= 10^{-18} cm^2) and the yields $\eta_f(=\sigma_f/\sigma_T)$ are in units of %.

λ(A)	σ_T(Mb)	σ_{Af}(Mb)	η_{Af}(%)	σ_{Bf}(Mb)	η_{Bf}(%)
462		2.3		1.5	
501		3.4		2.0	
526		3.9		3.6	
555		4.5		5.0	
589		4.7		7.5	
598		4.9		6.6	
610	35.7	4.8	13	6.2	17
625	36.2	4.6	13	5.2	14
637	37.8	5.1	13	6.1	16
645	38.1	4.8	13	5.9	15
689	45.1	4.9	11	9.5	21
702	44.8	5.7	13	10.8	24
716	46.3	6.3	14	9.7	21
731	46.5	6.9	15	6.9	15
769	48.0	8.3	17	8.9	19
772	49.5	8.8	18		
790	68.5	9.7	14	16.4	24
801	60.7	10.4	17	17.5	29
809	45.8			6.6	14
815	57.7			10.3	18
822	45.8			19.6	43
827	82.0	11.6	14	56.0	68
835	77.4	10.1	13	37.3	48
840	37.2			15.9	43
844	37.2	7.0	19	16.7	45
851	27.9	5.7	20	8.8	31
879	52.1	7.9	15		
894	43.2	7.6	18		
901	83.6	14.2	17		
923	45.4	30.2	67		
955	120.2	64.9	54		
977		1.7			

Figure Captions

Fig. 1 The fluorescence spectra of the $CS_2^+[B^2\Sigma_u^+ \rightarrow X^2\Pi_g]$ system produced by primary photons of wavelengths λ555, 827, 835 and 851 Å.

Fig. 2 The fluorescence spectrum of the $CS_2^+[B^2\Sigma_u^+ \rightarrow X^2\Pi_g]$ system produced by primary photons of wavelength λ835 Å. The band heads, a-y, given by Callomon are indicated. The suggested assignments for the α,c,β, and d bands are also indicated.

Fig. 3 The fluorescence spectrum of the $CS_2^+[A^2\Pi_u \rightarrow X^2\Pi_g]$ system produced by primary photons of wavelength λ923 Å. The suggested assignments for the observed bands are indicated.

Fig. 4 The production cross sections of the $CS_2^+[A^2\Pi_u \rightarrow X^2\Pi_g]$ and $CS_2^+[B^2\Sigma_u^+ \rightarrow X^2\Pi_g]$ fluorescence which are indicated by $\cdot$ and $\dot{x}$, respectively. The units are in Mb(= 10^{-18} cm^2).

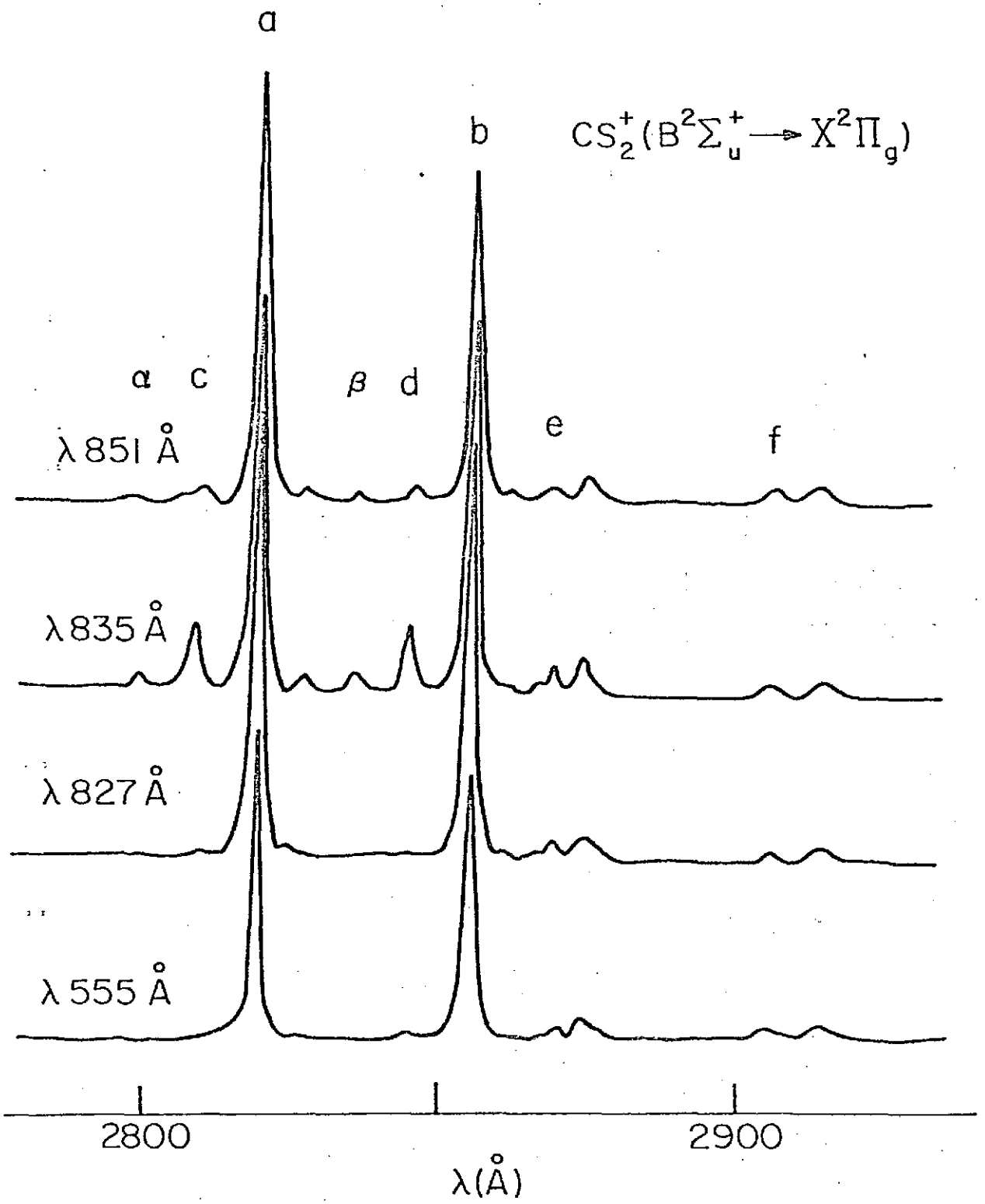
a
b
$CS_2^+(B^2\Sigma_u^+ \rightarrow X^2\Pi_g)$
α c
β d
e
f
λ 851 Å
λ 835 Å
λ 827 Å
λ 555 Å
2800
2900
λ(Å)

27

Fig. 1

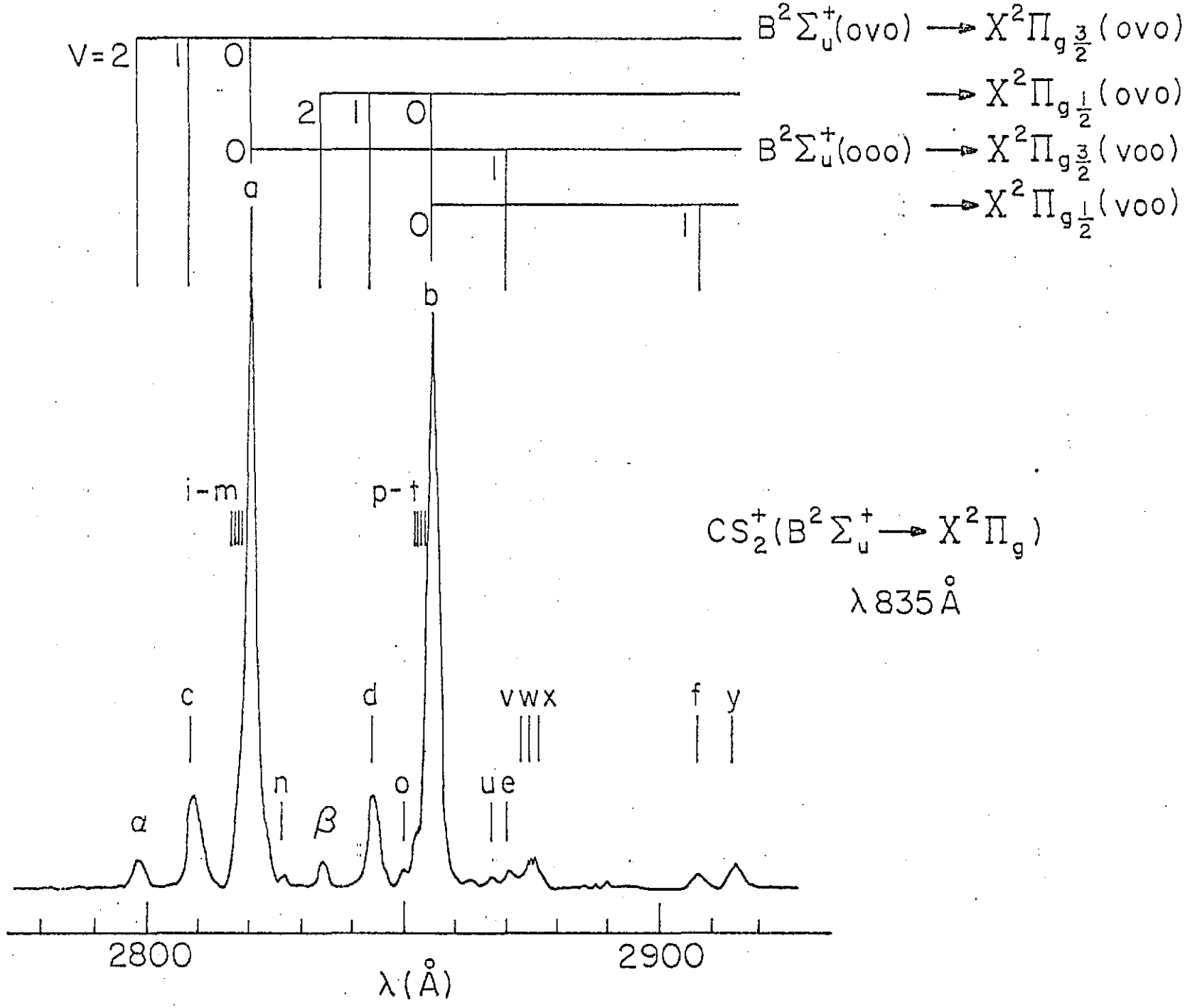
$B^2\Sigma_u^+(ovo) \rightarrow X^2\Pi_{g\frac{3}{2}}(ovo)$
$\rightarrow X^2\Pi_{g\frac{1}{2}}(ovo)$
$B^2\Sigma_u^+(ooo) \rightarrow X^2\Pi_{g\frac{3}{2}}(voo)$
$\rightarrow X^2\Pi_{g\frac{1}{2}}(voo)$
V=2
1
0
2
1
0
0
1
0
1
a
b
i-m
p-t
$CS_2^+(B^2\Sigma_u^+ \rightarrow X^2\Pi_g)$
λ835 Å
c
d
vwx
f
y
α
n
β
o
ue
2800
2900
λ(Å)

Figure 2

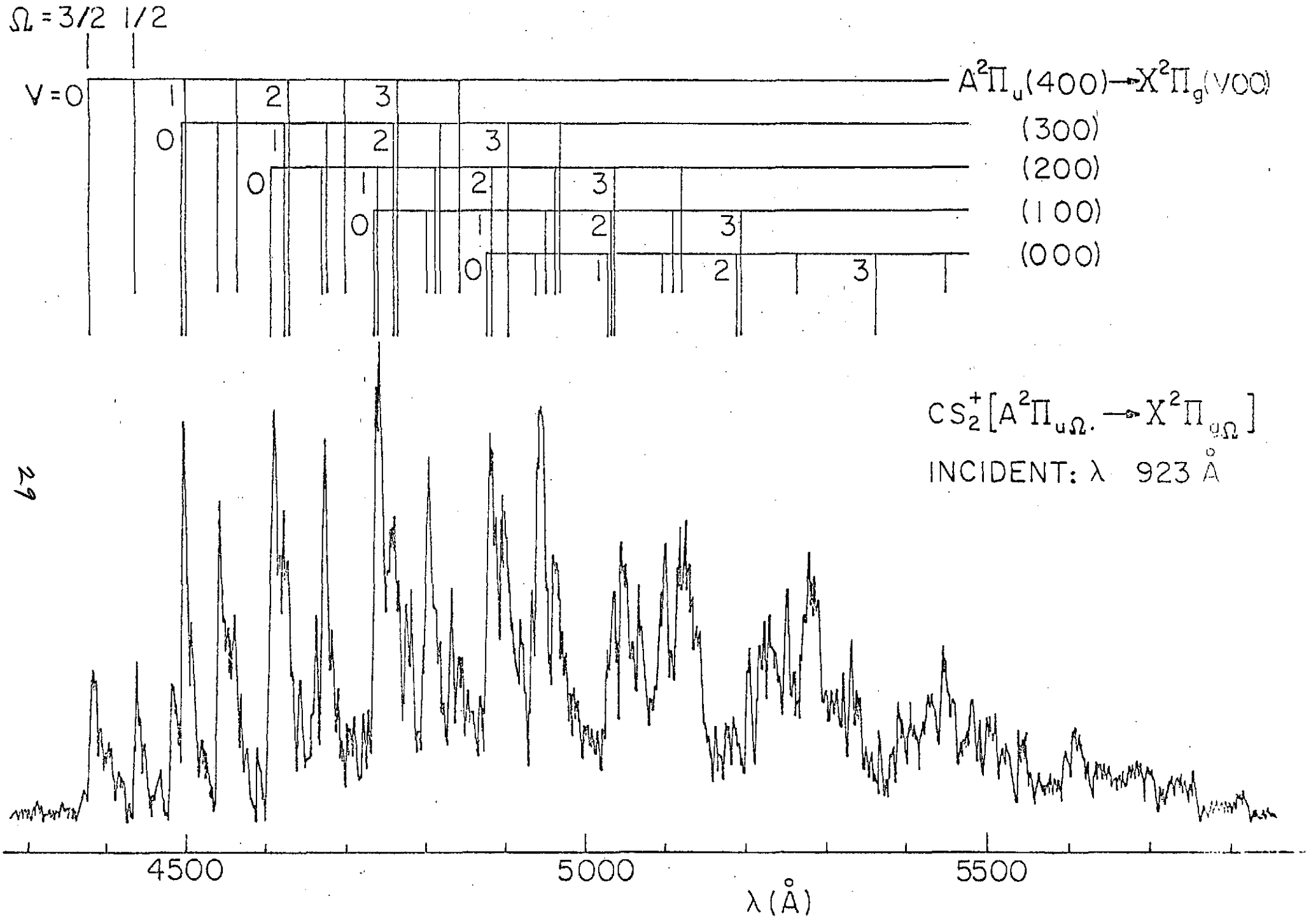
Ω = 3/2 1/2
V = 0
$A^2\Pi_u(400) \rightarrow X^2\Pi_g(V00)$
(300)
(200)
(100)
(000)
$CS_2^+[A^2\Pi_{u\Omega} \rightarrow X^2\Pi_{g\Omega}]$
INCIDENT: λ 923 Å
29
4500
5000
5500
λ(Å)

Fig. 3

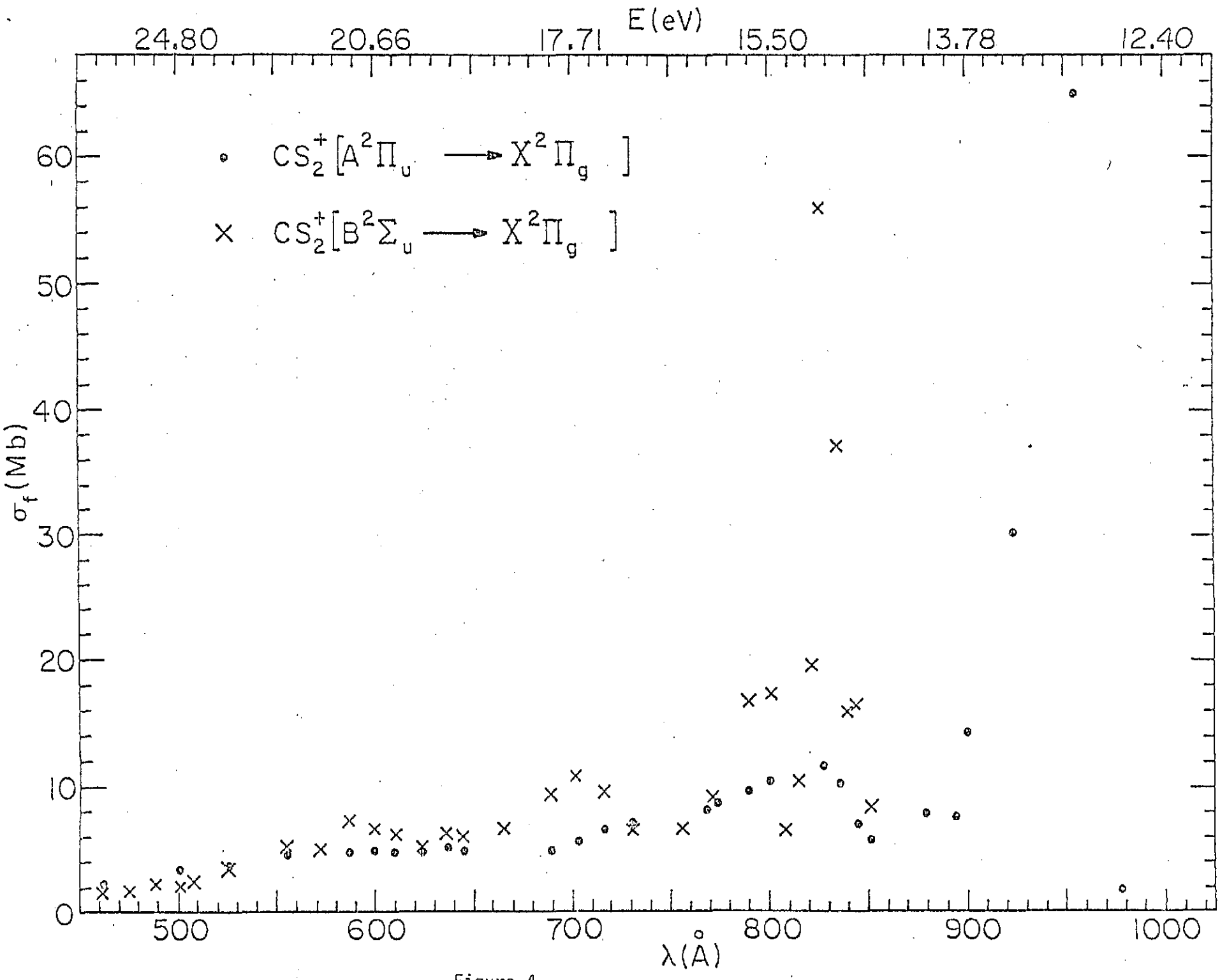
E(eV)
24.80
20.66
17.71
15.50
13.78
12.40
$CS_2^+[A^2\Pi_u \longrightarrow X^2\Pi_g]$
$CS_2^+[B^2\Sigma_u \longrightarrow X^2\Pi_g]$
σ_f(Mb)
0
10
20
30
40
50
60
500
600
700
800
900
1000
λ(Å)

Figure 4

$CS(A^1\Pi \rightarrow X^1\Sigma^+)$ FLUORESCENCE FROM PHOTODISSOCIATION OF CS_2 AND OCS

L. C. Lee and D. L. Judge

Department of Physics
University of Southern California
Los Angeles, California 90007

Abstract

The $CS(A^1\Pi \rightarrow X^1\Sigma^+)$ fluorescence resulting from photodissociation of CS_2 and OCS by vacuum ultraviolet emission lines from λλ686-1239 Å has been investigated. With the assumption that the electronic transition moment is constant, the Franck-Condon factors for the emission system and the population in the vibrational levels of the $CS(A^1\Pi)$ electronic state have been measured. The population data are approximately represented by a Poisson distribution, which is predicted from a theoretical argument. A population inversion between the $v = 0$ and 1 levels of the $CS(A^1\Pi)$ state is found. The production cross sections for the fluorescence are also measured.

I. INTRODUCTION

The $CS(A^1\Pi \rightarrow X^1\Sigma^+)$ fluorescence produced by photodissociative excitation of CS_2 produced by photons in the wavelength range from λλ1200-1337 Å has been observed by Okabe[1]. The excited photofragment $CS(A^1\Pi)$ is mainly produced by the process

$$CS_2 + h\nu \rightarrow CS(A^1\Pi) + S(^3P_2)$$

The ultraviolet fluorescence at wavelengths shorter than λ4500 Å, produced by OCS absorbing photons of wavelengths from λλ650-1000 Å, has been reported by Cook and Ogawa[2]. However, the source of the fluorescence was not identified.

The fluorescence spectra from photofragments provide data required for an understanding of photodissociation mechanisms. Recently, several theoretical arguments[3-6] have predicted the population distribution in the vibrational levels of a diatomic photofragment. Such theoretical predictions can be investigated by observing the fluorescence spectra as has been demonstrated in earlier work[7] and again in the present investigation.

II. EXPERIMENTAL

The experimental setup has been described in a previous paper[8]. The nominal vacuum UV emission lines selected for this investigation were 686, 765, 790, 834, 923, 955, 977, 992, 1037, 1085, and 1239 Å. The bandwidth of the 1-m normal incidence monochromator used for isolation of these lines was set at 5 Å or less. The absolute line intensities were measured with a nickel film photoelectric detector for which the quantum efficiency was known[9]. The fluorescence was dispersed by either of two gratings, one blazed at 2000Å and the other at 5000 Å, of which the first and the second orders were used, respectively. The bandwidth of the 0.3-m normal incidence monochromator used in the present investigations was set at 3 Å or less.

The combined response of the 0.3-m monochromator and cooled photomultiplier (EMI 9558 QB) was calibrated against the response of sodium salicylate, of which the fluorescent efficiency between 2200 and 3400 Å is known to be constant[10]. The spectral region of interest extends from λλ2400-2900 Å and throughout this range the detection system response (per photon/second) is found to be nearly constant.

CS_2 vapor was obtained from an analytical-reagent-grade liquid. The vapor was purified so that the fluorescence from the possible impurities, especially N_2, produced by vacuum ultraviolet radiation of λ555 Å was not detectable. OCS gas supplied by Matheson Gas Co. with a purity higher than 97.5% was used without further purification. The gas pressure inside the sample cell was monitored with a Baratron capacitance manometer and was limited to 20 mtorr or less where the fluorescence intensity is linearly proportional to the pressure.

III. RESULTS AND DISCUSSION

A. Fluorescence Spectra

The $CS(A^1\Pi \rightarrow X^1\Sigma^+)$ fluorescence produced by photodissociation of CS_2 with primary photons of wavelength $\lambda 1239$ Å is shown in Fig. 1. The radiation was dispersed and the second order spectrum was identified through the bandhead positions given by Pearse and Gaydon[11]. For primary photons of wavelength $\lambda 923$ Å the same CS fluorescence spectrum was produced by photodissociation of CS_2 and OCS. The resulting first order spectra may be seen in Fig. 2. At $\lambda 923$ Å the advantage of using the second order to obtain higher resolution is obscured by the emissions from CS_2^+, OCS^+ ions and/or other photofragments. Several spectra were taken at various primary photon wavelengths shorter than $\lambda 1239$ Å for CS_2 and shorter than $\lambda 992$ Å for OCS. These spectra are not significantly different from the spectra shown in Figures 1 and 2. According to the photodissociation energy of CS_2(= 4.463 eV) given by Okabe,[1] fluorescence emitted from levels higher than $v' = 5$ of $CS(A^1\Pi)$ is energetically possible for primary photon wavelengths shorter than $\lambda 1239$ Å. However, the fluorescence from these higher vibrational levels is rather weak.

B. Franck-Condon Factors of the $CS(A^1\Pi \rightarrow X^1\Sigma^+)$ System

The fluorescence radiation rate, $\dot{n}_{v'v''}$, for a band emitted from a vibrational level v' of the upper electronic state to a level v" of the lower electronic state can be obtained from the measured spectra. Because of the constancy of the detection system response the relative radiation rate for each emission is proportional to the area under its spectral envelope. The radiation rates for various emission bands resulting from CS_2 and OCS absorbing various primary photon wavelengths are listed in Table I. These values are averaged over several spectra obtained under similar

conditions and in which the (1-1) band of each spectrum is normalized to 1.

The radiation rate[12] has been given by

$$\dot{n}_{v'v''} = KN_{v'} Re^2_{v'v''} q_{v'v''} / \lambda^3_{v'v''}$$

where K is a constant, $N_{v'}$ is the population in the vibrational level v', $Re_{v'v''}$ is the electronic transition moment, $q_{v'v''}$ is the Franck-Condon Factor, and $\lambda_{v'v''}$ is the band wavelength.

If the electronic transition moment is assumed to be a constant, which is usually a good assumption for diatomic molecules[8], then the Franck-Condon factor can be calculated from the measured radiation rates and the known band wavelengths[11]. The Franck-Condon factors obtained from the spectra resulting from CS_2 absorbing photons of wavelength λ1239Å are listed in Table I. The sum of the Franck-Condon factors over the lower level v", $\Sigma\, q_{v'v''}$, for each upper level is equal to 1. The calculated Franck-Condon factors given by Felenbok[13] are also listed for comparison. In general, except for the $\Delta v = 0$ transitions, the measured values agree with the theoretical values. This agreement strengthens the validity of a constant electronic transition moment.

C. Population Distribution of the $CS(A^1\Pi)$ levels

If the electronic transition moment is assumed to be constant, the population $N_{v'}$ in an upper level, v', can be obtained from

$$N_{v'} = K' \sum_{v''} \dot{n}_{v'v''} \lambda^3_{v'v''}$$

The population distributions in the vibrational levels of $CS(A^1\Pi)$ produced by photodissociation of CS_2 with primary photon wavelengths of λ923 and λ1239 Å and OCS with λ923 Å are shown in Fig. 3 and 4, respectively. The population in the $v' = 1$ level is normalized to 1. The error bar shows the fluctuation of data obtained from various spectra.

A population inversion between the v = 0 and 1 levels is evident.

The photodissociation mechanism has been summarized and generalized by Simons and Tasker[3]. When a CS_2 or OCS molecule absorbs a photon it is excited to a repulsive state and the molecular CS fragments will occupy a range of initial vibrational states determined by the appropriate Franck-Condon factors. During the separation period the CS fragments are then forced into a set of final states by the recoil force. If we assume that the vibrational state of CS is that of a harmonic oscillator, and the recoil force corresponds to an exponentially repulsive potential, then the probability that $CS(A^1\Pi)$ in an initial state i will be transferred to a final vibrational level v' is given by [4,14-16]

$$P_{v'i} = i!\, v'!\, (\Delta E)^{i+v'}\, e^{-\Delta E} \left[\sum_{\ell=0}^{\min(i,v')} \frac{(-\Delta E)^{-\ell}}{\ell!(i-\ell)!\,(v'-\ell)!}\right]^2$$

where ΔE is the average number of vibrational quanta transferred.

If we assume that the initial states are only prepared in the ground state, i = o, then the population, $N_{v'}$, is a Poisson distribution,

$$N_{v'} \propto P_{v'o} = (\Delta E)^{v'}\, e^{-\Delta E}/v'!$$

The Poisson distribution best fit to the measured populations is shown in Figs. 3 and 4. The ΔE values for CS_2 dissociated by photons of wavelengths λ1239 and 923 Å, and for OCS by λ923 Å, are 1.66, 1.86, and 1.82, respectively.

As indicated in the figures the measured populations are only approximately represented by the Poisson distribution. It seems that the initial states are also prepared in higher excitation states. If we assume that both the i = o and 1 states are initially populated and that the number of vibrational quanta transferred is the same for both states, then the population in the vibrational level v' is given by

$$N_{v'} = N_1\, (\Delta E)^{v'-1}[(\Delta E)^2 + (\alpha - 2v')\,\Delta E + v'^2]/\{v'![(\Delta E)^2+(\alpha-2)\,\Delta E+1]\}$$

where α is the ratio of the population in the i= state to that in the i=1 state.

The result for the best fit of the observed populations using the above equation is shown in Figs. 3 and 4. The values of ΔE and α for the observed distributions are 1.665 and 12.60 for CS_2 photodissociated by photons of wavelength λ1239 Å, 1.951 and 4.48 for CS_2 photodissociated by λ923 Å, and 1.914 and 4.25 for OCS dissociated by λ923 Å. A comparison of the ΔE and α values of CS_2 dissociated by λ1239 Å with those by λ923 Å indicates that as the primary photon energy is increased more vibrational quanta are transferred and that the initial states include higher vibrational levels.

As indicated in the figures the measured populations are only approximately represented by the theoretical distribution modified to involve the initial state i=1. The initial populations in the other higher excited states and the anharmonicity of the $CS(A^1\Pi)$ potential well should be considered. On the other hand, Berry[17] and Band and Freed[18] have proposed different photodissociation models in which the interfragment force during the separation period is ignored and the final population distribution is solely determined by the initial Franck-Condon factors and the continua state densities. Such models may provide an alternative interpretation for the present measurements.

D. Production Cross Sections of the Fluorescence

At low gas pressure, P, the radiation rate produced by a primary photon of wavelength λ is proportional to the production cross section $\sigma_{v'v''}(\lambda)$ and is given by[19]

$$\dot{n}_{v'v''}(\lambda) = K\, \sigma_{v'v''}(\lambda)\, I_o\,(\lambda)\, P$$

where K is a constant and $I_o(\lambda)$ is the primary photon flux.

The absolute total cross section, $\sum_{v'v''} \sigma_{v'v''}(\lambda)$, at each primary wavelength is obtained by comparing the total fluorescence radiation $\sum_{v'v''} \dot{n}_{v'v''}$, with that of the CO^+ first negative band, for which the absolute cross section is known[8]. The cross sections for the $CS(A^1\Pi \rightarrow X^1\Sigma^+)$ fluorescence produced by photodissociation of CS_2 and OCS, at various primary photon wavelengths, are listed in Table II. The fluorescence production cross sections for the primary photon wavelengths from λ462 to 686 Å are estimated to be smaller than 0.02 Mb for both CS_2 and OCS.

E. The D(O - CS) Dissociation Energy

The threshold for the production of the $CS(A^1\Pi \rightarrow X^1\Sigma^+)$ fluorescence from photodissociation of CS_2 as measured by Okabe[1] is 1337 ± 2 Å. On the other hand, the threshold for the production of fluorescence from photodissociation of OCS has not been given. In the present measurement weak fluorescence has been observed at the primary photon wavelength of λ1010 Å and no detectable fluorescence signal has been produced by λ1037 Å photons. Therefore, the threshold for the production of $CS(A^1\Pi)$ fragments from photodissociation of OCS is 1024 ± 14 Å or 12.11 ± 0.16 eV. If we assume that the photodissociation is through the following process

$$OCS + h\nu \rightarrow CS(A^1\Pi) + O(^3P) \qquad (1)$$

which is spin forbidden, but corresponds to the CS_2 photodissociation process at threshold[1], the photodissociation energy D°_o (O - CS) is then found to be 7.30 ± 0.16 eV or 168 ± 3.7 KCal/mol, subtracting the 4.814 eV (λ2575.6Å) energy of the $CS(A^1\Pi, v'=o) \rightarrow CS(X^1\Sigma^+, v''=o)$ transition from the primary photon energy.

The presently obtained dissociation energy is comparable to that calculated from thermochemical data. Using $\Delta H^\circ_{f,o}(O) = 58.983$ and $\Delta H^\circ_{f,o}(OCS) = -33.991$ Kcal/mol given by Wagman et al.[20] and $\Delta H^\circ_{f,o}(CS) = 64.96 \pm 0.4$ Kcal/mol

derived from the photodissociation threshold of CS_2 given by Okabe,[1] the dissociation energy is

$$D_0^\circ (O - CS) = \Delta H_{f,0}^\circ(CS) - \Delta H_{f,0}^\circ(OCS) + \Delta H_{f,0}^\circ(O)$$
$$= 157.93 \text{ Kcal/mol}$$

This value is about 10 Kcal/mol lower than the presently measured value of 168 ± 3.7 Kcal/mol. However, these closely related values show that the process (1) is the main primary process at threshold. If we assume that the spin allowed process

$$OCS + h\nu \rightarrow CS\ (A^1\Pi) + O\ (^1D) \qquad (2)$$

is the primary process, then the photodissociation energy D_0° (O - CS) will be lowered by the 1.967 eV excitation energy of $O(^1D)$, and accordingly D_0° (O - CS) would be 5.33 ± 0.16 eV or, 123 ± 3.7 Kcal/mol. This value is much lower than that of 157.93 Kcal/mol and therefore, process (2) occurring at the photodissociation threshold is very unlikely.

Acknowledgments

The authors wish to thank Drs. Berry, Band, and Freed for the preprints describing their proposed photodissociation models. This work was supported by the National Aeronautics and Space Administration under Grant No. NGR 05-018-180.

REFERENCES

1. Hideo Okabe, J. Chem. Phys. 56, 4381 (1972).
2. G.R. Cook and M. Ogawa, J. Chem. Phys. 51, 647 (1969)
3. J.P. Simons and P.W. Tasker, Mol. Phys. 26, 1267 (1973)
4. K.E. Holdy, L.C. Klotz, and K.R. Wilson, J. Chem. Phys 52, 4588 (1970)
5. M. Shapiro and R. D. Levine, Chem. Phys. Lett. 5, 499 (1970)
6. Shaul Mukamel and Joshua Jortner, J. Chem. Phys. 60, 4760 (1974)
7. L.C. Lee and D. L. Judge, Can. J. Phys. 51, 378 (1973)
8. D.L. Judge and L.C. Lee, J. Chem Phys. 57, 455 (1972)
9. W.C. Walker, N. Wainfain, and G.L. Weissler, J. Appl. Phys. 26, 1366 (1955)
10. J.A.R. Samson, "Techniques of Vacuum Ultraviolet Spectroscopy" (Wiley, New York, 1967) P. 212
11. R.W. B. Pearse and A. G. Gaydon, "The Identification of Molecular Spectra," (Wiley, New York 1963), P. 125
12. G. Herzberg, "I. Spectra of Diatomic Molecules," (Van Nostrand, New Jersey 1967) P. 200
13. F. Felenbok, Proc. Phys. Soc. 86, 676 (1965)
14. E.H. Kerner, Can. J. Phys. 36, 371 (1958)
15. F.E. Heidrich, K.R. Wilson, and Donald Rapp, J. Chem. Phys. 54, 3885 (1971)
16. D. Rapp and T. Kassal, Chem. Rev. 69, 61 (1969)
17. M. J. Berry, Chem. Phys. Lett. 29, 329 (1974).
18. Y. B. Band and K. F. Freed, Chem. Phys. Lett. 28, 328 (1974).
19. D. L. Judge and L. C. Lee, J. Chem. Phys. 58, 104 (1973)
20. D.D. Wagman, W.H. Evans, V.B. Parker, I. Halow, S. M. Bailey and R.H. Schumm, Natl. Bur. Std. Tech. Note 270-3 (1968)

TABLE I

The radiation rates, $\dot{n}_{v'v''}$, and the Franck-Condon factors, $q_{v'v''}$, for the various bands of the CS($A^1\Pi \rightarrow X^1\Sigma^+$) system produced by photodissociation of CS_2 and OCS.

Molecules		CS_2			CS_2	OCS
Incident λ		1239 Å			923 Å	923 Å
Bands v'-v"	Bandheads $\lambda_{v'v''}$(Å)	$\dot{n}_{v'v''}$	$q_{v'v''}$	Calc. $q_{v'v''}$	$\dot{n}_{v'v''}$	$\dot{n}_{v'v''}$
0-0	2575.6	0.80	0.78	0.7747	0.67	0.73
0-1	2662.6	0.14	0.15	0.1937	0.09	0.11
0-2	2754.7	0.05	0.06	0.0283		
1-0	2507.3	0.24	0.13	0.1968	0.22	0.25
1-1	2589.6	1.00	0.61	0.4040	1.00	1.00
1-2	2677.0	0.31	0.20	0.3044	0.19	0.24
1-3	2769.2	0.07	0.05	0.0798		
2-0	2444.8	0.04	0.03	0.0260		
2-1	2523.2	0.32	0.25	0.3139	0.34	0.29
2-2	2605.9	0.44	0.37	0.1506	0.39	0.42
2-3	2693.2	0.31	0.29	0.3273	0.29	0.32
2-4	2785.7	0.06	0.06	0.1420		
3-1	2460.2	0.07	0.08	0.0764		
3-2	2538.7	0.27	0.33	0.3416	0.38	0.36
3-3	2621.6	0.12	0.16	0.0230	0.16	0.21
3-4	2708.9	0.21	0.31	0.2764	0.26	0.26
3-5	2801.5	0.09	0.14	0.1973		
4-2	2477.0	0.08	0.12	0.1404	0.10	0.10
4-3	2555.8	0.33	0.52	0.2912	0.40	0.42
4-4	2638.9	0.04	0.06	0.0034		
4-5	2726.7	0.15	0.29	0.1822	0.19	0.19

TABLE II

Cross sections for the $CS(A^1\Pi \rightarrow X^1\Sigma^+)$ fluorescence produced by photodissociation of CS_2 and OCS. The cross sections and the primary photon wavelengths are in units of Mb(= 10^{-18} cm^2) and Å, respectively.

λ(Å)	CS_2	OCS
686		0.03
765		0.04
790	0.02	0.08
834	0.04	0.09
923	0.28	0.24
955	0.18	0.21
977	0.17	0.29
992	0.24	0.28
1037	0.52	0
1085	0.39	0
1239	1.09	0

FIGURE CAPTIONS

Fig. 1. The $CS(A^1\Pi \rightarrow X^1\Sigma^+)$ fluorescence spectrum produced by photodissociation of CS_2 with primary photon wavelength of λ1239 Å. The bandhead positions given by Pearse and Gaydon are indicated.

Fig. 2. The $CS(A^1\Pi \rightarrow X^1\Sigma^+)$ fluorescence spectra produced by photodissociation of OCS and CS_2 with primary photon wavelength of λ923 Å.

Fig. 3. The vibrational population of the $CS(A^1\Pi)$ state produced by photodissociation of CS_2 with primary photon wavelengths of λ923 and 1239 Å. Both the best fit Poisson and modified distributions are indicated. The modified distribution has the initial population in both the $v = 0$ and 1 levels.

Fig. 4. The vibrational population of the $CS(A^1\Pi)$ state produced by photodissociation of OCS with primary photon wavelength of λ923 Å. Both the best fit Poisson and modified distributions are indicated.

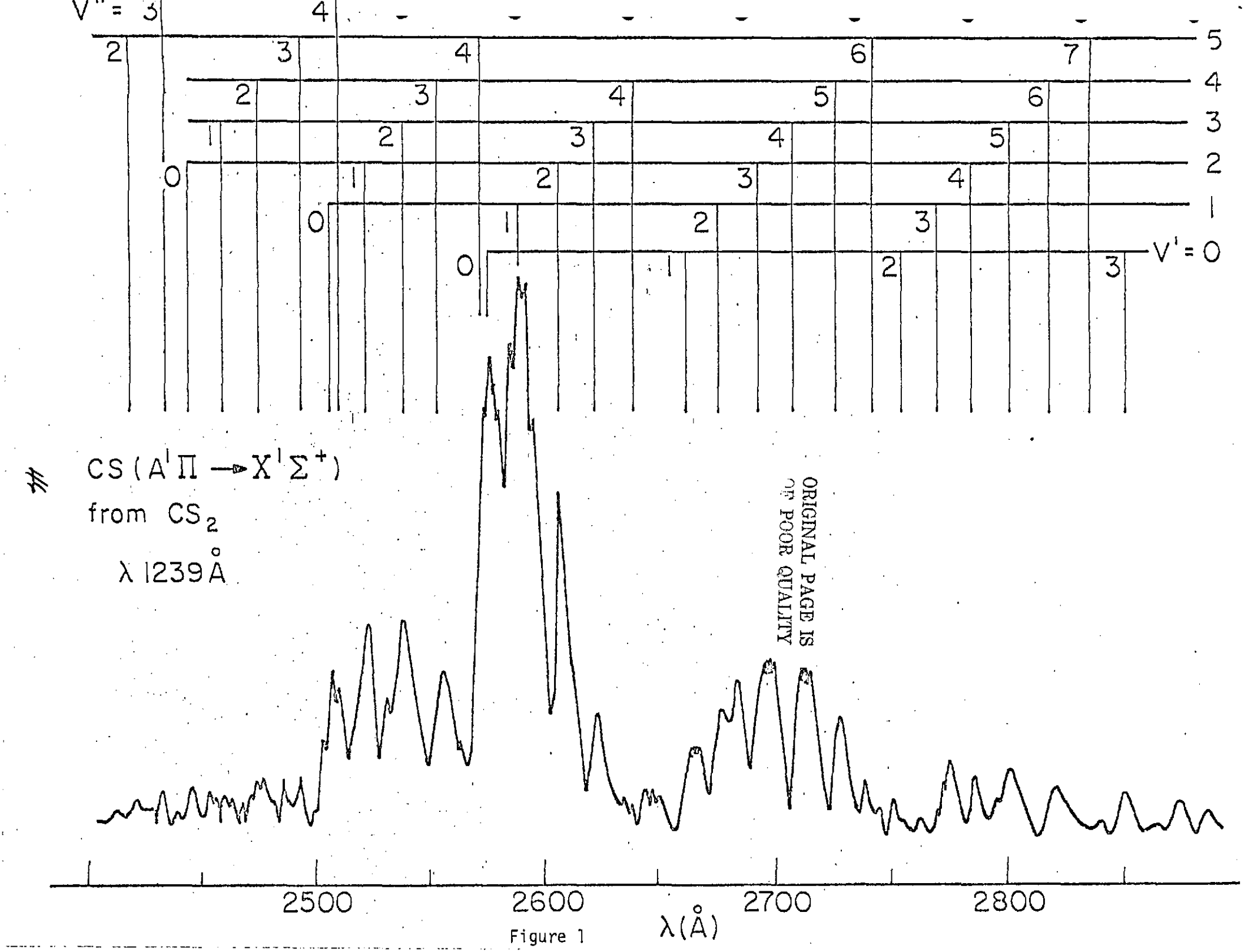
V'' = 3
4
2
3
4
6
7
5
2
3
4
5
6
4
1
2
3
4
5
3
0
1
2
3
4
2
0
1
2
3
1
0
1
2
3
V' = 0
2
3
CS (A¹Π → X¹Σ⁺)
from CS₂
λ 1239 Å
ORIGINAL PAGE IS
OF POOR QUALITY
2500
2600
2700
2800
λ(Å)

Figure 1

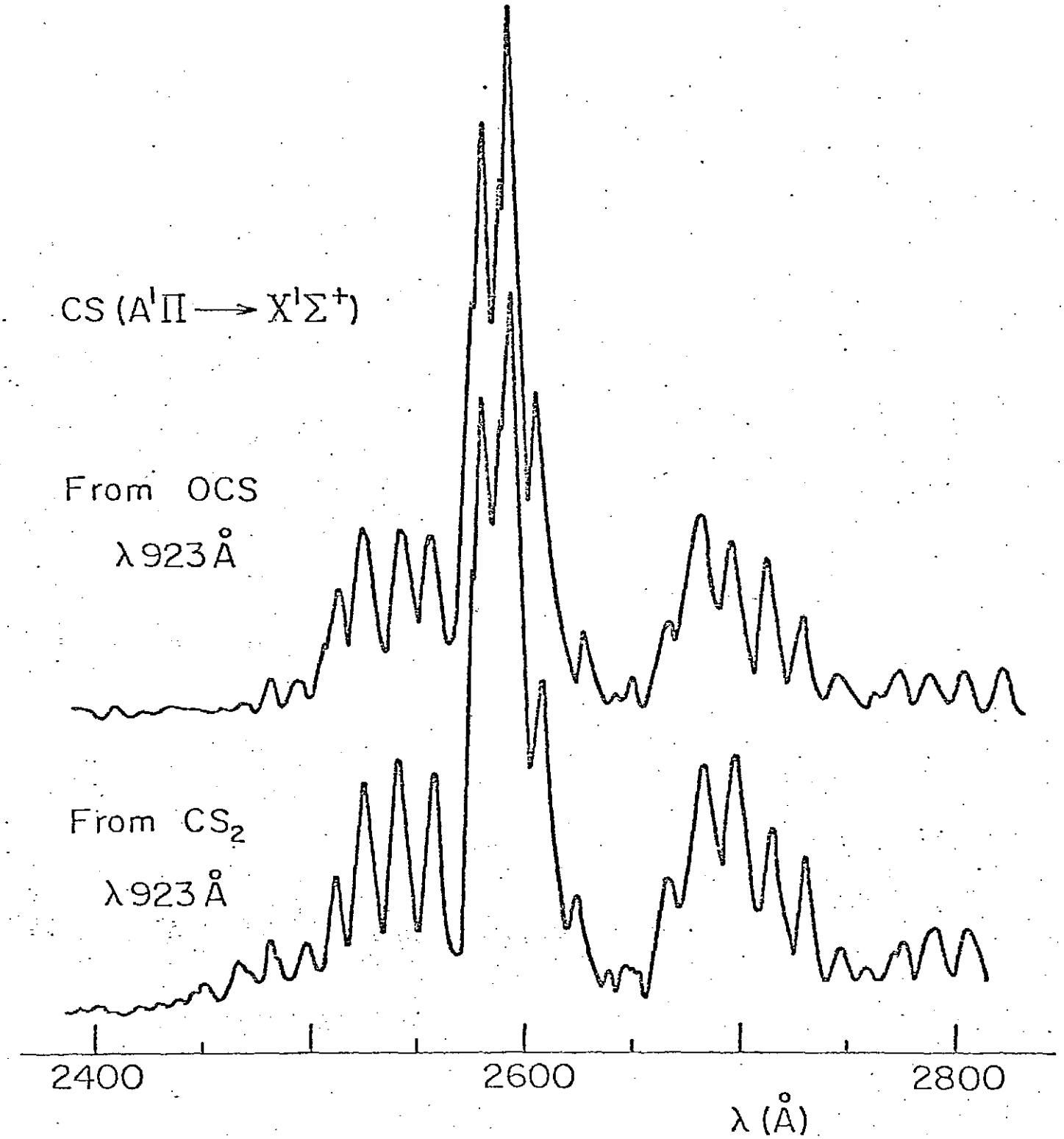

Figure 2

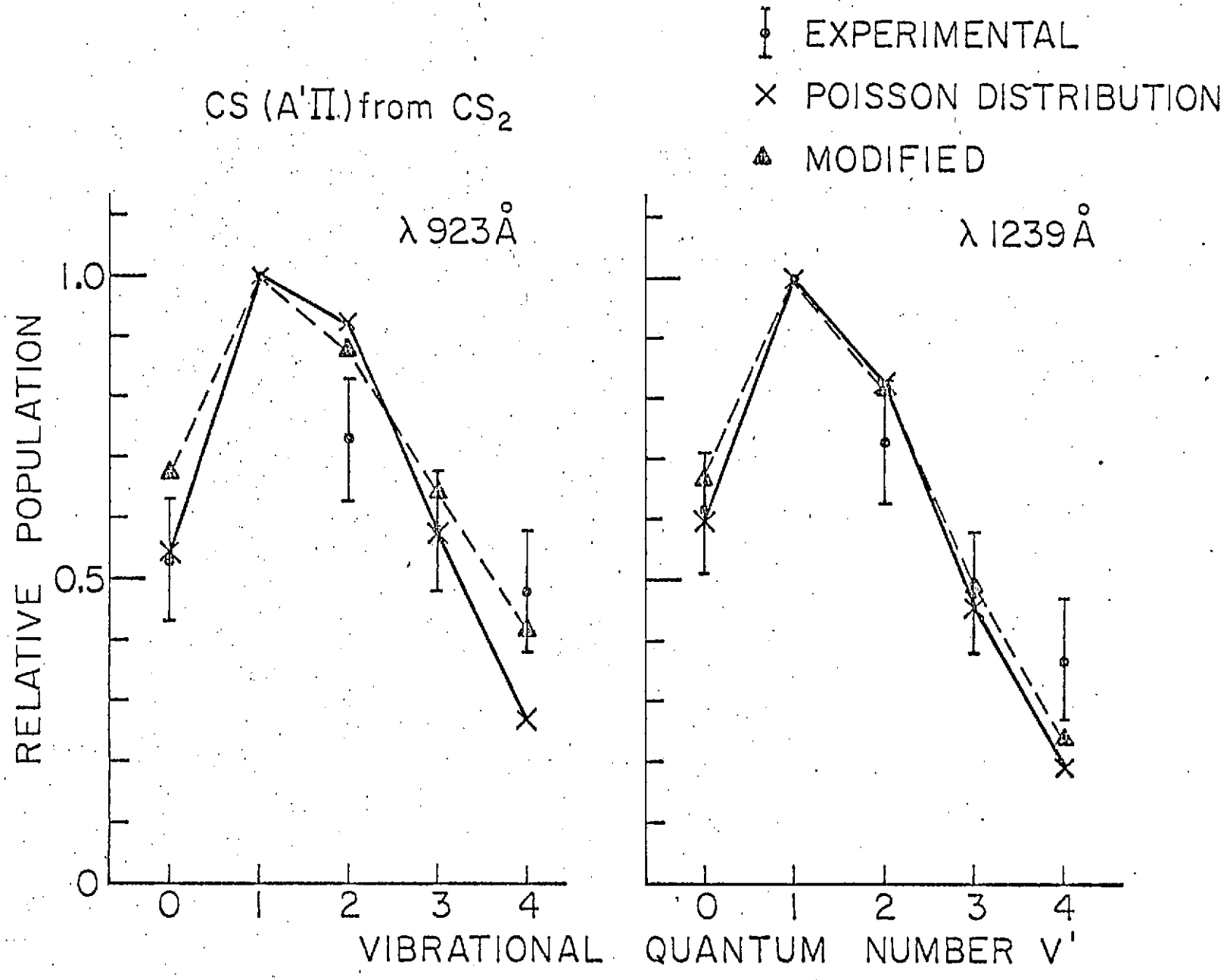
EXPERIMENTAL
POISSON DISTRIBUTION
MODIFIED
CS (A'Π) from CS2
λ 923Å
λ 1239Å
RELATIVE POPULATION
1.0
0.5
0
0 1 2 3 4
VIBRATIONAL QUANTUM NUMBER V'

Figure 3

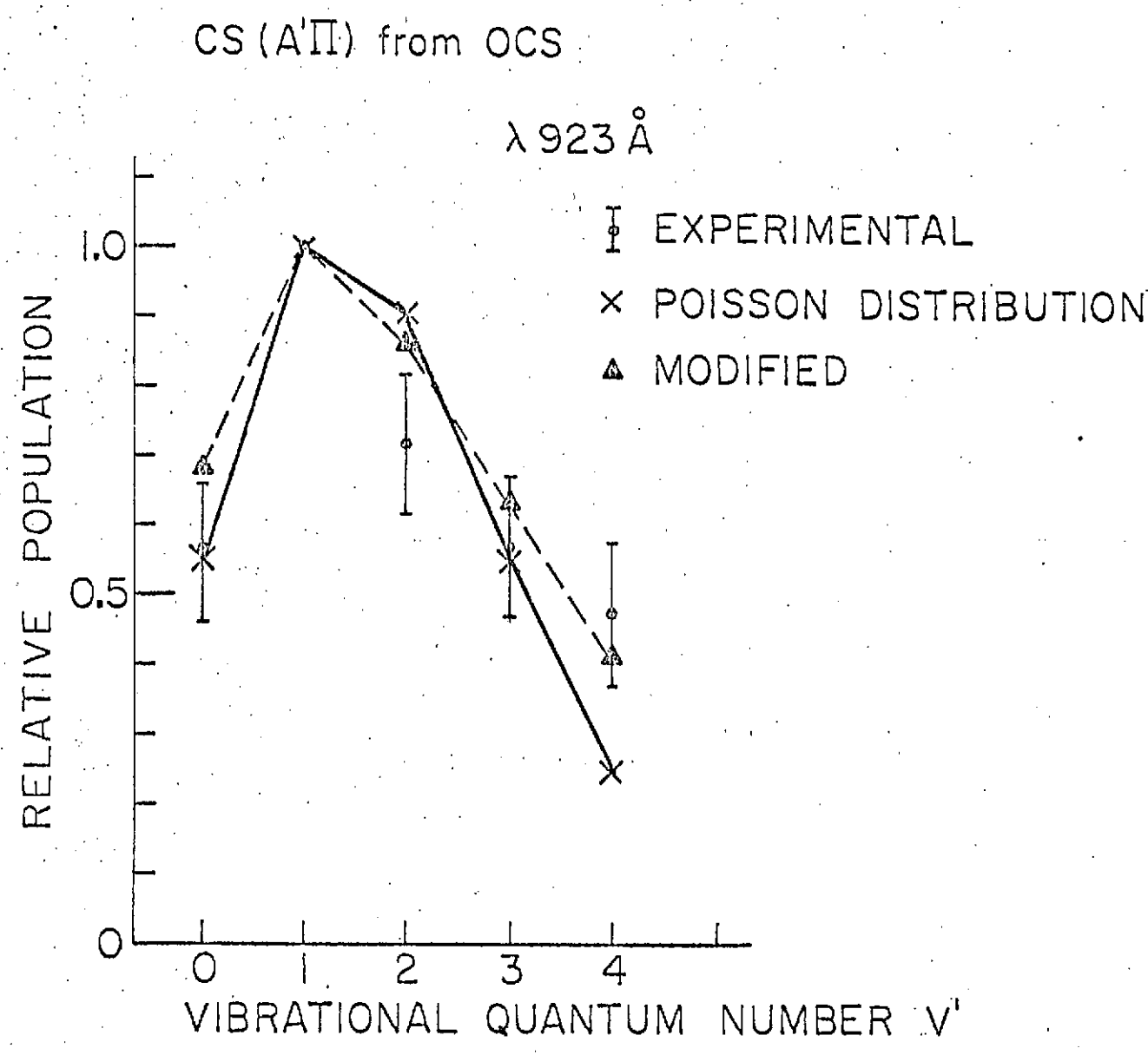
CS (A'Π) from OCS
λ 923 Å
EXPERIMENTAL
POISSON DISTRIBUTION
MODIFIED
RELATIVE POPULATION
1.0
0.5
0
0
1
2
3
4
VIBRATIONAL QUANTUM NUMBER V'

Figure 4

$OCS^+(A^2\Pi \rightarrow X^2\Pi)$ FLUORESCENCE FROM PHOTOIONIZATION OF OCS

D. L. Judge and L. C. Lee

Department of Physics
University of Southern California
Los Angeles, California 90007

Abstract

$OCS^+[A^2\Pi(000) \rightarrow X^2\Pi(v_1 0 v_3)]$ fluorescence bands produced by OCS photoabsorption of extreme ultraviolet emission lines from λλ637-801 Å were analyzed and the cross sections for the production of fluorescence were measured. Several weak emission bands were identified as $A^2\Pi(000) \rightarrow X^2\Pi(v_1 00)$ transitions. No fluorescence emitted from the OCS^+ ion, other than from the $A^2\Pi(000)$ vibrational level, was detected.

I. Introduction

The total fluorescence produced by OCS photoabsorption of extreme ultraviolet radiation has been observed by Cook and Ogawa [1]. The fluorescence was later dispersed by Judge and Ogawa [2] and determined to be in part emitted from the $OCS^+[A^2\Pi(000)(i) \rightarrow X^2\Pi(00v)(i)]$ transitions. Here, the identification of weak bands in the emission spectrum has been extended through the use of higher resolution spectra and the cross sections for the production of fluorescence have been measured.

II. Experimental

The experimental setup has been described in a previous paper [3]. The nominal wavelength of the emission lines used in this investigation were λ637, 689, 704, 716, 769, 790, and 801 Å. The bandwidth of the 1-m normal incidence monochromator used to isolate these lines was set at 10 Å or less. The bandwidth of the 0.3-m monochromator used to disperse the fluorescence was set at 15 Å or less.

The absolute source line intensities were measured with a nickel film photoelectric detector, and the fluorescence was detected with a cooled photomultiplier (EMI 9659BM) which is equipped with a glass window so that it responds in the wavelength region λλ3000-9000 Å. The response of the combination of the 0.3-m monochromator and the photomultiplier for wavelengths longer than λ3100 Å is essentially the same as that published in a previous paper [4].

OCS gas supplied by the Matheson Gas Company with a purity greater than 97.5% was used without further purification. The pressure inside the sample cell as monitored with a Baratron Capacitance Manometer and was limited to a maximum of 15 mtorr, below which the fluorescence intensity was linear with gas pressure.

III. Results and Discussion

A. Fluorescence Spectrum

The fluorescence spectrum produced by OCS photoabsorption of primary photons of wavelength $\lambda 801$ Å is shown in Figure 1. This spectrum was obtained with a bandwidth of 15 Å and has the characteristics of all spectra produced by other primary photon wavelengths. The bandhead positions of the $OCS^+[A^2\Pi_\Omega(000) \rightarrow X^2\Pi_\Omega(00v)$; $\Omega=\frac{1}{2}$ and $\frac{3}{2}$, v=0-4] emission bands given by Horani et al.,[5] are used to identify the strong emission bands and are indicated in the Figure. The bandhead positions for the v = 5 and 6 bands are calculated by using the data [5] that the average decrement of the vibrational quantum energy for each vibrational quantum is 45 cm^{-1}.

The weak bands distributed among the strong bands, which have also been observed by Horani et al., [5] are possibly in part attributable to the $A^2\Pi_\Omega(000) \rightarrow X^2\Pi_\Omega(v_1 0 v_3)$ emission bands, where v_1, v_3 = 1,2,.... Using the ν_1 value [6] of 650 cm^{-1} for the $OCS^+(X^2\Pi)$ state, the wave numbers and wavelengths for the various bandheads of the $OCS^+[A^2\Pi_\Omega(000) \rightarrow X^2\Pi_\Omega(v_1 0 v_3)]$ transition are calculated and listed in Table I. As indicated in the Figure several of the weak bands occur at the calculated positions of the $A^2\Pi_\Omega(000) \rightarrow X^2\Pi_\Omega(v_1 0 v_3)$ transitions.

B. Band Strengths

When the bandwidth of the 0.3-m monochromator was set at 8 Å the Ω components of each strong band shown in Figure 1 were completely separated. Therefore, the radiation rates, $\dot{n}$, for the components of various emission bands could be obtained and averaged over several spectra, are listed in Table II. The radiation rate is measured by the area under the spectral envelope and corrected by the detection response. The band strength, which is defined [7] as $P=Re^2q = k\,\dot{n}\,\lambda^3$, is also

calculated and given in Table II, where Re is the electronic transition moment and q is the Franck-Condon factor. The radiation rate for the $\Omega = \frac{3}{2}$ component and the band strengths for both the $\Omega = \frac{1}{2}$ and $\frac{3}{2}$ components of the $A^2\Pi_\Omega(000) \rightarrow X^2\Pi_\Omega(003)$ band are normalized to 1. The Franck-Condon factors previously published by Judge and Ogawa [2] were only estimated from their low resolution spectra and are somewhat different from the present values.

C. Production Cross Sections

At low gas pressure, P., the radiation rate is given [4] by

$$\dot{n} = K \sigma_f \, Io \, P \, F(\lambda_f)$$

where K is a constant, σ_f is the fluorescence production cross section, and Io is the primary photon flux and $F(\lambda_f)$ is the wavelength dependent response function of the detection system.

The production cross sections for the sum of the $OCS^+[A^2\Pi_\Omega(000) \rightarrow X^2\Pi_\Omega(00v)$; $\Omega = \frac{1}{2}$ and $\frac{3}{2}$, v = 2-5] bands are obtained from the measured fluorescence radiation rates, and calibrated against the known fluorescence cross section of the N_2^+ first negative system [8]. The results for the production cross sections are listed in Table III for the various primary photon wavelengths. The thresholds for the production of OCS^+ $[A^2\Pi_\Omega(000), \Omega = \frac{1}{2}$ and $\frac{3}{2}]$ ions are at λ821.14 and 822.26 Å, respectively. The total absorption cross sections, σ_T, given by Cook and Ogawa [1] are adopted to calculate the production yields, $\eta(= \sigma_f/\sigma_T)$, which are also listed in Table III. The cross sections are in units of Mb $(= 10^{-18}cm^2)$ and the yields are in %.

IV. Concluding Remarks

The photoelectron spectrum [6] of OCS^+ shows three well defined states, $A^2\Pi$, $B^2\Sigma^+$, and $C^2\Sigma^+$, which are very similar to CO_2^+. However, in contrast to CO_2^+ which emits fluorescence [3] from all excited vibrational levels of the $A^2\Pi_u$ state and the ground level of the $B^2\Sigma_u^+$ state, OCS^+ emits no fluorescence from levels higher than v = 0 of the $A^2\Pi$ state. Judge and Ogawa [2] have attributed the absence of fluorescence from the $V \geq 1$ levels of the $A^2\Pi$ state to predissociation. This assertion is further strengthened by the present observation that the cross section for production of fluorescence from the inverted $A^2\Pi_{1/2}$ (000) level is only 75% of that in the $A^2\Pi_{3/2}$(000) level. The relative fluorescence cross sections are measured by the sum of $\dot{n}\lambda$ [3] over all the bands listed in Table II.

The absence of fluorescence from the OCS^+($B^2\Sigma^+$ and $C^2\Sigma^+$) states indicates that these states are also predissociated.

Table I

The wave numbers, $\nu(cm^{-1})$, and the wavelengths, $\lambda(\mathring{A})$, for the various band heads of the $A^2\Pi_\Omega(000) \rightarrow X^2\Pi_\Omega(v_1 0 v_3)$ transitions.

Ω	v_1		v_3 = 0	1	2	3	4	5	6
$\frac{1}{2}$	0	ν	31154*	29091*	27066*	25088*	23158*	21269	19425
		λ	3208.9*	3436.5*	3693.6*	3984.9*	4317.0*	4700.3	5146.5
	1	ν	30504	28441	26416	24438	22508	20619	18775
		λ	3277.3	3515.0	3784.5	4091.0	4041.6	4848.5	5324.7
	2	ν	29854	27791	25766	23788	21858	19969	18125
		λ	3348.7	3597.2	3880.0	4202.6	4573.7	5006.3	5519.5
$\frac{3}{2}$	0	ν	31408*	29339*	27316*	25334*	23400*	21511	19667
		λ	3183.0*	3407.4*	3659.8*	3946.2*	4272.2*	4647.2	5083.2
	1	ν	30758	28689	26666	24684	22750	20861	19017
		λ	3250.2	3484.7	3749.0	4050.0	4394.3	4792.0	5257.0
	2	ν	30108	28039	26016	24034	22100	20211	18367
		λ	3320.1	3565.5	3842.7	4159.6	4521.5	4946.0	5443.0

*Adopted from the data given by Horani et al.

Table II

The radiation rates, $\dot{n}$, and the band strengths, P, for the various bands of the $A^2\Pi_\Omega(000) \rightarrow X^2\Pi_\Omega(00v_3)$ emission system. The band positions, λ, are in units of Å.

Ω \ v_3		2	3	4	5
$\frac{1}{2}$	λ(Å)	3693.6	3984.9	4317.0	4700
	$\dot{n}$	0.45	0.75	0.59	0.41
	P	0.48	1.00	0.99	0.89
$\frac{3}{2}$	λ(Å)	3659.8	3946.2	4272.2	4647.2
	$\dot{n}$	0.69	1.00	0.84	0.52
	P	0.55	1.00	1.07	0.82

Table III

Cross sections, σ(Mb), and the production yield, η(%), for fluorescence from the sum of the $OCS^{+}[A^{2}\Pi_{\Omega}(000) \rightarrow X^{2}\Pi_{\Omega}(00v_3)$; $\Omega = \frac{1}{2}$ and $\frac{3}{2}$, $v_3 = 2\text{-}5]$ bands. The total absorption cross sections, σ_T(Mb), for various primary photon wavelengths, $\lambda(\mathring{A})$, are adopted from the data given by Cook and Ogawa.

$\lambda(\mathring{A})$	σ_f(Mb)	σ_T(Mb)	η(%)
637	0.05	41.8	0.12
689	0.06	45.8	0.13
704	0.05	45.5	0.11
716	0.05	45.0	0.11
769	0.06	46.1	0.13
790	0.06	42.4	0.14
801	0.11	71.5	0.15

Figure Caption

Fig. 1. Fluorescence spectra of the $OCS^+[A^2\Pi_\Omega(000) \rightarrow X^2\Pi_\Omega(v_1 0 v_3)]$ system produced by primary photons of wavelength λ801 Å. The bandhead positions given in Table I are indicated.

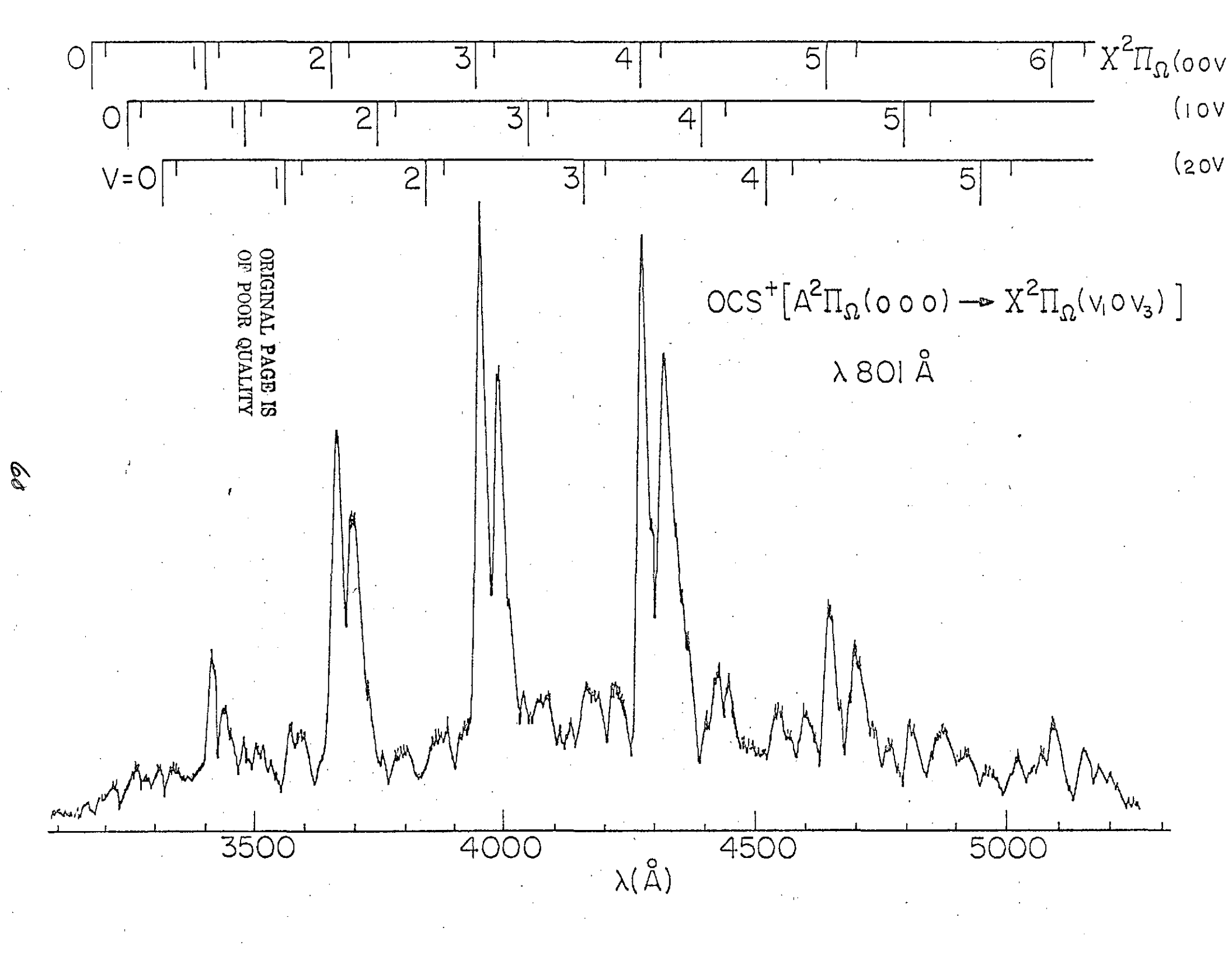
0 1 2 3 4 5 6 $X^2\Pi_\Omega$(00v
0 1 2 3 4 5 (10v
V=0 1 2 3 4 5 (20v
ORIGINAL PAGE IS
OF POOR QUALITY
$OCS^+[A^2\Pi_\Omega(0\,0\,0) \rightarrow X^2\Pi_\Omega(v_1\,0\,v_3)]$
λ 801 Å
3500
4000
4500
5000
λ(Å)

Acknowledgment

This work was supported by the National Aeronautics and Space Administration under Grant No. NGR 05-018-180.

REFERENCES

1 G. R. Cook and M. Ogawa, J. Chem. Phys., 51 (1969) 647.

2 D. L. Judge and M. Ogawa, J. Chem. Phys., 51 (1969) 2035.

3 D. L. Judge and L. C. Lee, J. Chem. Phys., 57 (1972) 455.

4 L. C. Lee and D. L. Judge, J. Chem. Phys., 57 (1972) 4443.

5 M. Horani, S. Leach, J. Rostas, and G. Berthier, J. Chem. Phys., 63 (1966) 1015.

6 C. R. Brundle and D. W. Turner, Int. J. Mass Spectrosc. Ion Phys., 2 (1969) 195.

7 R. W. Nicholls, J. Quant. Spectrosc. Radiat. Transfer, 2 (1962) 433.

8 D. L. Judge and G. L. Weissler, J. Chem. Phys., 48 (1968) 4590.

REEVALUATION OF THE $CO_2^+(X^2\Pi_g)$ BENDING QUANTUM

D. L. Judge and L. C. Lee
Department of Physics
University of Southern California
Los Angeles, California 90007

and

M. J. Haugh
Department of Chemistry
Temple University
Philadelphia, Pennsylvania 19122

The index classification of this paper is 5.442

ABSTRACT

With the assumption that the splitting of the $CO_2^+[X^2\Pi_g(100)(\frac{3}{2})]$ level is caused by perturbation of the $CO_2^+[X^2\Pi_g(020)(\frac{3}{2})\ G^+]$ level, the bending vibrational levels are calculated and the bending frequency, ω_2, is found to be 514.8 cm^{-1}. This value is comparable to the observed frequency of 513±10 cm^{-1} obtained from the $CO_2^+(A^2\Pi_u \rightarrow X^2\Pi_g)$ fluorescence spectra which are selectively produced by vacuum ultraviolet radiation.

I. Introduction

The bending quantum of the $CO_2^+(X^2\Pi_g(i))$ molecule has been previously measured by Judge et al. (1969). However, due to limited spectral resolution only an approximate value was given. Here its value has been remeasured using significantly higher resolution spectra.

The bending vibrational levels of $CO_2^+(X^2\Pi_g)$ are split by the spin-orbit and the vibronic interactions (Herzberg 1966). The lowest vibrational level splits into two sublevels and their terms are given by

$$G(0,1,\pm\tfrac{1}{2}) = \omega_2 \pm \tfrac{1}{2} A - \tfrac{1}{4}\varepsilon^2\omega_2 \qquad (1)$$

where $\pm\frac{1}{2}$ is the spin quantum number, ω_2 is the bending frequency, A is the spin-orbit interaction constant, and ε is the Renner parameter.

Each excited bending vibrational level is split into four sublevels and their terms are

$$G^+(v_2,1,\pm\tfrac{1}{2}) = \omega_2(1 - \tfrac{1}{8}\varepsilon^2)(v_2+1) + \tfrac{1}{2}A^*_{v_2,1} \mp \frac{\varepsilon^2 A\,\omega_2(v_2+1)}{8\,A^*_{v_2,1}} \qquad (2)$$

and, $$G^-(v_2,1,\pm\tfrac{1}{2}) = \omega_2(1 - \tfrac{1}{8}\varepsilon^2)(v_2+1) - \tfrac{1}{2}A^*_{v_2,1} \pm \frac{\varepsilon^2 A\,\omega_2(v_2+1)}{8\,A^*_{v_2,1}} \qquad (3)$$

where $A^*_{v_2,1} = \sqrt{A^2 + \varepsilon^2\omega_2^2\, v_2(v_2+2)}$

Mrozowski (1941, 1942, 1947a, and 1947b) has observed that the sublevel $\Omega = \frac{3}{2}$ of the $X^2\Pi_g(100)$ state is very strongly perturbed and splits into 1^a and 1^b sublevels. He suggested that the perturbation is probably caused by the $X^2\Pi_g(020)$ state. If we assume that the perturbing level is the $X^2\Pi_g(020)(\frac{3}{2})$ G^+ sublevel and its position is halfway between

the 1^a and 1^b levels, i.e., $G^+(2,1,+\frac{1}{2}) = 1264.6\ cm^{-1}$ measured from the $X^2\Pi_g(000)(3/2)$ level, then ω_2, calculated from equations (1) and (2) and the known values of $\epsilon\omega_2(= -93\ cm^{-1})$ and $A(= -159.5 cm^{-1})$(Herzberg 1966), is found to be $514.8\ cm^{-1}$. The Renner parameter is therefore $\epsilon = -0.18$. Using these ω_2 and ϵ values the positions of the bending vibrational levels are calculated as shown in Fig. 1.

II. Analysis

Fig. 2 shows the spectra obtained by photoionization of CO_2 at the primary photon wavelengths of λ715, 709, and 703 Å, of which the highest possible excited vibrational levels are $A^2\Pi_u(000)$, (100), and (200), respectively. The spectrum obtained by photon excitation at a wavelength of λ587 Å is shown in Fig. 3. The spectral bandwidth of the 0.3 m monochromator used to obtain these spectra was set at 4 Å or less.

As indicated in the spectra shown in Fig. 2 and 3, the emission bands of the $A^2\Pi_u(v_1 00)(\Omega) \rightarrow X^2\Pi_g(020)(\Omega)\ G^{\pm}$ transitions always accompany those of the $A^2\Pi_u(v_1 00)(\Omega) \rightarrow X^2\Pi_g(000)(\Omega)$ transitions. With the present spectra the wavelength for an emission band is determined within 3 Å (~30 cm^{-1}). However, checking with the previously published emission spectra (Smyth 1931; Fox et al., 1927) the positions of the emission bands are further confined and their wave numbers are determined within 10 cm^{-1}. The observed wave numbers for the various $A^2\Pi_u(v_1 00)(\Omega) \rightarrow X^2\Pi_g(020)(\Omega)\ G^{\pm}$ transitions are listed in Table 1. The calculated wave numbers, which are obtained from the known positions of the $A^2\Pi_u(v_1 00)$ levels (Mrozowski 1941, 1942, 1947a, 1947b) and the calculated energy levels shown in Fig. 1, are also listed in the table for comparison. The correctness of the assignment for the $A^2\Pi_u(v_1 00)(\Omega) \rightarrow X^2\Pi_g(020)(\Omega)\ G^-$ transitions is corroborated by

the fact that the vibrational energy of a $A^2\Pi_u(v_1 00)$ level obtained from its presently assigned transition to the $X^2\Pi_g(020)G^-$ level agrees with its transition to the $X^2\Pi_g(000)$ level assigned by Mrozowski (1941, 1942 and 1947a). The vibrational energies of the $A^2\Pi_u(v_1 00)$ levels obtained from their transitions to the different $X^2\Pi_g$ levels are listed in Table 2 for comparison.

The positions of the $X^2\Pi_g(020)(\frac{3}{2})$ and $(\frac{1}{2})$ G^- levels obtained from the observed emission bands listed in Table 1 and Table 2 are listed in Table 3. The average values for the positions of the $X^2\Pi_g(020)$ $(\frac{3}{2})$ and $(\frac{1}{2})$ G^- levels are 935 and 963 cm^{-1}, and in reasonable agreement with the calculated values 950.2 and 956.7 cm^{-1}, respectively.

From the spectrum produced by the primary photons of wavelength $\lambda 715$ Å the positions of the various $A^2\Pi_u(000)(\Omega) \rightarrow X^2\Pi_g(0v_2 0)(\Omega)$ $G^{\pm}$ emission bands are obtained and listed in Table 4. The position of the $A^2\Pi_u(000)(\frac{3}{2}) \rightarrow X^2\Pi_g(020)(\frac{3}{2})$ G^+ band is estimated from the 1^a and 1^b levels given by Mrozowski (1941 and 1942). The calculated positions of the expected emission bands are also listed in Table 4 for comparison. The positions of the bending vibrational levels obtained from these observed emission bands are comparable to the calculated levels and are shown in Fig.1, in which the positions of the $X^2\Pi_g(020)(\frac{3}{2})$ and $(\frac{1}{2})$ G^- levels are adopted from the average values listed in Table 3.

Since the quantity $\frac{1}{8}\varepsilon^2\omega_2$ is $\simeq 2$ cm^{-1} and within the experimental error, it may be neglected in the experimental determination of ω_2. The observed vibrational levels are plotted against the quantum number as shown in Fig. 4, in which the energy centroid of the sublevels is linear with quantum number. The observed bending frequency determined from such data is 513 ± 10 cm^{-1}.

Acknowledgment

The authors wish to thank professor Ogawa for his encouragement and comments on this analysis. This work was supported by the National Aeronautics and Space Administration under Grant No. NGR 05-018-180.

References

Fox, G.W., Duffendack, O.S., and Baker, E.F. 1927. Proc. Nat. Acad. 13, 302

Herzberg, G. (Editor), 1966. Electronic Spectra and Electronic Structure of Polyatomic Molecules (Van Nostrad Reinhold Co., N.Y.), pp. 36 and 594.

Judge, D.L., Bloom, G.S., and Morse, A.L. 1969 Can. J. Phys. 47, 489

Mrozowski, S. 1941 Phys. Rev. 61, 730

_____ 1942 Phys. Rev. 62, 270

_____ 1947a Phys. Rev. 72, 682

_____ 1947b Phys. Rev. 72, 691

Smyth, H.D. 1931 Phys. Rev. 38, 2000

. Table 1

Comparison between the calculated and the observed* wave numbers, ω_c and ω_o, for the $A^2\Pi_u(v_1 00)(\Omega) \rightarrow X^2\Pi_g(020)(\Omega)$ G^- transitions.

v_1 \ Ω	$\frac{1}{2}$			$\frac{3}{2}$		
	Wave Number (cm^{-1})			Wave Number (cm^{-1})		
	ω_c	ω_o	$\omega_c-\omega_o$	ω_c	ω_o	$\omega_c-\omega_o$
0	27671.3	27651	20	27582.3	27600	-18
1	28797.2	28802	-5	28709.1	28721	-12
2	29918.5	29911	8	29831.8	29844	-12
3	31034.1	31035	-1	30952	30972	-20

* Values are taken from Smyth (1931) and Fox et al. (1927)

Table 2

Comparison of the vibrational energies of the $A^2\Pi_u(v_1 00)(\Omega)$ levels obtained from their transitions to the $X^2\Pi_g(020)(\Omega)$ G^- level with their transitions to the $X^2\Pi_g(000)(\Omega)$ level.

V_1	Ω	$\omega_p^*(v_1)$ cm^{-1}	$\omega_o^*(v_1)$ cm^{-1}	Present $\omega_o(v_1) - \omega_o(0)$	Mrozowski $\omega(v_1)^{**} - \omega(0)$
0	$\frac{1}{2}$	27620±30	27651±10		
	$\frac{3}{2}$	27550	27600		
1	$\frac{1}{2}$	28790	28802	1151	1127
	$\frac{3}{2}$	28730	28721	1121	1126
2	$\frac{1}{2}$	29890	29911	2260	2250
	$\frac{3}{2}$	29820	29844	2244	2247
3	$\frac{1}{2}$	31050	31035	3384	3370
	$\frac{3}{2}$	30960	30972	3372	3372

* $\omega_p(v_1)$ and $\omega_o(v_1)$ are the wave numbers for the $A^2\Pi_u(v_1 00)(\Omega) \rightarrow X^2\Pi_g(020)(\Omega)$ G^- transition obtained from the present and Smyth's Spectra, respectively.

** $\omega(v_1)$ is the wave number for the $A^2\Pi_u(v_1 00)(\Omega) \rightarrow X^2\Pi_g(000)(\Omega)$ transition adopted from Mrozowski.

Table 3

The observed $X^2\Pi_g(020)(\Omega)$ G^- energy levels relative to the $X^2\Pi_g(000)(3/2)$ level. These levels are obtained from the observed wave numbers of the $A^2\Pi_u(v_1 00)(\Omega) \rightarrow X^2\Pi_g(020)(\Omega)$ G^- transitions listed in Table 1.

v_1 \ Ω	$\frac{1}{2}$	$\frac{3}{2}$
0	977±10 cm^{-1}	932±10 cm^{-1}
1	952	938
2	965	938
3	956	930
Aver-age	963	935

Table 4

Comparison between the calculated and the observed* wave numbers ω_c and ω_o, for the $A^2\Pi_u(000)(\Omega) \div X^2\Pi_g(0v_20)(\Omega)$ $G^{\pm}$ transitions.

v_1	Ω	$\frac{1}{2}$			$\frac{3}{2}$		
		Wave Number (cm^{-1})			Wave Number (cm^{-1})		
		ω_c	ω_o	$\omega_c-\omega_o$	ω_c	ω_o	$\omega_c-\omega_o$
2	G^+	27370.2	27390	-20	27268.2	27268.2	0
	G^-	27671.3	27651	20	27582.3	27600	-18
4	G^+	26257.5	26241	17	26155.0	26152	3
	G^-	26733.2	26718	15	26644.7	26661	-16

*Values are taken from Smyth (1931) and Fox et al. (1927)

FIGURE CAPTIONS

Fig. 1. The calculated and observed vibrational energies of the $CO_2^+[X^2\Pi_g(0v_20)(\Omega)]$ levels. The vibrational energies are relative to the $X^2\Pi_g(000)(\frac{3}{2})$ level and in units of cm^{-1}.

Fig. 2. The fluorescence spectra of the $CO_2^+(A^2\Pi_u \rightarrow X^2\Pi_g)$ system produced by primary photon wavelengths λ715, 709, and 703 Å. The positions of the $A^2\Pi_u(v_1'00) \rightarrow X^2\Pi_g(v_1''00)$ and $X^2\Pi_g(0v_2''0)$ G transitions are indicated.

Fig. 3. The fluorescence spectrum of the $CO_2^+(A^2\Pi_u \rightarrow X^2\Pi_g)$ system produced by primary photon wavelengths λ587 Å. The positions of the $A^2\Pi_u(300) \rightarrow X^2\Pi_g(v_1''00)$ and $X^2\Pi_g(020)$ transitions are indicated.

Fig. 4. The plot of the observed vibrational energies, $\omega(cm^{-1})$, versus the vibrational bending quanta, v_2, for the $X^2\Pi_g(0v_20)$ levels. A line through the energy centroid is drawn.

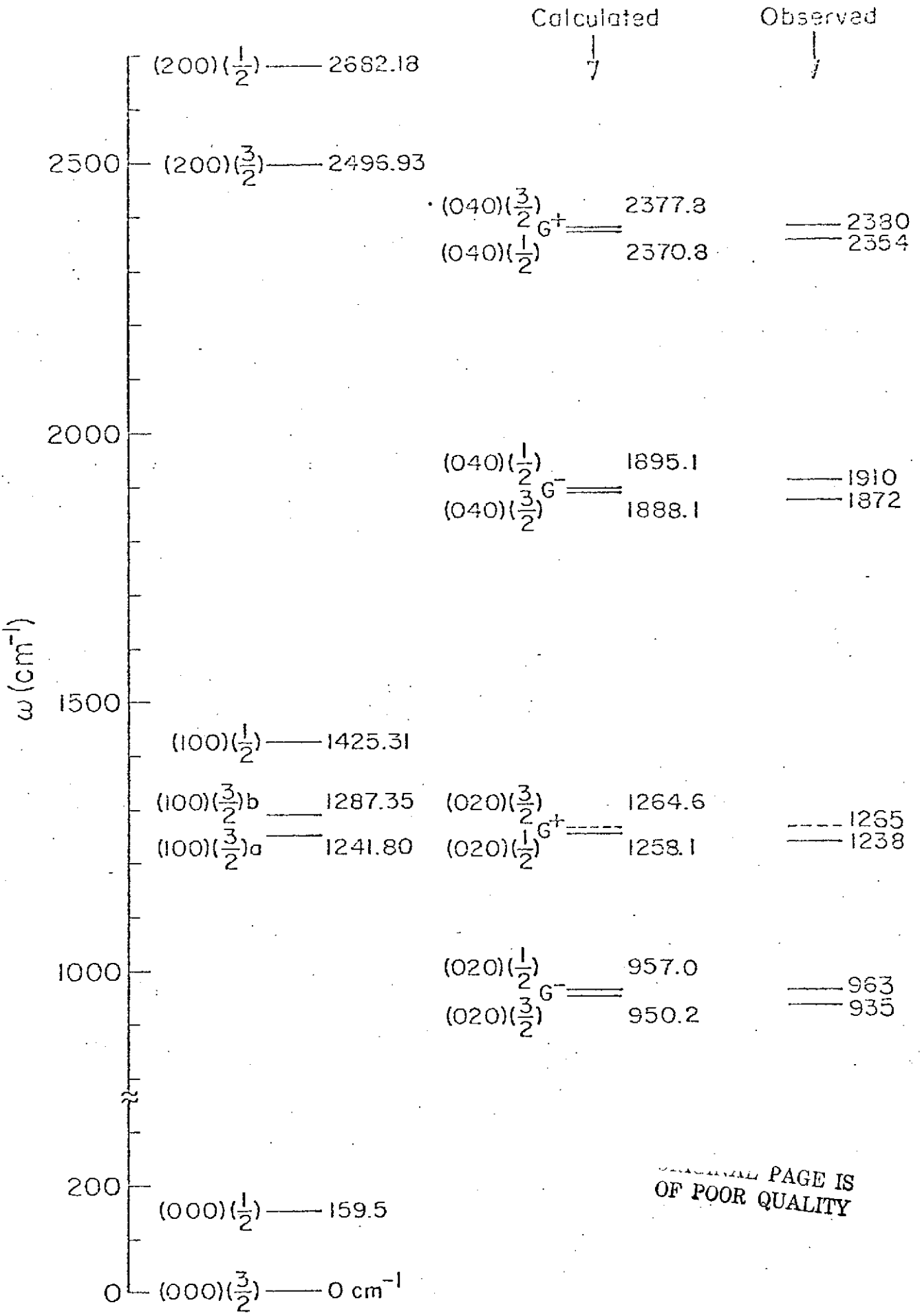

Figure 1

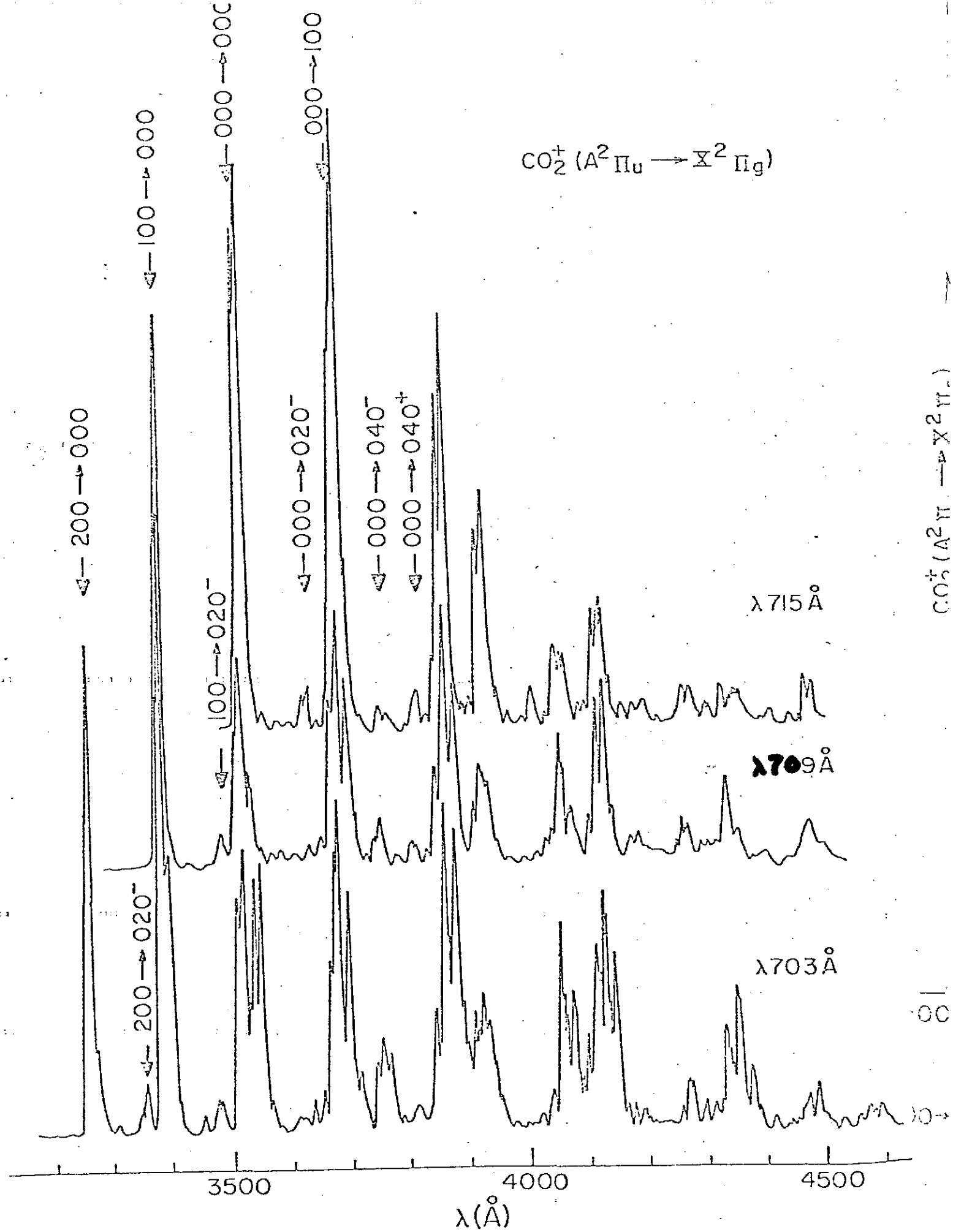
$CO_2^+ (A^2\Pi_u \rightarrow X^2\Pi_g)$
000 → 100
000 → 000
100 → 000
200 → 000
000 → 020⁻
100 → 020⁻
200 → 020⁻
000 → 040⁻
000 → 040⁺
λ715 Å
λ709 Å
λ703 Å
3500
4000
4500
λ(Å)

Figure 2

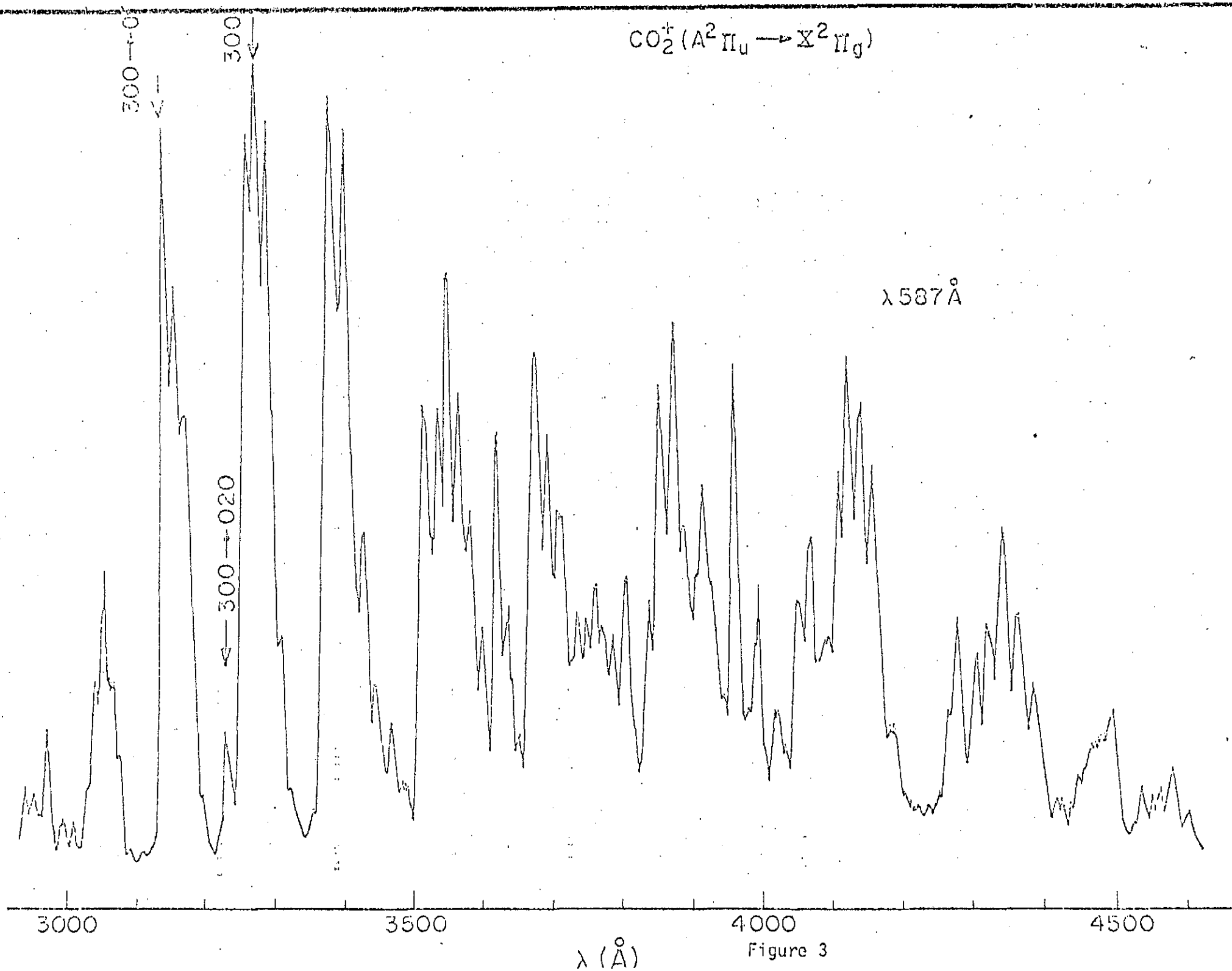
$CO_2^+(A^2\Pi_u \rightarrow X^2\Pi_g)$
λ587Å
300→0
300
300→020
3000
3500
4000
4500
λ (Å)

Figure 3

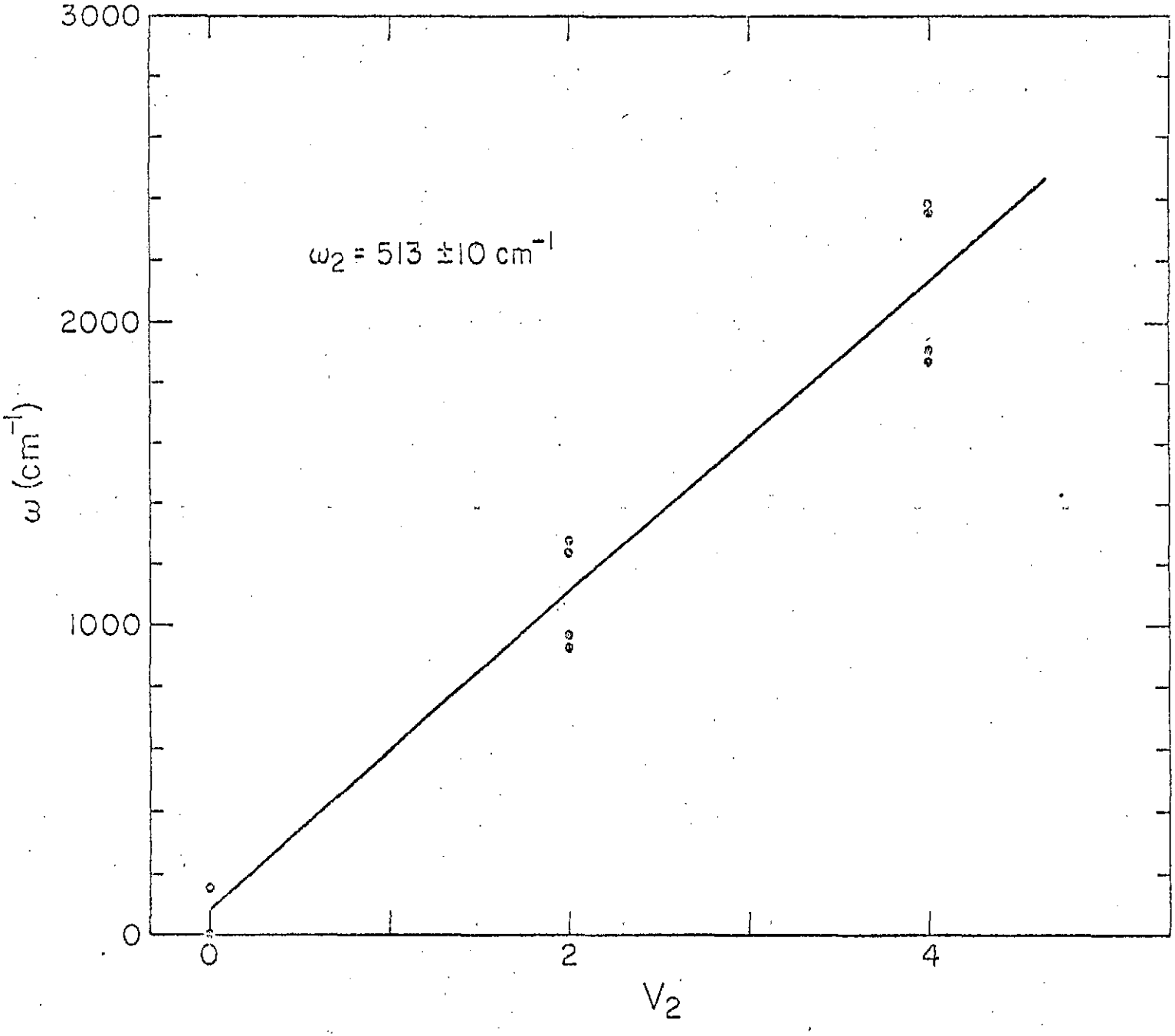

Figure 4

APPENDIX A

CONTINUATION PROPOSAL (April 26, 1972)

INTRODUCTION

The following proposal indicates the areas of work successfully pursued during the past funding period and suggests a logical extension of the past effort. Our work is concerned with the measurement of absolute photodissociation cross sections for the formation of specific products of the atmospheric gases and long term evaluation of channeltrons.

PHOTON IMPACT STUDIES OF MOLECULAR GASES

I. Measurements of the Absolute Cross Sections

The cross sections for the production of molecular fragments by XUV irradiation have been measured by observing the fluorescence radiation rates from those fragments. The experimental arrangement is shown in Fig. 1. The XUV light was produced by a spark discharge through a boron nitride capillary and dispersed with a 1-m normal incidence monochromator (McPherson 225). The fluorescence produced by the molecular fragments was dispersed with a 0.3-m normal incidence monochromator (McPherson 218) and detected synchronously with a cooled EMI 9558 QB photomultiplier. The absolute cross sections were determined by comparing the fluorescence radiation rates of the molecular fragments with that of $N_2^+(B\ ^2\Sigma_u^+)$. The absolute cross sections for the production of some excited fragments from CH_4, and CO_2 have been measured in this laboratory (see Appendix A and B). Using the same facilities and techniques, the absolute cross sections for the gases of interest in planetary atmospheres, such as NH_3, H_2O, NO, N_2O, NO_2, etc. will be measured during the next funding period.

II. The Population Distribution of Excited Vibrational Levels Produced by Photodissociation

The mechanism for the production of the CO Cameron bands through photodissociation of CO_2 has been studied in this laboratory during the past year. It is found that the dominant mechanism is as given below:

$$CO_2 + h\nu \rightarrow CO_2^*$$

$$\rightarrow CO(a'\,^3\Sigma^+,\ d\ ^3\Delta_i,\ e\ ^3\Sigma^-) + O(^3p)$$

$$\rightarrow CO(a\ ^3\Pi) + O(^3p) + h\nu'$$

The population distribution of the vibrational levels of $CO(a'^3\Sigma^+$ and $d\ ^3\Delta_i)$ has been found to be a Poisson distribution and agrees with the prediction of a quasidiatomic model, which is characterized only by the phase-average transfer energy during the separation period (see Appendix C). This model should, however, be tested in the photodissociation of other gases of atmospheric interest. In particular, it would be highly desirable to test the validity of the model by observing the photodissociation of other linear molecules, such as N_2O, NO_2 and CS_2. The fluorescence from the fragments of these molecules has been previously observed in photodissociation. The fragments formed are,

$$N_2O + h\nu \rightarrow N_2^* + O \rightarrow N_2 + O + h\nu'$$

$$NO_2 + h\nu \rightarrow NO^* + O \rightarrow NO + O + h\nu'$$

and

$$CS_2 + h\nu \rightarrow CS^* + S \rightarrow CS + S + h\nu'$$

The population distribution of the vibrational levels of these fragments can be measured by the same technique as used to study CO_2.

III. Constancy of the Transition Dipole Moments vs. Internuclear Distances for Molecular Transitions

The electronic transition dipole moment of a molecular transition can be calculated using the measured radiation rates and the relative Franck-Condon factors. Its variation with internuclear distance has been studied by several authors, but substantial errors are present in the many of the published papers. Using the line emission light source and the synchronous detection system, it is possible to produce accurate data, and accordingly to determine the transition dipole moments with

precision. The transition dipole moments of the A→X, B→X, and B→A systems of CO^+ have been investigated. In contrast to a previous result indicating that the transition dipole moment of the A→X system of CO^+ varies with the internuclear separation it is found that each system has a constant transition dipole moment (see Appendix D). Since the transition dipole moment is a principal factor in the determination of the band strength, its measurement is important for the investigation of airglow measurements in planetary atmospheres. The measurement of transition dipole moments will be extended to several transitions of N_2, NO, and CS, during the next funding period.

IV. Quenching

In the study of the pressure dependence of the fluorescence intensity, it is, in general, observed that the fluorescence intensities for the lower vibrational levels decrease slower than the higher levels as the pressure increases. This relative intensity enhancement for the lower vibrational levels is attributed to the vibrational relaxation of the higher levels into the lower ones. The vibrational relaxation time may be obtained from a quantitative study of the pressure dependence of the fluorescence intensity. On the other hand, the measurement of the vibrational relaxation times will aide in the determination of the pressure of the gases in planetary atmospheres. Further study of this subject is planned.

V. Resonance Scattering Experiments

Consider the problem of determining the absolute cross section for the following photon-molecule interaction;

$$CO_2(\tilde{X}\ ^1\Sigma_g^+) + h\nu \rightarrow CO(a\ ^3\Pi) + O(^3p)$$

Assuming the incident photon flux is known, cross sections can be experimentally determined if the abundance of $O(^3p)$ is known. The amount of $O(^3p)$ present can be determined through the technique of resonance scattering.

Previously, cross sections in this laboratory have been determined through fluorescence studies of excited fragments. For the above reaction this would be a poor method since the fluorescence results from the "forbidden" transition [$CO(a\ ^3\Pi) \rightarrow CO(X\ ^1\Sigma^+)$]. Thus many of the $CO(a\ ^3\Pi)$ states would be depopulated through collisions. To determine this loss, deactivation rates are required. This makes the experiment difficult to perform and increases the possibility of error. Lawrence[1] has, however, observed this fluorescence and obtained a value for the deactivation coefficient and for the cross section for the production of $CO(a\ ^3\Pi)$. Nonetheless, an independent measurement not subject to the same experimental difficulties would be highly desirable.

Furthermore, there are many reactions which only yield fragments in their ground state. Resonance scattering could be used to assign cross sections to these processes. The reverse experiment can also be performed; if the reaction cross section is known and the resonance scattering cross section unknown, then it can be found experimentally.

Realizing the abundance of information that can be gathered through such scattering experiments this laboratory has intiated a study of resonance scattering. The following describes this work.

A. Work in Progress

Succesful observation of resonance scattering in helium have been made in this laboratory. Using the 584Å line of He I, resonance scattering

has been observed at right angles to the incident 584Å radiation when helium was introduced into the sample cell. An rf discharge through helium was used to generate the 584Å line. The self-absorption of this line by the source itself, has been studied using a 3-meter spectrograph in 4th order. It was found that the center of the line showed total absorption having a 0.01Å width at 100μ pressure through a path length of 4 cm. The self-absorption by the source is expected to be much less for diatomic gases such as O_2. Since the dominant background gas will be O_2, rather than O from which the 1304 radiation is obtained. The direction of gas flow through the discharge tube can also be used to further reduce the absorption.

At the present time an experiment is being assembled to study reactions through resonance scattering. The first reaction to be studied is $CO_2 + h\nu \rightarrow CO(a\ ^3\Pi) + O(^3p)$. What follows is a description of the experiment and an outline of the equipment available.

A photomultiplier, 1/2-meter Seya-Namioka type monochromator, and a 0.3-meter McPherson 218 monochromator are all attached to a sample cell. The optic axes of the components are connected in such a manner as to be mutually orthogonal. Also attached to the cell and on the optic axis of the McPherson monochromator is a Wood's horn light trap. A schematic diagram of the apparatus is shown in Fig. 2.

The McPherson monochromator is used to isolate the 1302Å resonance line of OI generated in an rf discharge tube containing O_2. After passing through the cell this radiation is trapped by the light trap. Thus the only 1302Å radiation which can reach the detector must be resonantly scattered. The present detector will use sodium salicylate in conjunction with a photomultiplier with a

blue sensitive photocathode. For the future a photomultiplier with a potassium bromide photocathode is proposed.to cover the wavelength range from 1050-1600Å.

The CO_2 will be dissociated primarily by radiation exiting from the 1/2-meter Seya-Namioka type monochromator. This monochromator is being built at USC and is just nearing completion. It employs differential pumping slits, sine bar drive, fast pumping, 1/2 meter Rowland circle for increased light gathering power and a stainless steel vacuum chamber.

A condensed spark discharge light source will be mounted at the monochromator entrance slit. Since this source generates a line emission spectrum resolution is generally not sacrificed by using the 1/2-meter monochromator.

Platinum and sodium salicylate coated photomultiplier detectors will be used to monitor the resonance line intensity and the incident photon intensity. These detectors will be calibrated using an argon ionization cell.

The output from the resonance scattering detector will be processed by gated pulse counting electronics synchronized with the spark source in order to increase the signal to noise ratio.

B. Summary

It is proposed that the technique of resonance scattering be established as a useful method for detecting ground state fragments. To this end it is suggested that a study be made of the reaction $CO_2 + h\nu \rightarrow CO(a\ ^3\Pi) + O(^3P)$, through resonance scattering from the $O(^3P)$, to yield an absolute cross section for the formation of CO in the a $^3\Pi$ state.

Ideally the only radiation reaching the detector would be 1302Å resonant scattered radiation. However since the sodium salicylate coated photomultiplier has a wide spectral response it will be necessary to make a difference measurement between the signal output when the resonant light source is turned on and when it is off. Thus non-resonant radiation, namely fluorescence, can be discriminated against. This method is applicable if radiation does not result from fluorescence excited by the resonance line.

Any "contaminating" fluorescence will result primarily from the Cameron bands, $CO(a\ ^3\Pi \rightarrow X\ ^1\Sigma^+)$, and excited CO_2^*. Other energetically possible processes are $CO_2 + h\nu \rightarrow CO(X\ ^1\Sigma^+) + O(^1D)$ and $CO_2 + h\nu \rightarrow CO(X\ ^1\Sigma^+) + O(^1S)$, but it is extremely difficult to detect any radiation from these long lifetime metastable states.

For those cases where competing fluorescence is a great problem a third monochromator could be used to isolate the scattered radiation. An alternate choice, which is less effective but also less expensive, is to use a narrow spectral response detector, such as the proposed potassium bromide photocathode photomultiplier.

[1] G. M. Lawrence, to be published in J. Chem. Phys. April 1972.

CHANNELTRON EVALUATION

I. Bendix 4028 Lifetime Studies

The evaluation of Bendix 4028 Channeltron multipliers is continuing with primary emphasis on determining their lifetime. Five of these devices are presently being tested and have accumulated $\approx 3 \times 10^{11}$ counts. They are now accumulating counts at the rate of $\approx 36{,}000$ counts/sec. Periodically their gain and pulse height distribution is checked. To date no significant change in their characteristics has been observed after the initial "burn in" of $\approx 10^{9}$ counts. A sixth multiplier having an accumulated counts of 6×10^{11} counts is being transferred to the ion-pumped chamber containing the above referenced multipliers. Details of the channeltron characteristics will be included in the next progress report.

It is proposed that the lifetime evaluation be continued during the next funding period in order to provide further data on their expected behavior during multiyear missions such as those planned for the outer planets.

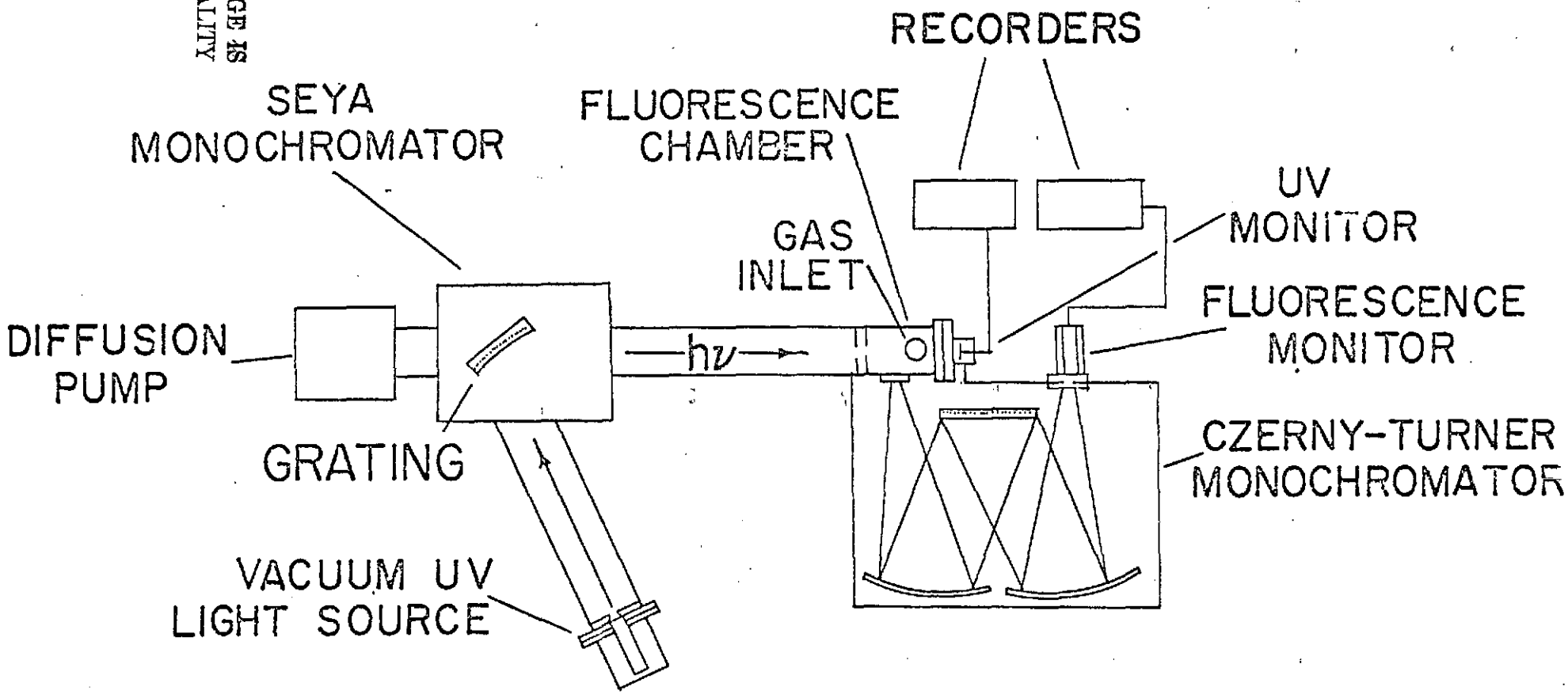

FIG. I. EXPERIMENTAL APPARATUS

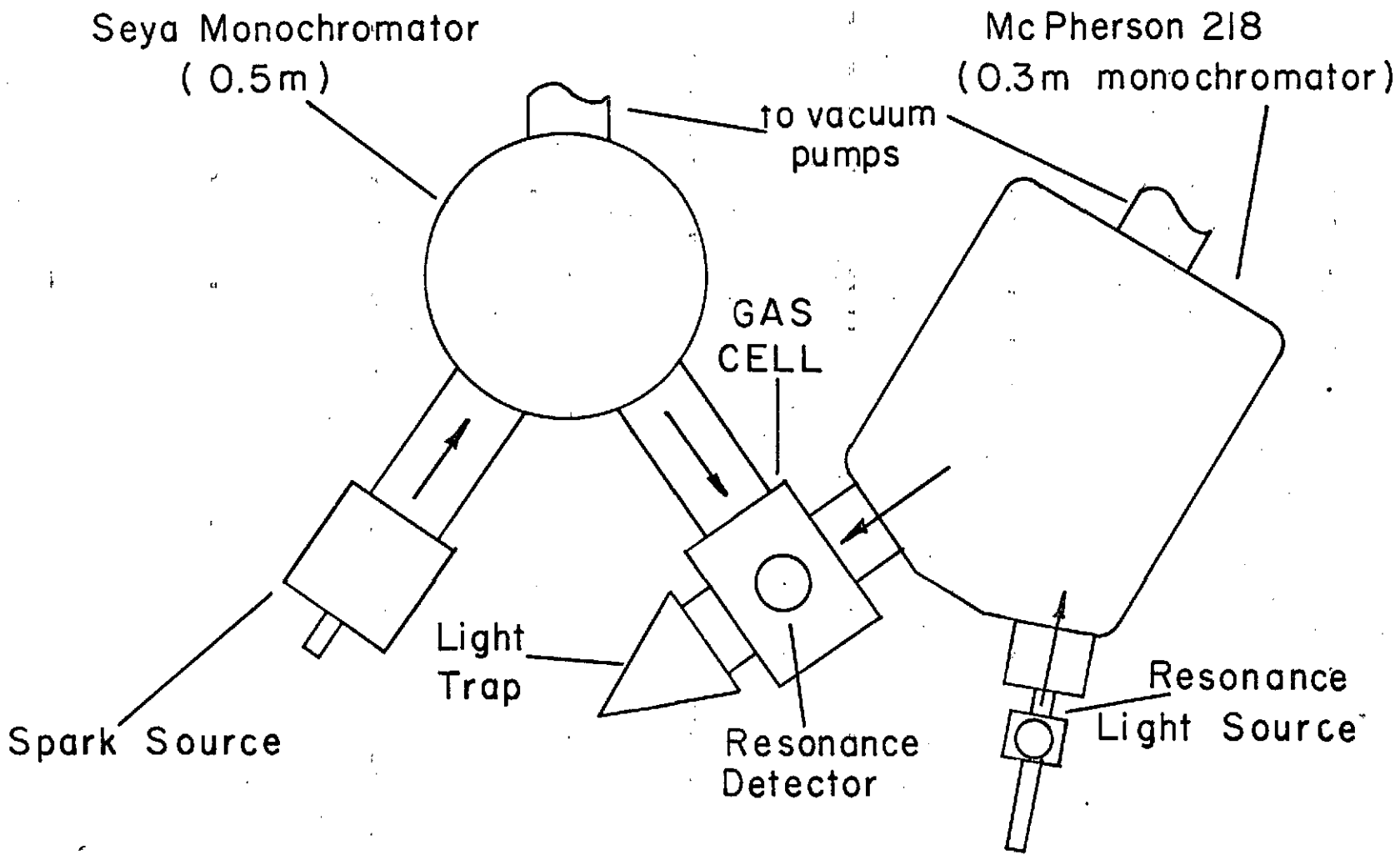

Fig. 2. Resonance Scattering Experimental Arrangement.

APPENDIX B

CONTINUATION PROPOSAL (July 10, 1973)

Abstract

The research proposed in the following sections represents a continuation of our laboratory investigations of processes of interest in planetary atmospheres. Primary emphasis will be placed on photodissociation processes leading to ground state or metastable fragments as outlined in Section I. Continuation of our evaluation of the long term characteristics of channeltrons is also proposed.

PHOTON-MOLECULE INTERACTION STUDIES OF THE ATMOSPHERIC GASES

I. DISSOCIATION CROSS SECTION MEASUREMENTS

INTRODUCTION

It is proposed to extend our preliminary investigation of gaseous photodissociation and photoionization processes which result in the formation of ground state and metastable atoms and molecules. Previous work in this laboratory has been involved primarily with the production of excited states in photon-molecule interactions. Such excitation processes were investigated by observation of the resulting fluorescence radiation. In the proposed extension these fluorescence emissions will be absent or weak owing to the long lifetime and deactivation of the metastable states. In this case detection of the ground state and metastable photo-fragments will be accomplished through resonance scattering. In addition to our own initial efforts such techniques have been used in the laboratory, for example, by Slanger and Black (1970) to detect ground state atomic oxygen and by Melton and Klemperer (1972) for NO detection. In the following paragraphs we discuss some of the specific processes to be investigated, considering O_2 as an example, followed by a brief discussion of the experimental aspects.

DISSOCIATION OF MOLECULAR OXYGEN

The absorption spectrum of oxygen exhibits the well known Schumann continuum in the 1400-1800Å region. This absorption is thought ot occur via excitation to the continuum of the $B^3\Sigma_u^-$ state followed by dissociation to produce $O(^3P) + O(^1D)$. Fluorescence of the $O(^1D)$ atoms produces the 6300Å multiplet. This feature is a strong component in the airglow spectrum and is attributed, in part, to photodissociative excitation by the solar ultraviolet. In recent years, however, concern has been

expressed that other states which could produce two $O(^3P)$ atoms rather than the $O(^3P) + O(^1D)$ products may be involved in the Schumann continuum. If such processes do occur, the quantum yield of $O(^1D)$ could be significantly different than previous assumptions would give. Laboratory information concerning the relative yields of $O(^3P)$ and $O^1D)$ are necessary for comparison with airglow measurements and the importance of photodissociation relative to other excitation mechanisms.

A somewhat similar situation is found for the OI λ5577Å line arising from $O(^1S)$. Recent airglow measurements (for example, Schaeffer et al., 1972) have suggested that a photodissociative excitation mechanism is important for $O(^1S)$ in addition to $O(^1D)$. This mechanism was discussed almost twenty years ago by Bates and Dalgarno (1954) who found that a lack of basic laboratory data prevents any reliable estimate of the contribution to the green airglow line due to photodissociation. This situation continues to be true, although the photodissociative excitation of $O(^1S)$ has been verified in observing 5577Å fluorescence produced by the ultraviolet flash photolysis of O_2 (Filseth and Welge, 1969). Tanaka (1952) has examined the absorption spectrum of O_2 and found minor peaks, one of which at 1293Å he suggests results in the formation of $O(^1S)$. At present, however, the cross section and states involved must be considered unknown.

At shorter wavelengths, oxygen still undergoes photodissociation. The total photodissociation cross section below ~ 1000Å has been obtained by Matsunaga and Watanabe (1967) and Cook et al. (1972). Certain of these continua have been identified but a complete description of the underlying processes has not yet been determined.

At shorter wavelengths the process of dissociative ionization can produce atoms (and atomic ions) in ground or excited states. Recent measurements indicate a rather high efficiency for this process not only for oxygen but other molecules also. Detection of the resulting photofragments and determination of the cross sections may be accomplished by resonance scattering.

EXPERIMENTAL ASPECTS

Measurements of the production of ground state and metastable atoms can be obtained through resonance scattering with the following basic experimental elements: a pulsed ultraviolet source to photodissociate the molecules in the experimental chamber, a source of resonance line photons, and a detector of the resonantly scattered radiation. Proper interpretation of the detected scattered radiation requires that several precautions be taken. First, if one is detecting ground state atoms (for example) one should insure that these atoms are created in the photodissociation process and not through secondary reactions. Some of these secondary processes of concern are the deactivation of metastable atoms produced in photodissociation, ground state atoms resulting from the radiative decay of excited photodissociation products, and atomic fragments arising from dissociative recombination and photoelectron excitation.

In order to estimate the relative contributions of these processes it is useful to envision a typical experiment. With sample gas partial pressures of 10 - 100 μ the absorption coefficient of the dissociating ultraviolet will be approximately 10^{-2} to 10^{-1} cm^{-1}. The mean free path at these total pressures is $\sim$ 0.05 to 0.5 cm with collision times of $\sim$

1 - 10 μ sec. Thus, the time to diffuse 1 cm is ~ 40 μ sec at 10 μ total pressure and 400 μ sec at 100 μ. If a buffer gas, for example a rare gas, is added, the diffusion time will vary approximately as the pressure. A 1 torr buffer gas will then increase the diffusion time to a few msec.

The light sources employed frequently in this laboratory are condensed spark discharges operated at pulse rates of ~ 50 Hz, each pulse lasting for times of a few μ sec. Typical line fluxes measured at the exit slit are ~ 2×10^8 photons/pulse, corresponding to an instantaneous rate of ~ 10^{14} photons/sec. Thus, with 1 percent absorption per cm each pulse produces ~ 10^{12} absorptions cm^{-1} sec^{-1}. While several other sources might be used for such work, data quality and subsequent interpretation are significantly enhanced by using a pulsed source having high instantaneous flux levels.

We can now estimate the order of magnitude contributions of the secondary processes. For dissociative recombination, each pulse will contribute $kn_+n_-\tau$ recombinations where k is the recombination coefficient, n_+, n_- are the ion and electron densities and τ is the diffusion time. The electrons will, of course, diffuse much faster than the ions, but we use here the ion diffusion time as a generous upper limit. In doing so, we find the rate of dissociative recombination is of order 1 - 10 per pulse and is much less than expected photodissociative processes. If one is working at wavelengths greater than the ionization potential, there will be no dissociative recombination contribution.

The photoelectron excitation rate can be estimated by assuming a cross section of 10^{-17} cm^2, a reasonably optimistic value considering

the low photoelectron energies that will be encountered. The probability of excitation is then approximately 3% of the primary absorption rate. If the photodissociation cross section is only a small fraction of the total absorption cross section, and if the electron dissociation cross section is as large as estimated, then this secondary process may be of concern. Pressure dependence measurements will be of value in experimentally evaluating the effect. Of course, at the longer wavelengths, there will be an absence of photoelectrons with sufficient energy for subsequent dissociative reactions and the effect can be neglected.

The production of ground state and metastable atoms from the radiative decay of excited photodissociation products will occur at the radiative transition rate, typically a few n-sec, and will be proportional to the photodissociative excitation rate. Since this time is much shorter than the primary light source pulses, no experimental discrimination of these products can be employed. Fortunately, these cross sections can be measured by observation of the resulting fluorescence giving a means of determining the cross section for the direct production of ground and metastable state atoms.

Deactivating collisions will destroy the metastable atoms and increase the concentration of ground state atoms over that produced directly in the photodissociation process. Consequently, measurement of either metastable or ground state atoms by resonance scattering must take this process into account for proper interpretation of the results. The time scale for this process can be estimated using measured deactivation coefficients. For the $O(^1D)$ state deactivated by O_2, $k \cong 5 \times 10^{-11}$ cm^3/sec

and at 100 μ partial pressure of O_2, $\tau \sim 7$ μ sec. For $O(^1S)$ the rate is approximately two orders of magnitude less, giving a mean life for $O(^1S)$ atoms of ~ 1 msec. Working at lower O_2 partial pressures will increase the lifetime against deactivation in proportion (if the buffer gas doesn't also participate), at the same time decreasing the primary rate of excitation.

These considerations suggest the experimental arrangement to be employed in further experiments. A pulsed spark source and vacuum spectrometer will be used to provide the initial photodissociation. Synchronously with this primary excitation, a condensed discharge lamp will be fired which will provide the necessary resonance line, e.g. λ 1302, 4, 6 Å radiation for detection of $O(^3P)$, λ 1152 Å for $O(^1D)$, and λ 1217 Å for $O(^1S)$. The sample time of the scattered resonance line should be a few μ sec for $O(^1D)$, $O^3P)$ and can be greater for $O(^1S)$. The deactivation coefficient and the relative contribution of these processes can be studied by varying the time delay between the primary light flash and the resonance scattering emission sampling time. In these experiments the resonance emission light source should directly illuminate the absorption cell and a solar blind photomultiplier directly view the resonantly scattered radiation. Either filters or a high throughput monochromator can be used to isolate the emission of interest.

II. CROSS SECTIONS FOR THE PRODUCTION OF FLUORESCENCE

Cross sections for production of fluorescence from $CO^+(A^2\Pi_i, B^2\Sigma^+ \rightarrow X^2\Sigma^+)$, $CO_2^+(A^2\Pi_u, B^2\Sigma_u^+ X^2\Pi g)$, and $N_2O^+(A^2\Sigma^+ \rightarrow X^2\Pi)$ (see appendices A, B, C) and from fragments of CH_4 and CO_2 (see appendices D and E) have been observed in the wavelength region from 462-1250Å. Using similar techniques the fluorescence production cross sections for these gases and others of interest in planetary atmospheres (O_2, N_2, NO, COS, H_2O, H_2S etc.) will be measured during the next funding period. Particular consideration will be given to resolving an existing problem concerning the production of the $CO_2^+(A, B \rightarrow X)$ fluorescence. Photoelectron spectroscopy results give, at 584Å, a production cross section for A/B = 0.65 while the fluorescence data imply A/B = 2.7. At present there is no satisfactory theoretical explanation for such a result. A possible source of the discrepancy is a systematic error introduced by the experimental arrangement. It is accordingly desirable to repeat the photoelectron data at 584Å using a 4π geometry in order to be sure that all photoelectrons are properly analyzed.

In addition to the work cited in the appendices, the fluorescence from the fragments of N_2 and NO by photodissociation of N_2O have been observed in this laboratory. However, an improvement of the present detection system is required to enhance the signal to noise ratio.

The relative fluorescence cross sections for the fragments of N, O and CO by photodissociation of N_2, O_2 and CO_2 have been observed using synchrotron radiation of 175-800Å (for example, see appendix F). Absolute measurement of the fluorescence cross sections using a strong line emission source in this laboratory will permit an absolute calibration of these relative measurements. It is accordingly proposed that the absolute cross section measurements be continued.

III. MEASUREMENTS OF THE POPULATION DISTRIBUTION OF EXCITED VIBRATIONAL LEVELS PRODUCED BY PHOTODISSOCIATION

The population distribution of triplet vibrational levels of CO produced by photodissociation of CO_2 has been measured in the previous funding period (see appendix G). The population is reasonably represented by a Poisson distribution and an internal collision mechanism was suggested to interpret the photodissociation process. For further study of this mechanism the vibrational populations of the CO, N_2, NO and CS fragments produced by the following photodissociation processes will be measured:

$$CO_2 + h\nu \rightarrow CO\ (A^1\Pi) + O$$

$$N_2O + h\nu \rightarrow N_2\ (B^2\Pi_g,\ C^3\Pi_u) + O$$

$$N_2O + h\nu \rightarrow NO\ (A^2\Sigma^+,\ B^2\Pi) + N$$

$$COS + h\nu \rightarrow CO\ (A^1\Pi,\ \text{triplet}) + S$$

$$COS + h\nu \rightarrow CS\ (A^1\Pi) + O$$

$$CS_2 + h\nu \rightarrow CS\ (A^1\Pi) + S$$

Although the production cross sections for some of these fragments are small, fluorescence from the excited fragments is observable and the vibrational populations should be measureable. As an example of the application of such data it should be noted that the mechanism for the production of the vibrational population of CO ($A^1\Pi$) as measured by the Mariner 6 and 7 UV spectrometer* has not yet been clarified. Photodissociation of CO_2 by solar radiation at $\lambda<1000$Å is thought to be the dominant mechanism. Measurement of the vibrational population produced by photodissociation is indeed required to help clarify the observed processes.

*C. A. Barth, C. W. Hord, J. B. Pearce, K. K. Kelly, C. P. Anderson and A. I. Stewart, J. Geophys. Res. 76, 2213 (1971).

IV. MEASUREMENT OF ELECTRONIC TRANSITION MOMENTS

The electronic transition dipole moments for the CO^+ ($A^2\Pi_i$, $B^2\Sigma^+ \rightarrow X^2\Sigma^+$), N_2^+ ($B^2\Sigma_u^+ \rightarrow X^2\Sigma_g^+$), and CO_2^+ ($A^2\Pi_u \rightarrow X^2\Pi_g$) systems have been measured in the previous funding period (see appendix A, H, I). For the diatomic systems the transition dipole moment was found constant but for the CO_2^+ system it fluctuated drastically. The transition dipole moment is a principal factor in the determination of band strengths and its measurement is important to the investigation of emission bands in planetary atmospheres. Transition dipole moments for the CO ($A^1\Pi \rightarrow X^1\Sigma$), N_2 ($B^3\Pi_g \rightarrow A^3\Sigma_u^+$), N_2 ($C^3\Pi_u \rightarrow B^3\Pi_g$), and CS ($A^1\Pi \rightarrow X^1\Sigma$) systems will be measured during the next funding period.

Franck-Condon factors for transitions in linear triatomic molecules are quite limited. Measurements of the band strengths for these transitions will hopefully stimulate reliable calculations of the Franck-Condon factors of interest.

V. STUDY OF THE PRESSURE DEPENDENCE OF THE FLUORESCENCE INTENSITY

The pressure dependence of the CO_2^+ ($B^2\Sigma_u^+ \rightarrow X^2\Pi_g$) and CO_2^+ ($A^2\Pi_u \rightarrow X^2\Pi_g$) fluorescence was measured during the previous funding period, and the two systems were found to yield similar results. No collisional "dumping" from CO_2^+ ($B^2\Sigma_u^+$) to the CO_2^+ ($A^2\Pi$) states was observed.

To simplify the analysis of the pressure dependence data, a uniform gas pressure inside the gas cell is required. Accordingly, an aluminum thin film was used to separate the gas cell from the main chamber of our normal incidence monochromator McPherson 225. However, the resulting reduction of the light incident on the gas cell to only 5% of the windowless intensity resulted in an unacceptably low fluorescence intensity for the individual bands. A revision of the present detection system to a more sensitive photon counting system is planned, and will be pursued during the next funding period. Measurement of the pressure dependence of the fluorescence intensity for planetary gases may aid in a determination of the pressure of such gases in planetary atmospheres.

VI. IDENTIFICATION OF UNCLASSIFIED MOLECULAR BANDS

Identification of vibrational bands of the N_2O^+ [$A^2\Sigma^+(0,0,0) \rightarrow X^2\Pi(n_1,n_2,n_3)$] system has been a part of our work during the previous funding period (see appendix J). The conventional methods (gaseous discharges) for exciting the gas whose spectrum is to be analyzed invariably yield numerous emission bands and atomic lines from the molecules and their fragments. In the present work a monochromatic photon beam is used to produce photoionization excitation and accordingly a relatively simple spectrum results, permitting unambiguous analysis. A determination of the vibrational bandhead positions is not proposed as a primary effort; it is a natural extension of our other work.

REFERENCES

Bates, D. R. and A. Dalgarno, J. Atm. Terr. Phys. 5, 329 (1954).

Cook, G. R. and P. H. Metzger, J. Opt. Soc. Amer. 54, 968 (1964).

Filseth, S. V. and K. H. Welge, J. Chem Phys. 51, 839 (1969).

Matsunaga, F. M. and K. Watanebe, Sci. Light 16, 37 (1967).

Melton, L. A. and W. Klemperer, Planet. Space Sci. 20, 157 (1972).

Schaeffer, R. C., P. D. Feldman, and E. C. Zipf, J. Geophys. Res. 77, 6828 (1972).

Slanger, J. G. and G. Black, J. Chem. Phys. 54, 1889 (1971)

Tanaka, Y., J. Chem. Phys. 20, 1728 (1952).

File with N75-21091

75-18041

N75-21091

REPORT NO. 6 AND 7

Section VII - X

J. Phys. B: Atom. Molec. Phys., Vol. 6, May 1973. Printed in Great Britain.

LETTER TO THE EDITOR

The electronic transition moment of the N_2^+ ($B\,^2\Sigma_u^+ \rightarrow X\,^2\Sigma_g^+$) system

L C Lee and D L Judge

Department of Physics, University of Southern California, University Park, Los Angeles, California, 90007

MS received 2 April 1973

Abstract. The $N_2^+(B\,^2\Sigma_u^+)$ ions were produced through vacuum ultraviolet irradiation at λ462, 555, 630 and 637 Å and the intensities of the $N_2^+(B\,^2\Sigma_u^+ \rightarrow X\,^2\Sigma_g^+)$ bands were measured. The electronic transition moment of the system was found to be reasonably constant.

The intensities of the $N_2^+(B\,^2\Sigma_u^+ \rightarrow X\,^2\Sigma_g^+)$ bans produced in discharge tubes, have been measured by Wallace and Nicholls (1955). Using the Franck–Condon factors given by Jarmain *et al* (1953), Nicholls (1962) found the electronic transition moment of the N_2^+ first negative system to be given by

$$R_e(r) = \text{const.} \times (10{\cdot}134\,r^2 - 23{\cdot}497\,r + 14{\cdot}473)$$

for $0{\cdot}974 < r < 1{\cdot}265$ Å. Brown and Landshoff (1971) remeasured the relative intensities of the (1,3) and (1,2) bands and applied the new Franck–Condon factors and r-centroids given by Generosa *et al* (1971) to rescale the equation to

$$R_e(r) = \frac{\text{const.}}{(r - 0{\cdot}72)^{1/2}}.$$

However, such a variation of the electronic transition moment was not found in the present work. The transition moment was found approximately constant for $0{\cdot}974 < r < 1{\cdot}153$ Å.

The present experimental arrangement has been described in a previous paper (Judge and Lee 1972). The vacuum ultraviolet source lines used to produce the $N_2^+(B\,^2\Sigma_u^+)$ ions were λ462, 555, 630 and 637 Å. The gas pressure in the absorption cell was set at 10 mTorr or less. The fluorescence spectrum, shown in figure 1, was produced by incident photons of wavelength 637 Å, and was typical of the spectra obtained with other source lines. The upper trace is an amplified spectrum showing the weak bands. The bandhead positions of the $N_2^+(B\,^2\Sigma_u^+ \rightarrow X\,^2\Sigma_g^+)$ system given by Pearse and Gaydon (1963) are indicated in figure 1 to identify the observed bands.

The fluorescence radiation rate, $\dot{n}_{v'v''}$, which was measured by the area under the spectral envelope of a band divided by the detection response published in a previous paper (Lee and Judge 1972), may be written (Wallace and Nicholls 1955, Judge and Lee 1972) as

$$\dot{n}_{v'v''} = kN_{v'}R_e^2(\bar{r}_{v'v''})q_{v'v''}/\lambda_{v'v''}^3$$

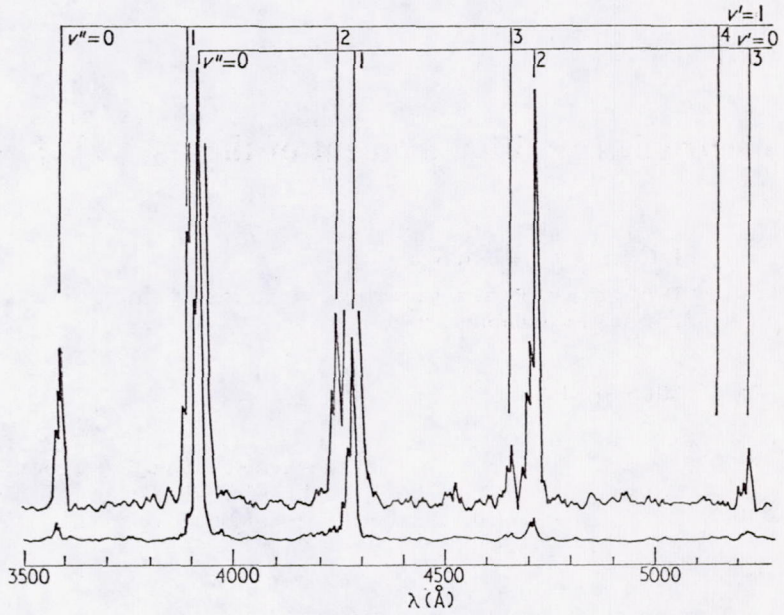

Figure 1. Dispersed flourescence of the $N_2^+(B\,^2\Sigma_u^+ \rightarrow X\,^2\Sigma_g^+)$ system produced by incident photons of λ637 Å. The bandhead positions given by Pearse and Gaydon are indicated.

where k is a constant, $N_{v'}$ is the population of the $N_2^+(B\,^2\Sigma_u^+)$ ions in the v' level, $R_e(\bar{r}_{v'v''})$, $\bar{r}_{v'v''}$, $q_{v'v''}$, and $\lambda_{v'v''}$ are respectively the electronic transition moment, r-centroid, Franck–Condon factor, and wavelength of the (v', v'') band. If the Franck–Condon factors and r-centroids given by Generosa *et al* (1971), which are not significantly different from those given by Nicholls (1961) for the lower vibrational levels, are adopted, the relative electronic transition moments can be calculated and plotted

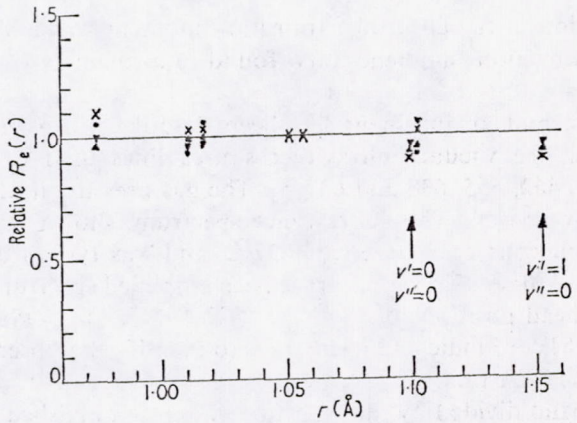

Figure 2. A plot of the relative electronic transition moment $R_e(r)$ against r for the vibrational bands of the $N_2^+(B\,^2\Sigma_u^+ \rightarrow X\,^2\Sigma_g^+)$ system. The data indicated by ▼, ▲, ×, and ● were, respectively, obtained using incident photons of λ462, 555, 630, and 637 Å.

as shown in figure 2. The transition moments for the (0,1) and (1,2) bands are normalized to 1. As shown in figure 2, the deviation of $R_e(r)$ from a constant is not significantly different from the experimental uncertainty which was estimated to be within 10% of the given values. The constancy of $R_e(r)$ was also indicated by Koppe *et al* (1971) in the measurement of the effective cross sections of the N_2^+ first negative bands. Since R_e is approximately constant, the absolute value of the electronic transition moment, $R_e = 0{\cdot}75$ au, given by Hesser (1968) is meaningful.

The band strengths, $p_{v'v''} = R_e^2(\bar{r}_{v'v''})q_{v'v''}$, averaged over all the observed spectra are shown in table 1. The sum, $\Sigma_{v''} p_{v'v''}$, is normalized to 1 for each upper v'. The data given by Nicholls (1962) are also shown in table 1 for comparison.

Table 1. Band Strength of the $N_2^+(B\,^2\Sigma_u^+,\ v' = 0, 1 \rightarrow X\,^2\Sigma_g^+,\ v'' = 0, 1, 2, 3)$ transitions.

v' \ v''		0	1	2	3
0	a	0·62	0·29	0·07	0·02
	b	0·54	0·23	0·07	0·02
1	a	0·27	0·26	0·32	0·15
	b	0·21	0·27	0·26	0·26

a. Present work.
b. Nicholls (1962).

This work was supported by NASA Grant No. NGR 05-018-180.

References

Brown W A and Landshoff R K 1971 *J. Quant. Spectrosc. Radiat. Transfer* **11** 1143–5
Generosa J I, Harris R A and Sullo L A 1971 *Air Force Wes. Lab. Tech. Rept. No.* AFWL-TR-70-108
Hesser J E 1968 *J. chem. Phys.* **48** 2518–35
Jarmain W R, Fraser P A and Nicholls R W 1953 *Astrophys. J.* **118** 228–33
Judge D L and Lee L C 1972 *J. chem. Phys.* **57** 455–61
Koppe V T *et al* 1971 *Soviet Phys.–JETP* **32** 1016–8
Lee L C and Judge D L 1972 *J. chem. Phys.* **57** 4443–5
Nicholls R W 1961 *J. Res. Natn. Bur. Stand.* **65A** 451–60
——1962 *J. atmos. terr. Phys.* **24** 749
Pearse R W B and Gaydon A G 1963, *The Identification of Molecular Spectra* 3rd edn (New York: John Wiley) p 219
Wallace L V and Nicholls R W 1955 *J. atmos. terr. Phys.* **1** 101–5

J. Phys. B: Atom. Molec. Phys., Vol. 6, October 1973. Printed in Great Britain.

Band strengths for the $CO_2^+(A\ ^2\Pi_u \rightarrow X\ ^2\Pi_g)$ system produced through photoionization excitation of CO_2

D L Judge and L C Lee

Department of Physics, University of Southern California, University Park, Los Angeles, California 90007

Received 2 April 1973

Abstract. The CO_2^+ ions in the various vibrational levels of the $A\ ^2\Pi_u$ electronic state were selectively produced by vacuum ultraviolet radiation of λ703, 709, and 715 Å. The emission band strengths of the $CO_2^+(A\ ^2\Pi_u \rightarrow X\ ^2\Pi_g)$ system were obtained and compared with other previous results established by different excitation methods. Good agreement with the earlier work was found. Using existing Franck–Condon factors, the electronic transition moments for the $CO_2^+(A\ ^2\Pi_u \rightarrow X\ ^2\Pi_g)$ bands are also presented.

1. Introduction

The individual emission band strengths of the $CO_2^+(A\ ^2\Pi_u \rightarrow X\ ^2\Pi_g)$ system have been investigated by using various excitation methods: McCallum and Nicholls (1972) by a CO_2 discharge in a hollow cathode, Wauchop and Broida (1972) by the interaction of CO_2 with He($2\ ^3S$), Ajello (1971) by electron impact, and Poulizac and Dufay (1967) by proton impact. The $CO_2^+(A\ ^2\Pi_u \rightarrow X\ ^2\Pi_g)$ fluorescence has also been studied by Judge *et al* (1969), Wauchop and Broida (1971), and Lee and Judge (1972) using photon impact. But, in this case, the emission intensities for individual bands were not analysed. Since the $CO_2^+(A\ ^2\Pi_u \rightarrow X\ ^2\Pi_g)$ radiation observed in the dayglow of Mars (Barth *et al* 1969, 1971) is predominantly produced by the interaction of solar radiation with the Martian atmosphere (Stewart 1972), and direct photoionization of CO_2 is the most important mechanism (Dalgarno *et al* 1970, Dalgarno and Degges 1971), measurement of the individual emission band intensities produced by photon impact seemed desirable.

2. Experimental

The details of the experimental setup have been described in a previous paper (Judge and Lee 1972). The source lines used in the present study were λ703, 709 and 715 Å, and were isolated with a 1 m normal incidence monochromator (McPh 225) set at a bandwidth of 2·5 Å. A 0·3 m normal incidence monochromator (McPh 218) was used to disperse the fluorescence and was set at a bandwidth of 3·5 Å.

The combined response of a grating blazed at 5000 Å and a cooled photomultiplier (EMI 9558QB) was calibrated with a NBS quartz iodine standard lamp. The detection system response (per photon s^{-1}) as a function of wavelength is essentially the same as published in a previous paper (Lee and Judge 1972).

CO_2 gas supplied by Airco with a purity of 99·99 % was used for this study without further purification. The CO_2 pressure was measured with a Baratron capacitance manometer (MKS Instruments, Inc.) which was remote from the absorption cell on the high pressure side of the flow system, and was set at 30 mTorr or less for the entire experiment.

3. Results and discussion

3.1. Fluorescence spectra

Typical $CO_2^+(A\ ^2\Pi_u \rightarrow X\ ^2\Pi_g)$ fluorescence spectra for incident photons of wavelengths λ703, 709 and 715 Å are shown in figure 1. The bandhead positions of the $CO_2^+(A\ ^2\Pi_{\frac{1}{2}u} \rightarrow X\ ^2\Pi_{\frac{1}{2}g})$ subsystem given by Judge *et al* (1969) are indicated to identify the observed bands. Referring to the known energy levels of the $CO_2^+(A\ ^2\Pi_u)$ states (Tanaka and Ogawa 1962), the energetically possible levels of excitation at λ703, 709 and 715 Å are (2, 0, 0), (1, 0, 0), and (0, 0, 0), respectively. The fluorescence bands from these possible levels are observed as shown in figure 1.

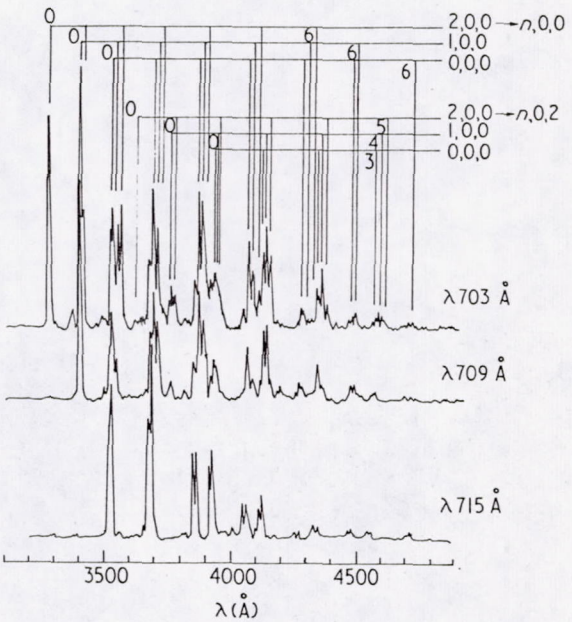

Figure 1. The fluorescence spectrum of CO_2^+ produced by incident photons of λ703, 709, and 715 Å. The bandhead positions of the $CO_2^+(A\ ^2\Pi_{\frac{1}{2}u} \rightarrow X\ ^2\Pi_{\frac{1}{2}g})$ system given by Judge *et al* (1969) are indicated.

3.2. Analysis technique

The fluorescence radiation rate, $\dot{n}_{v'v''}$, for the transition from an upper level v' to a lower level v'' is given (Herzberg 1967) by

$$\dot{n}_{v'v''} = KN_{v'}A_{v'v''}$$

where K is a normalization constant, $N_{v'}$ is the population of the v' level, and $A_{v'v''}$ is

the transition probability. The fluorescence radiation rate, $\dot{n}_{v'v''}$, is measured by the area under the spectral envelope of the fluorescence band ($v' \rightarrow v''$) divided by the detection system response.

For incident photons of λ715 Å, only the (0, 0, 0) level of $CO_2^+(A\ ^2\Pi_u)$ is excited. As shown in figure 1, the fluorescence bands are well-separated. The fractional transition probability for the upper (0, 0, 0) level may be written as

$$\tau A_{0v''} = \dot{n}_{0v''}/(\Sigma \dot{n}_{0v''})$$

where $\tau = 1/(\Sigma A_{0v''})$ is the lifetime of the (0, 0, 0) level of the $CO_2^+(A\ ^2\Pi_u)$ state, and $\dot{n}_{0v''}$ is the measured radiation rate.

For incident photons of λ709 Å, both the (1, 0, 0) and (0, 0, 0) levels of the $CO_2^+(A\ ^2\Pi_u)$ state are excited. The fluorescence bands from these two levels are mixed in the observed spectrum. However, the fractional transition probability $\tau A_{0v''}$ is known from the 715 Å spectrum thus permitting $\tau A_{1v''}$ for the (1, 0, 0) level to be obtained from the spectrum according to the relation,

$$(q_{00}\tau A_{0v''} + q_{01}\tau A_{1v''+1})/(q_{00}+q_{01}) = (\dot{n}_{0v''} + \dot{n}_{1v''+1})/(\Sigma \dot{n}_{0v''} + \Sigma \dot{n}_{1v''})$$

where q_{00} and q_{01} are the Franck–Condon factors for the production of the upper level populations, N_0 and N_1, $(\dot{n}_{0v''} + \dot{n}_{1v''+1})$ is the measured radiation rate of the mixed bands, $(\Sigma \dot{n}_{0v''} + \Sigma \dot{n}_{1v''})$ is the measured total radiation rate, and τ is the common lifetime (Hesser 1968) of the vibrational levels of the $CO_2^+(A\ ^2\Pi_u)$ state. The production Franck–Condon factors have been given by Brundle and Turner (1969), Eland and Danby (1968), and Spohr and Puttkamer (1967).

Similarly, using the constant level independant and the known absorption Franck–Condon factors, the fractional transition probability for the (2, 0, 0) level of the $CO_2^+(A\ ^2\Pi_u)$ state can be obtained from the fluorescence spectrum produced by incident photons of λ703 Å.

3.3. Transition probabilities and band strengths

Using the average values of the Franck–Condon factors given by the above authors (Brundle and Turner 1969, Eland and Danby 1968, Spohr and Puttkamer 1967) it is found that $q_{00}:q_{01}:q_{02} = 0{\cdot}40:0{\cdot}80:1{\cdot}0$. Adopting these values, the fractional transition probabilities for the $CO_2^+(A\ ^2\Pi_u)$ (2, 0, 0), (1, 0, 0), and (0, 0, 0) levels have been determined and are as given in table 1. These results represent the average of several spectra and are accurate within 15% of the given value. The data given by McCallum and Nicholls (1972), Wauchop and Broida (1972), Ajello (1971), and Poulizac and Dufay (1967) are also shown in table 1 for comparison. The data given by previous authors are so normalized that the sum of the existing fractional transition probabilities is equal to that of the corresponding present measurement. For the data given by Ajello (1971), only the well-separated bands are given in table 1. It may be noted that there is good agreement among the various sets of data.

Using the relation $A_{v'v''} = \text{const.} \times p_{v'v''}/\lambda^3_{v'v''}$ the relative band strengths, $p_{v'v''}$, can be calculated and are shown in table 1. The sum of $p_{v'v''}$ over v'' is normalized to 1.

3.4. Transition dipole moment

The Franck–Condon factors, $q_{v'v''}$, and the r-centroids for the $CO_2^+(A\ ^2\Pi_u \rightarrow X\ ^2\Pi_g)$ bands have been calculated by McCallum and Nicholls (1971) and Petropoulos (1968).

Table 1. The fractional transition probabilities and the band strengths of the $CO_2^+(A\ ^2\Pi_u \rightarrow X\ ^2\Pi_g)$ system

		$(v'', 0, 0)$							$(v'', 0, 2)$					
$(v', 0, 0)$		0	1	2	3	4	5	6	0	1	2	3	4	5
0	a	0·27	0·30	0·13	0·05	0·02	0·02	0·02	0·10	0·06	0·02	0·01		
	b	0·27	0·30	0·13	0·05				0·05	0·10	0·04			
	c	0·31	0·26	0·14	0·04	0·02			0·05	0·11				
	d	0·26	0·30		0·07				0·09					
	e	0·24	0·30	0·15	0·07	0·04								
	f	0·21	0·26	0·13	0·06	0·03	0·03	0·04	0·11	0·08	0·03	0·02		
1	a	0·36	0·08	0·12	0·14	0·05	0·01	0·02	0·03	0·05	0·08	0·03	0·02	
	b	0·47	0·07	0·10	0·07	0·04			0·07	0·05	0·04	0·03		
	c	0·46	0·04	0·08	0·14	0·03			0·06	0·05	0·05			
	d	0·37	0·07						0·04	0·03				
	e	0·34	0·08	0·11	0·15	0·08	0·02	0·01						
	f	0·26	0·07	0·12	0·15	0·06	0·02	0·03	0·03	0·06	0·11	0·05	0·04	
2	a	0·33	0·13	0·16	0·02	0·07	0·05	0·01	0·01	0·05	0·02	0·07	0·05	0·02
	b	0·35	0·10	0·16	0·01	0·10			0·03	0·06	0·03		0·02	
	c	0·39	0·10	0·11	0·02	0·04			0·02	0·06	0·02	0·05		
	d	0·34	0·14	0·14					0·03	0·03				
	e	0·34	0·11	0·17	0·03	0·07	0·04	0·02						
	f	0·23	0·10	0·15	0·02	0·08	0·07	0·02	0·01	0·05	0·03	0·10	0·08	0·04

a Present results for the fractional transition probabilities, $\tau A_{v'v''}$.
b The $\tau A_{v'v''}$ from McCallum and Nicholls (1972).
c The $\tau A_{v'v''}$ from Wauchop and Broida (1972).
d The $\tau A_{v'v''}$ from Ajello (1971).
e The $\tau A_{v'v''}$ from Poulizac and Dufay (1967).
f The band strengths calculated from the present fractional transition probabilities.

Using the relation $p_{v'v''} = R_e^2(r)q_{v'v''}$, the relative transition dipole moment, $R_e(r)$, can be obtained. A plot of $R_e(r)$ for the $(v', 0, 0)$–$(v'', 0, 0)$ transitions versus r is shown in figure 2. Because the r-centroids for the (0, 0, 0)–(0, 0, 0), (1, 0, 0)–(1, 0, 0), and (2, 0, 0)–(2, 0, 0) transitions are nearly the same, their $R_e(r)$ values should be equal (Fraser 1954) and have been normalized to 1. The average of the Franck–Condon factors and the r centroids for the two components of the $CO_2^+(A\ ^2\Pi_u \rightarrow X\ ^2\Pi_g)$ bands given by McCallum and Nicholls (1971) were adopted in this plot since they yield the least fluctuation of R_e.

As shown in figure 2 there is no clear trend for the variation of $R_e(r)$. Further, it seems very unlikely that $R_e(r)$ should fluctuate so drastically. Since the experimental data for the band strengths established by different techniques are in good agreement, but the published Franck–Condon factors (McCallum and Nicholls 1972, Petropoulos 1968) are significantly different, further refinement of the Franck–Condon factor calculations would appear to be required.

Acknowledgments

This work was supported by NASA Grant No. NGR 05-018-180.

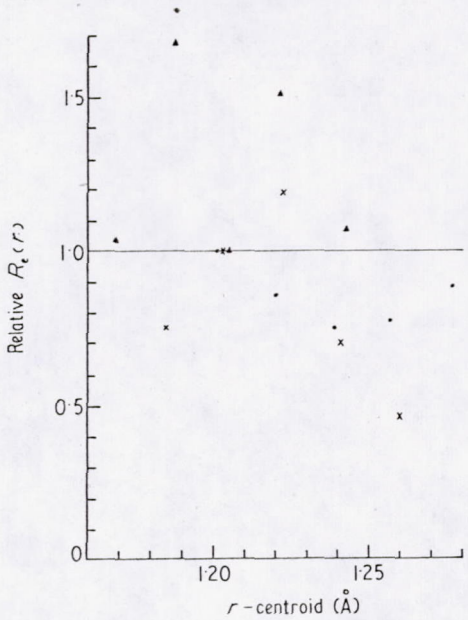

Figure 2. The relative electronic transition moment R_e versus the r-centroid for the emission bands of the $CO_2^+(A\ ^2\Pi_u \rightarrow X\ ^2\Pi_g)$ system. The data indicated by ·, ×, and ▲ are, respectively, for the upper levels (0, 0, 0), (1, 0, 0) and (2, 0, 0).

References

Ajello J M 1971 *J. chem. Phys.* **55** 3169–77

Barth C A, Fastie W G, Hord C W, Pearce J B, Kelly K K, Stewart A I, Thomas G E, Anderson G P and Raper O F 1969 *Science* **165** 1004–5

Barth C A, Hord C W, Pearce J B, Kelly K K, Anderson G P and Stewart A I 1971 *J. geophys. Res* **76** 2213–27

Brundle C R and Turner D W 1969 *Int. J. Mass. Spectrosc. Ion. Phys.* **2** 195–220

Dalgarno A and Degges T C 1971 *Planetary Atmospheres* ed C Sagan (Dordrecht, Holland: Reidel-Dordrecht) p 337–45

Dalgarno A, Degges T C and Stewart A I 1970 *Science* **167** 1490–1

Eland J H D and Danby C J 1968 *Int. J. Mass. Spectrosc. Ion. Phys.* **1** 111–9

Fraser P A 1954 *Can. J. Phys.* **32** 515–21

Herzberg G (ed) 1967 *Spectra of Diatomic Molecules* (New York: Van Nostrand) p 20

Hesser J E 1968 *J. chem. Phys.* **48** 2518–35

Judge D L, Bloom G S and Morse A L 1969 *Can. J. Phys.* **47** 489–97

Judge D L and Lee L C 1972 *J. chem. Phys.* **57** 455–62

Lee L C and Judge D L 1972 *J. chem. Phys.* **57** 4443–5

McCallum J C and Nicholls R W 1971 *J. Phys.* B: *Atom. molec. Phys.* **4** 1096–101

—— 1972 *J. Phys.* B: *Atom. molec. Phys.* **5** 1417–26

Petropoulo B 1968 *C.R. Acad. Sci., Paris* **266** 276–8

Poulizac M C and Dufay M 1967 *Astrophys. Lett.* **1** 17–20

Stewart A I 1972 *J. geophys. Res.* **77** 54–68

Spohr R and Puttkamer E 1967 *Z. Naturf.* **22** (A) 705–10

Tanaka Y and Ogawa M 1962 *Can. J. Phys.* **40** 879–86

Wauchop T S and Broida H P 1971 *J. geophys. Res.* **76** 21–6

—— 1972 *J. Quant. Spectrosc. Radiat. Transfer* **12** 371–8

J. Phys. B: Atom. Molec. Phys., Vol. 7, No. 5, 1974. Printed in Great Britain.

Cross sections and band strengths for the N_2O^+ ($A\ ^2\Sigma^+ \rightarrow X\ ^2\Pi$) system produced by vacuum ultraviolet radiation

L C Lee and D L Judge

Department of Physics, University of Southern California, University Park, Los Angeles, California 90007, USA

Received 12 October 1973

Abstract. Cross sections for producing the $N_2O^+(A\ ^2\Sigma^+ \rightarrow X\ ^2\Pi)$ bands, using vacuum ultraviolet radiation between 462–755 Å, have been measured. Band strengths for the $N_2O^+[A\ ^2\Sigma^+(0,0,0) \rightarrow X\ ^2\Pi(n_1, n_2, 0)]$ bands are also given.

1. Introduction

Using a continuum background the photoabsorption and photoionization cross sections of N_2O have been measured by Cook *et al* (1968) in the 600–1000 Å region while Lee *et al* (1973) have measured the photoabsorption cross section in the 180–700 Å region. In addition, Bahr *et al* (1972) have determined the partial photoionization cross section for the various N_2O^+ electronic states in the 584–890 Å region using photoelectron spectroscopy. However, the cross section for production of the N_2O^+ ($A\ ^2\Sigma^+ \rightarrow X^2\Pi$) fluorescence has not been measured.

Further, since N_2O is a simple linear molecule in its ground state the band strength data are of theoretical interest. Although band strengths and Franck–Condon factors for diatomic molecules have been reasonably well investigated both theoretically and experimentally, only limited results are available on triatomic or more complex molecules.

2. Experimental

The experimental setup has been described in a previous paper (Judge and Lee 1972). The nominal source lines used in the present investigation were 462, 526, 555, 586, 625, 637, 666, 686, 700, 704, 716, 726 and 755 Å. The bandwidth of the 1 m normal incidence monochromator (McPherson 225) used to isolate these lines was set at 4 Å or less, while the bandwidth of the 0·3 m normal incidence monochromator (McPherson 218) used to disperse the fluorescence was set at 3 Å. The detection system and the response were essentially the same as that described in a previous paper (Lee and Judge 1972).

N_2O gas supplied by the Matheson Company, with a purity greater than 98%, was used in the present investigation without further purification and the pressure in the experimental chamber was set at 25 m Torr or less.

3. Results

3.1. Fluorescence spectra

The fluorescence spectra produced using incident photons of λ715·6 and 754·9 Å are shown in figure 1. The band head positions for the $N_2O^+[A\ ^2\Sigma^+(0,0,0) \rightarrow X\ ^2\Pi(n_1, n_2, 0)]$ system, given by Judge and Lee (1973), are indicated in the figure to identify the bands. The λ754·9 Å photons have only enough energy to excite the ground state neutral molecules to the $N_2O^+[A\ ^2\Sigma^+(0,0,0)]$ level (Tanaka *et al* 1960, Brundle and Turner 1969), so that the fluorescence is dominated by progressions originating from this upper state. However, at room temperature, about 6% of the neutral molecules are in the $X\ ^1\Sigma^+(0,1,0)$ level, thus fluorescence from the $N_2O^+[A\ ^2\Sigma^+(0,1,0)]$ level is also evident in the spectrum.

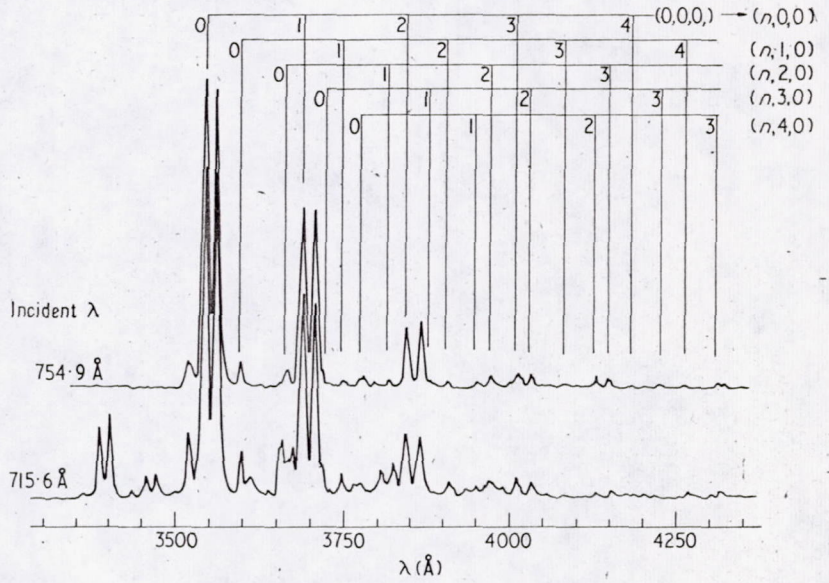

Figure 1. Fluorescence spectra of the $N_2O^+(A\ ^2\Sigma^+ \rightarrow X\ ^2\Pi)$ system produced by primary photons of wavelengths 715·6 and 754·9 Å. The bandhead positions given by Judge and Lee (1973) are indicated.

The spectrum produced by primary photons of λ715·6 Å is characteristic of all spectra resulting from primary photons of wavelength less than 726 Å. This result is consistent with Brundle and Turner's (1969) data showing that the Franck–Condon factors for production of the $N_2O^+(A\ ^2\Sigma^+)$ state have significant values only for the levels at or below the (0, 0, 1) level (16·7 eV), implying that the fluorescence spectra produced by the primary photons of λ742 Å should be generally similar.

3.2. Fluorescence cross sections for the individual bands

The fluorescence cross section $\sigma_f(\lambda, \lambda_f)$, for a band at wavelength λ_f produced by a primary photon of wavelength λ, is proportional to the fluorescence radiation rate $\dot{n}_f(\lambda, \lambda_f)$ (Lee and Judge 1972). For all primary photons of wavelengths shorter than 726 Å, the relative fluorescence cross sections for the various bands are essentially the same and are given

Table 1. Relative fluorescence cross sections for the observed bands of the $N_2O^+(A\ ^2\Sigma^+ \rightarrow X\ ^2\Pi)$ system

λ(Å)	3381 3396	3454 3470	3521	3542 3558	3595 3608	3661 3673	3689 3707
σ	0·186	0·061	0·096	1·00	0·088	0·122	0·515

λ(Å)	3746 3764	3803 3823	3845 3864	3902	3945	3970	4007 4030
σ	0·061	0·071	0·129	0·019	0·018	0·028	0·026

in table 1. Here the cross section for the $A\ ^2\Sigma^+(0,0,0) \rightarrow X\ ^2\Pi(0,0,0)$ band has been normalized to 1. The experimental error is about 10% of the given values. The absolute cross section for each band may be determined by referring to the total production cross section at each incident wavelength (§ 3.3).

3.3. Absolute N_2O^+ ($A\ ^2\Sigma^+ \rightarrow X\ ^2\Pi$) fluorescence cross sections

The absolute cross section, $\Sigma_f \sigma_f(\lambda, \lambda_f)$, for production of the $N_2O^+(A\ ^2\Sigma^+ \rightarrow X\ ^2\Pi)$ system can be obtained by comparing the total fluorescence radiation rate, $\Sigma_f \dot{n}_f(\lambda, \lambda_f)$, with that of the $N_2^+(B\ ^2\Sigma_u^+, v' = 0) \rightarrow N_2^+(X\ ^2\Sigma_g^+, v'' = 0)$ band, for which the absolute cross section is known (Judge and Weissler 1968). The spatial distribution of the fluorescence is assumed isotropic for both systems since the molecular rotational frequencies are much greater than the transition rates.

The absolute fluorescence cross sections at each of the primary photon wavelengths are shown in figure 2 and agree well with the corresponding photoelectron spectroscopy results of Bahr *et al* (1972) in marked contrast with a similar comparison of data on CO_2 (Lee and Judge 1972, Samson *et al* 1972). The present experimental error is estimated to be within 15% of the given values.

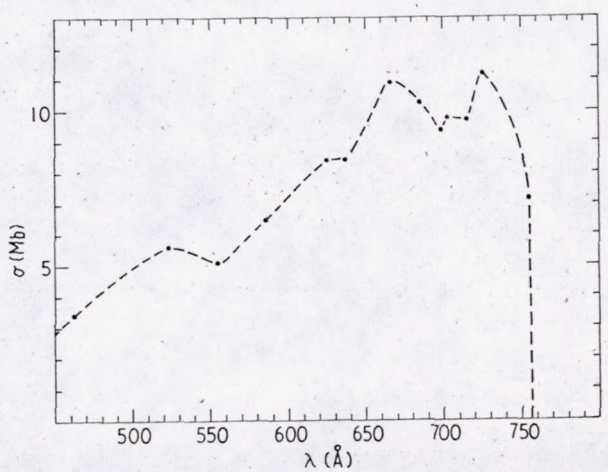

Figure 2. Cross sections for the production of $N_2O^+(A\ ^2\Sigma^+ \rightarrow X\ ^2\Pi)$ fluorescence by vacuum ultraviolet radiation of wavelengths 462, 526, 555, 625, 637, 666, 686, 700, 704, 716, 726, and 755 Å. The cross section is in units of Mb (10^{-18} cm^2).

3.4. Band strengths for the $A\,^2\Sigma^+(0,0,0) \rightarrow X\,^2\Pi(n_1, n_2, 0)$ fluorescence

The band strength is given (Nicholls 1962) by $P_{v'v''} = K\dot{n}_{v'v''}\lambda^3_{v'v''}$, where K is a constant, and $n_{v'v''}$ and $\lambda_{v'v''}$ are, respectively, the fluorescence radiation rate (photons/second) and wavelength of the (v', v'') band. The presently determined relative band strengths for the $A\,^2\Sigma(0, 0, 0) \rightarrow X\,^2\Pi(n_1, n_2, 0)$ system are given in table 2. The wavelength indicated corresponds to the shortest wavelength member of each band. The sum of the band strengths, $\Sigma_{v''}p_{v'v''}$, is normalized to 1.

Table 2. The $N_2O^+[A\,^2\Sigma^+(0, 0, 0) \rightarrow X\,^2\Pi(n_1, n_2, 0)]$ band strengths

n_1		n_2 = 0	1	2	3
0	λ	3541	3595	3661	3720
	p	0·51	0·019	0·005	0·002
1	λ	3689	3746	3815	3874
	p	0·3	0·012	0·004	0·001
2	λ	3845	3902	3970	
	p	0·10	0·009	0·014	
3	λ	4007			
	p	0·020			

λ wavelength (Å); p band strength

Acknowledgments

The assistance of Edward Phillips in obtaining and reducing the data is gratefully acknowledged. This work was supported by NASA grant No. NGR 05-018-180.

References

Bahr J L, Blake A J, Carver J H, Gardner J L and Kumar V 1972 *J. Quant. Spectrosc. Radiat. Transfer* **12** 59–73

Brundle C R and Turner D W 1969 *J. Mass Spectrosc. Ion Phys.* **2** 195–220

Cook G R, Metzger P H and Ogawa M 1968 *J. Opt. Soc. Am.* **58** 129–36

Judge D L and Lee L C 1972 *J. chem. Phys.* **57** 455–62

—— 1973 *J. Molec. Spectrosc.* submitted for publication

Judge D L and Weissler G L 1968 *J. chem. Phys.* **48** 4590–6

Lee L C, Carlson R W, Judge D L and Ogawa M 1973 *J. Quant. Spectrosc. Radiat. Transfer* **13** 1023–31

Lee L C and Judge D L 1972 *J. chem. Phys.* **57** 4443–5

Nicholls R W 1962 *J. Quant. Spectrosc. Radiat. Transfer* **2** 433–9

Samson J A R, Gardner J L and Mental J E 1972 *J. Geophys. Res.* **77** 5560–6

Tanaka Y, Jursa A S and LeBlanc F J 1960 *J. chem. Phys.* **32** 1205–14

JOURNAL OF MOLECULAR SPECTROSCOPY 53, 317 (1974)

NOTE FROM THE EDITOR'S OFFICE

Identification of the $N_2O^+[A^2\Sigma^+(0,0,0) \rightarrow X^2\Pi(n_1,n_2,n_3)]$ Vibrational Bands

The emission spectrum of the $N_2O^+(A^2\Sigma^+ \rightarrow X^2\Pi)$ system has been studied by both Brocklehurst (*1*) and Callomon (*2*). However, due to overlying bands of the N_2 second positive, N_2^+ first negative, and the NO(β) system only the strong bands of the N_2O^+ spectrum have been assigned (*2*). In order to make a complete analysis, Callomon (*2*) noted that a pure N_2O^+ emission spectrum would be required. To obtain such a result we have selectively produced the $N_2O^+[A^2\Sigma^+(0, 0, 0)]$ ions using vacuum ultraviolet radiation of wavelength 754.9 Å, and thereby obtained a spectrum of the $N_2O^+(0, 0, 0) \rightarrow X^2\Pi(n_1, n_2, n_3)]$ system (*3*). The observed bands were found to be well represented by the progressions, $1/\lambda = 1/\lambda_0 - (n_1\nu_1 + n_2\nu_2)$, with $n_1, n_2 = 0, 1, \ldots$. Such selective photon excitation demonstrates a powerful technique for obtaining a pure and simple spectrum, and thus permits a rather straightforward analysis of the resulting bands.

REFERENCES

1. B. BROCKLEHURST, *Nature* (*London*) 182, 1366 (1958).
2. J. H. CALLOMON, *Proc. Chem. Soc.*, p. 313 (1959); also, private communication.
3. L. C. LEE AND D. L. JUDGE, *J. Phys. B* 7, 626 (1974).

DARRELL L. JUDGE AND LONG C. LEE

University of Southern California
Received June 1, 1974

Reprinted from:

THE JOURNAL OF CHEMICAL PHYSICS VOLUME 57, NUMBER 1 1 JULY 1972

Absolute Specific Photodissociation Cross Sections of CH_4 in the Extreme Ultraviolet*

A. R. WELCH AND D. L. JUDGE

Department of Physics, University of Southern California, Los Angeles, California 90007

(Received 21 January 1972)

The photodissociation of methane has been studied at 16 different incident wavelengths in the range 555–1242 Å. Absolute partial cross sections have been determined for those processes yielding excited fragments which fluoresce in the range 3500–8000 Å. The fluorescence was dispersed and found to result from the $A\,^2\Delta \rightarrow X\,^2\Pi$ and $B\,^2\Sigma \rightarrow X\,^2\Pi$ systems of CH, the $\tilde{b}\,^1B_1 \rightarrow \tilde{a}\,^1A_1$ system of CH_2, and the H_α, H_β, and H_γ transitions of H. Absolute cross sections have been assigned to the processes $CH_4+h\nu \rightarrow CH(A\,^2\Delta)+H_2(X\,^1\Sigma_g^+)+H(1\,^2S_{1/2})$, $CH_4+h\nu \rightarrow CH(B\,^2\Sigma)+H_2(X\,^1\Sigma_g^+)+H(1\,^2S_{1/2})$, and $CH_4+h\nu \rightarrow CH_2(\tilde{b}\,^1B_1)+H_2(X\,^1\Sigma_g^+)$. Emission cross sections have been assigned to the Balmer lines H_α, H_β, and H_γ. The process $CH_4+h\nu \rightarrow CH_3(X\,^2A_2'')+H^*$ is believed to be responsible for the Balmer lines. The largest cross section measured, $\sigma = 8\times10^{-20}$ cm², occurred at 923 Å for the process leading to $CH(A\,^2\Delta)$. Cross sections of this magnitude are three orders of magnitude less than the total peak absorption cross section for methane.

I. INTRODUCTION

The investigation presented here is concerned with the dispersed fluorescence of fragments resulting from the dissociation of methane, irradiated by monochromatic vacuum ultraviolet photons. Since methane is a relatively small molecule there is some hope that if the fluorescence can be identified, simple energy arguments can be made to identify the photodissociation processes. Absolute cross sections can be assigned to specific processes using this approach, if the energy of the excited fragments is lost through radiative transitions.

The only other known study of the fluorescence from methane, in the region report here, has been made by Metzger and Cook.[1] However, they only measured the relative total fluorescence over a portion of the range, making no attempt to disperse it, or suggest its source.

The total absorption cross section for methane has been established by previous experimenters. Notable papers include work by Wilkinson and Johnson,[2] Moe and Duncan,[3] Sun and Weissler,[4] Ditchburn,[5] Metzger and Cook,[1] and Rustgi.[6] Together their work assigns a cross section from 190 Å to greater than 1400 Å. It is known that between 400 Å and 900 Å this absorption is due primarily to photoionization.[4,5] Dibeler, Krauss, Reese, and Harlee,[7] have identified the processes $CH_4+h\nu \rightarrow CH_4^+ + e$, $CH_4+h\nu \rightarrow CH_3^+ + H + e$, and $CH_4+h\nu \rightarrow CH_2^+ + H_2 + e$ over most of this region. These cross sections have also been calculated by Dalgarno, using self-consistent wavefunctions.[8] Other theoretical calculations for the decomposition of methane have been made by Lindholm,[9] using molecular orbital theory.

The processes responsible for the absorption at wavelengths greater than 900 Å are not, however, well known. In view of the abundance of methane around Jupiter, these unknown processes would be valuable in forming a model for the Jovian atmosphere, especially those processes which occur at L_α (1216 Å).[10] Furthermore, it is possible that other simpler molecules and atoms found in space could have their origin in methane, for example, the CH observed in comets.

II. EXPERIMENT

The experimental apparatus is illustrated in Fig. 1. The ultraviolet radiation was generated by a condensed spark discharge through a water-cooled boron nitride capillary containing hydrogen, nitrogen or oxygen. The discharge was operated at a rate of 38 pulses/sec by means of a rotary spark gap. An evacuated 1-m monochromator adjusted for 2 Å resolution was used to disperse the source radiation. The intensity incident on the methane was measured at shorter wavelengths using a platinum photocathode, the photoelectron yield of which is known,[11] and was measured at the longer wavelengths using a sodium salicylate coated photomultiplier.[12] An absolute calibration for the sodium salicylate was obtained by using the platinum since the response of these two detectors overlap. The intensity of the incident radiation ranged from 1.2×10^{10} photons/sec for the strongest line, down to 8×10^8 photons/sec for the weakest useful line.

The methane gas sample was admitted into the cell through a leak valve and was pumped out through the exit slit of the 1-m monochromator. The cell pressure was maintained at 1.5×10^{-1} torr. The fluorescence resulting from the photodissociation was viewed through a quartz window by a second monochromator.

Cooled EMI 9558QB and 9514S photomultiplier tubes were employed as part of a synchronous pulse counting system to detect the dispersed fluorescence. Only the signal received during the 10 μsec discharge of the light source was detected. The small duty cycle and cooled detector limited the noise level to 0.3 dark counts/min.

The methane was obtained from the Matheson Company. It was specified as 99.5% pure, and was used without further purification. The impurities included ethane (C_2H_6), propane (C_3H_8), carbon dioxide (CO_2), nitrogen (N_2), and oxygen (O_2).

III. RESULTS

The dispersed fluorescence, resulting from the irradiated methane was recorded for 16 different

incident energies with photon energies ranging from 10 eV (1242 A) to 22.4 eV (555 Å).

For incident wavelengths less than 1032 Å, the spectra were dominated by CH emission bands. These bands are well known and have been observed by other experimenters in hydrocarbon flames, discharge tubes containing carbon and hydrogen, carbon arcs in hydrogen, and the emission from comet heads.[13] The 3900 Å system ($B\,^2\Sigma \rightarrow X\,^2\Pi$) and the 4300 Å system ($A\,^2\Delta \rightarrow X\,^2\Pi$) of CH were identified using Pearse and Gaydon band head data.[13] The spectra taken at shorter incident wavelengths were of particular interest since they showed line emission resulting from excited atomic hydrogen. For these spectra the H_α, H_β, and H_γ lines of the Balmer series were identified. The intensities of these lines were corrected for the system response, and compared with published oscillator strengths. They indicate the initial states were of nearly equal population. Figure 2 shows the resulting fluorescence spectrum taken at 555 Å incident wavelength where most features of interest appear.

For incident wavelengths greater than 1032 Å only the spectrum taken at L_α (1216 Å) resulted in any significant fluorescence. This has been identified as the ($\tilde{b}\,^1B_1 \rightarrow \tilde{a}\,^1A_1$) system of CH_2. This system has been seen previously only in absorption spectra, found to extend from 5000 Å to 9000 Å.[14,15] The observed emission spectrum appears to cover nearly the same region, starting at 5500 Å and extending beyond the 8000 Å limit of this experiment. Since it was not possible to measure all the radiation resulting from the CH_2 only an estimate of the cross section for the responsible process could be made.

To obtain an absolute cross section for the observed processes, an emission spectrum of N_2^+ was taken. The emission spectrum of N_2^+ in the range 3500–5500 Å following irradiation of N_2 by photons of wavelength 555 Å (22.4 eV), was taken at the same scan speed and resolution as the photodissociation fluorescence spectra. By comparing the fluorescence from the first negative system of nitrogen ($B\,^2\Sigma_u^+ \rightarrow X\,^2\Sigma_g^+$) with the fluorescence yields for the various processes observed in CH_4, it was possible to assign absolute cross sections to these processes.[16]

The absolute cross sections versus incident wavelength for the processes resulting in the transitions $A\,^2\Delta \rightarrow X\,^2\Pi$, and $B\,^2\Sigma \rightarrow X\,^2\Pi$ of CH, H_α, H_β, and H_γ of H and ($\tilde{b}\,^1B_1 \rightarrow \tilde{a}\,^1A_1$) of CH_2 are given in Fig. 3. The cross sections were found by integrating the area under the spectrum for each process, and at each incident wavelength, and comparing these areas with the area under the spectrum of N_2^+ for the process $B\,^2\Sigma_u^+ \rightarrow X\,^2\Sigma^+$. The radiation from these processes was assumed to be isotropic. Corrections for system response were incorporated into these calculations; that is, photomultiplier and platinum detector efficiencies, incident intensities, optics, electronic amplification, scan speeds and pulse pile-up.

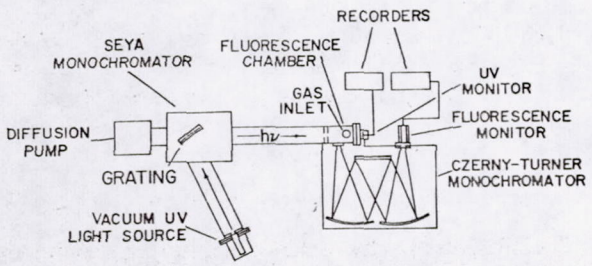

FIG. 1. Experimental Apparatus.

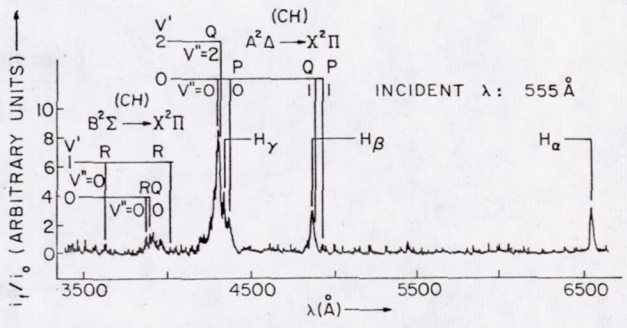

FIG. 2. Fluorescence from CH and H, resulting from CH_4 irradiated by 555 Å photons.

The calculated thresholds for many of the processes considered are identified in Fig. 3. They were found by adding together the energy necessary to dissociate the molecule and excite the labelled fragments. A discussion of the suggested dissociation processes is given below; their cross sections are given in Fig. 3.

A. $CH_4 + h\nu \rightarrow CH(A\,^2\Delta) + H_2(X\,^1\Sigma_g^+) + H(1\,^2S_{1/2})$

Figure 3 strongly suggests the reaction $CH_4 + h\nu \rightarrow CH(A\,^2\Delta) + H_2(X\,^1\Sigma_g^+) + H(1\,^2S_{1/2})$, since the threshold for the production of excited CH is observed within 0.05 eV of the calculated threshold at 1028 Å.

There is also an energetically possible threshold for the process, $CH_4 + h\nu \rightarrow CH(A\,^2\Delta) + 3H(1\,^2S_{1/2})$ at 750 Å. However no threshold appears at this wavelength. Thus, if this reaction is present, its threshold must occur at an energy higher than its calculated minimum value. This process could account for the increasing emission from $CH(A\,^2\Delta \rightarrow X\,^2\Pi)$ found between 555 and 626 Å. If this process is absent, then the reaction $CH_4 + h\nu \rightarrow CH(A\,^2\Delta) + H_2(X\,^1\Sigma_g^+) + H(1\,^2S_{1/2})$ must account for all excitation to the $CH(A\,^2\Delta)$ state. The presence of the reaction $CH_4 + h\nu \rightarrow CH^* + H_2 + H$ and the absence of the reaction $CH_4 + h\nu \rightarrow CH^* + 3H$ would also suggest that upon photon impact the CH_4 molecule is distorted bringing at least two H atoms close enough together that when CH_4 dissociates these H atoms bond together forming H_2.

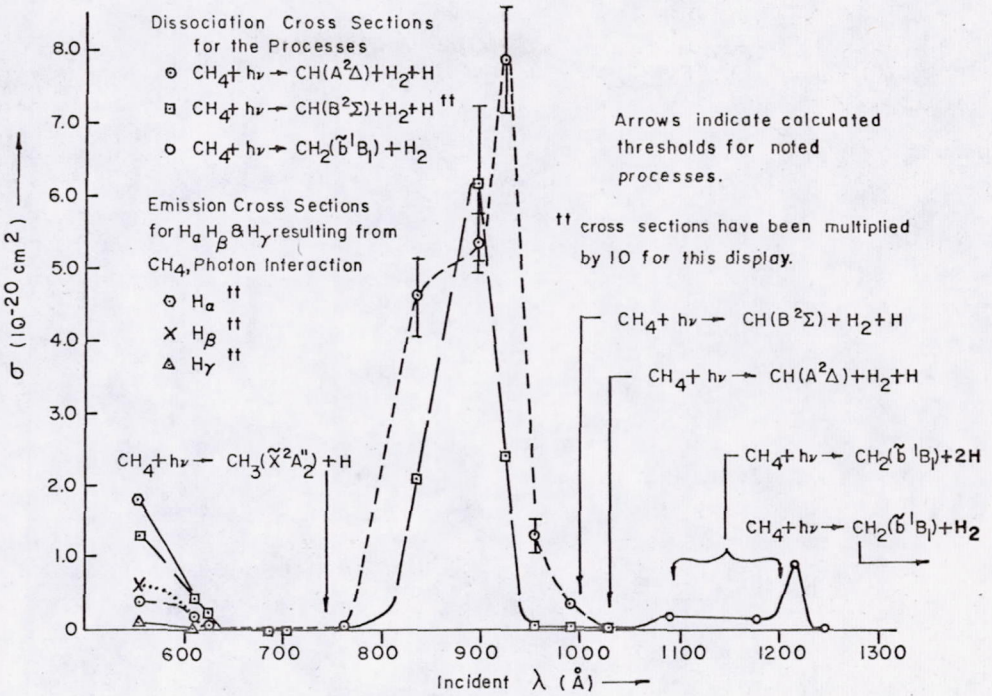

FIG. 3. Cross sections for the specific dissociation processes observed in methane.

B. $CH_4+h\nu \rightarrow CH(B\,^2\Sigma)+H_2(X\,^1\Sigma_g^+)+H(1\,^2S_{1/2})$

From energy arguments, the threshold for the process $CH_4+h\nu \rightarrow CH(B\,^2\Sigma)+H_2(X\,^1\Sigma_g^+)+H(1\,^2S_{1/2})$ cannot occur at wavelengths longer than 1005 Å. For the process $CH_4+h\nu \rightarrow CH(B\,^2\Sigma)+3H(1\,^2S_{1/2})$, the threshold must occur at wavelengths less than or equal to 736 Å. The experimentally found threshold for the transition $CH(B\,^2\Sigma) \rightarrow CH(X\,^2\Pi)$ is near 950 Å. Thus, of the above two processes the experimental data are consistent only with the process $CH_4+h\nu \rightarrow CH(B\,^2\Sigma)+H_2(X\,^1\Sigma_g^+)+H(1\,^2S_{1/2})$. This is a reasonable process to expect since the process yielding $CH(A\,^2\Delta)$ and ground state H_2 and H has also been identified. Here again, it is possible that the reaction $CH_4+h\nu \rightarrow CH(B\,^2\Sigma)+3H(1\,^2S_{1/2})$ could account for the excitation to the $CH(B\,^2\Sigma)$ state which results in the $CH(B\,^2\Sigma \rightarrow X\,^2\Pi)$ transition for incident photons between 555 and 626 Å.

C. $CH_4+h\nu \rightarrow CH_3(X\,^2A_2'')+H^*$

The threshold for production of H atoms in the fifth principal quantum state ($n=5$), through the process $CH_4+h\nu \rightarrow CH(X\,^2\Pi)+H_2(X\,^1\Sigma_g^+)+H^*$ is 559 Å. From this state the third Balmer line H_γ is possible. The threshold decreases to 567 Å for radiation resulting from the second Balmer line, H_β, and 585 Å for H_α, the first Balmer line.

For the process

$$CH_4+h\nu \rightarrow CH_2(X\,^3\Sigma_g^-)+H(1\,^2S_{1/2})+H^*,$$

the calculated threshold wavelength for H_γ is 564 Å, H_β, 572 Å and H_α, 590 Å.

For the process $CH_4+h\nu \rightarrow CH_3(\tilde{X}\,^2A_2'')+H^*$, the calculated threshold wavelength for H_γ is 712 Å, H_β 725 Å, and H_α 754 Å, respectively.

The experimental results show thresholds between 610 and 626 Å for the first three Balmer lines. Thus, the process $CH_4+h\nu \rightarrow CH_3(\tilde{X}\,^2A_2'')+H^*$ appears to be a likely process for the production of excited H atoms.

Because the threshold for excited H atoms coincides with the "threshold" for fluorescence resulting from excited CH, the processes

$$CH_4+h\nu \rightarrow CH(A\,^2\Delta)+H_2(X\,^1\Sigma_g^+)+H^*$$

and

$$CH_4+h\nu \rightarrow CH(A\,^2\Delta)+2H(1\,^2S_{1/2})+H^*$$

were considered. However, neither of these processes can occur for incident photon wavelengths longer than 500 Å.

The possibility of secondary reactions giving rise to excited H atoms was rejected by measuring the pressure dependence of the H_α line. The pressure dependence, over the range $10\text{–}300\times10^{-3}$ torr, was linear at pressures less than 200×10^{-3} torr and showed quenching at the higher pressures.

D. $CH_4+h\nu \rightarrow CH_2(\tilde{b}\,^1B_1)+H_2(X\,^1\Sigma_g^+)$

Spectra for lower energy incident photons were taken at 1086, 1176, L_α (1216 Å) and 1242 Å. For incident photons at the three shorter wavelengths fluorescence

resulted from $CH_2(\tilde{b}\,^1B_1 \rightarrow \tilde{a}\,^1A_1)$. This radiation was identified by comparison with the results of Herzberg and Johns for the absorption of CH_2.[15] No fluorescence resulted at 1242 A. There are two possible processes to consider that yield CH_2^*: $CH_4+h\nu \rightarrow CH_2^*+H_2(X\,^1\Sigma_g^+)$ and $CH_4+h\nu \rightarrow CH_2^*+2H(1\,^2S_{1/2})$. The first must be considered since the photodetachment of H_2 has been found to be a primary process at 1236 Å in studies made by Mahan and Mandel[17] although their experiment was not capable of detecting excited states. The threshold for producing the lowest energy excited CH_2 fragment in the second process was calculated, using simple energy arguments, to be in the range 1090–1200 Å. Only the range can be specified since the energy of the first singlet state of CH_2 above the triplet ground state is uncertain, although Herzberg believes the energy to be less than 1 eV.[18] Thus the process $CH_4+h\nu \rightarrow CH_2(\tilde{b}\,^1B_1)+H_2(X\,^1\Sigma_g^+)$ appears to be responsible for the CH_2^* radiation, since the other process would have to violate threshold arguments.

E. Other Possible Processes

The $(A\,^2\Delta \rightarrow X\,^2\Pi)$ and $(B\,^2\Sigma \rightarrow X\,^2\Pi)$ transitions of CH, the first three lines of the Balmer series and the $(\tilde{b}\,^1B_1 \rightarrow \tilde{a}\,^1A_1)$ system of CH_2 appear to account for the total emission spectra resulting from CH_4 irradiated by vacuum uv photons over the observed range. The possibility of fluorescence from other fragments such as: C, H_2, CH^+, CH_2^+, CH_4, and CH_4^+ resulting from dissociation and/or ionization processes was also considered. With the exceptions of C and H_2 fluorescence from these fragments is either not possible in the observed range or the incident energies used were not adequate to yield sufficient excitation of the fragments.

For carbon it is possible that emission could result from the process $CH_4+h\nu \rightarrow C^*+2H_2(X\,^1\Sigma_g^+)$. It is possible to ionize C through this process for incident photons of wavelength less than 636 Å thus, for longer wavelengths it is possible to excite those C transitions which fall within the observed range. However, no transitions corresponding to atomic carbon were observed.

Possible transitions resulting from excited H_2 could result from the primary processes

$$CH_4+h\nu \rightarrow CH(X\,^2\Pi)+H_2(2s\sigma\,^3\Sigma_g^+)+H(1\,^2S_{1/2}), \quad (1)$$

$$CH_4+h\nu \rightarrow C(^3P)+H_2(X\,^1\Sigma_g^+)+H_2^*, \quad (2)$$

and

$$CH_4+h\nu \rightarrow CH_2(X\,^3\Sigma_g^-)+H_2^*. \quad (3)$$

For the first of these processes, fluorescence would result from the transition $H_2(2s\sigma\,^3\Sigma_g^+) \rightarrow H_2(2p\sigma\,^3\Sigma_u^+)$. However, the $2p\sigma\,^3\Sigma_u^+$ state is unstable and gives rise to a broad continuum thus, unless this process has a large cross section it is not expected that the fluorescence would be detectable.

In Processes (2) and (3) it is possible to excite higher singlet and triplet states of H_2 than were energetically possible in Process (1). However, if the H_2 is being highly excited, the spectrum from 4000 to 6000 Å should consist of many band systems, as reported by Gale, Monk, and Lee.[19] Thus if any H_2 is excited upon dissociation of CH_4, it has a small cross section compared to the processes observed.

IV. SUMMARY

Fluorescence, in the range 3500–8000 Å is observed from the dissociation fragments of CH_4 when it is irradiated by vacuum ultraviolet light in the range 555–1242 Å. The fluorescence is due to the $A\,^2\Delta \rightarrow X\,^2\Pi$ and $B\,^2\Sigma \rightarrow X\,^2\Pi$ systems of CH, the $CH_2(\tilde{b}\,^1B_1 \rightarrow \tilde{a}\,^1A_1)$ system of CH_2, and the first three Balmer lines of H. Other low intensity transitions may have been present, but were indistinguishable from the noise.

The irradiation wavelength threshold for electronically excited CH occurs near 1032 Å, and results in the process $CH_4+h\nu \rightarrow CH(A\,^2\Delta)+H_2(X\,^1\Sigma_g^+)+H(1\,^2S_{1/2})$. The calculated and measured threshold for the process agree to within 0.05 eV. The maximum absolute cross section occurs near 923 Å and has a value of 7.8×10^{-20} cm².

The threshold for exciting CH to the $B\,^2\Sigma$ state occurs near 950 Å with a maximum absolute cross section of 6.1×10^{-21} cm² near 898 Å. It is suggested that this state results from the process, $CH_4+h\nu \rightarrow CH(B\,^2\Sigma)+H_2(X\,^1\Sigma_g^+)+H(1\,^2S_{1/2})$.

The fluorescence, for all processes observed, approaches zero for incident photons between 626 and 760 Å.

A second measured "threshold" for excitation into the states $CH(A\,^2\Delta)$ and $CH(B\,^2\Sigma)$ occurs at 626 Å. It has not been uniquely determined which of the two possible processes,

$$CH_4+h\nu \rightarrow CH^*+H_2(X\,^1\Sigma_g^+)+H(1\,^2S_{1/2})$$

or

$$CH_4+h\nu \rightarrow CH^*+3H(1\,^2S_{1/2}),$$

is responsible for the excitation at these shorter incident photon wavelengths. However, the absolute cross sections for the responsible process are down an order of magnitude from those associated with $CH_4+h\nu \rightarrow CH^*+H_2(X\,^1\Sigma_g^+)+H(1\,^2S_{1/2})$, identified for incident photons of 900 Å wavelength. In addition, 626 Å corresponds approximately to the threshold for the process $CH_4+h\nu \rightarrow CH_3(X\,^2A_2'')+H^*$ which is suggested as the process resulting in the first three Balmer lines. The process $CH_4+h\nu \rightarrow CH_2(\tilde{b}\,^1B_1)+H_2(^1\Sigma_g^+)$ is suggested as the process responsible for the CH_2 fluorescence. Its maximum cross section is estimated to be $\sigma=1\times10^{-20}$ cm².

* This research was supported under NASA Grants #NGR 05-018-138 and #NGL 05-018-044.

[1] P. H. Metzger and G. R. Cook, J. Chem. Phys. 41, 642 (1964).
[2] P. G. Wilkinson and H. L. Johnston, J. Chem. Phys. 18, 190 (1950).
[3] G. Moe and A. B. F. Duncan, J. Am. Chem. Soc. 74, 3140 (1952).

[4] H. Sun and G. L. Weissler, J. Chem. Phys. **23**, 1160 (1954).
[5] R. W. Ditchburn, Proc. Roy. Soc. (London) A**229**, 44 (1955).
[6] O. P. Rustgi, J. Opt. Soc. Am. **54**, 464 (1964).
[7] V. H. Dibeler, M. Krauss, R. M. Reese, and F. N. Harllee, J. Chem. Phys. **42**, 3791 (1965).
[8] A. Dalgarno, Proc. Phys. Soc. (London) A**65**, 663 (1952).
[9] E. Lindholm, Arkiv Fysik **37**, 37 (1968).
[10] D. F. Strobel, J. Atmospheric Sci. **26**, 906 (1969).
[11] W. C. Walker, N. Wainfan, and G. L. Weissler, J. Appl. Phys. **26**, 1366 (1955).
[12] J. A. R. Samson, J. Opt. Soc. Am. **54**, 6 (1964).
[13] R. W. B. Pearse and A. G. Gaydon, *The Identification of Molecular Spectra* (Wiley, New York, 1963), 3rd ed.
[14] G. Herzberg, Proc. Roy. Soc. (London) A**262**, 291 (1961).
[15] G. Herzberg and J. W. C. Johns, Proc. Roy. Soc. (London) A**295**, 107 (1966).
[16] D. L. Judge and G. L. Weissler, J. Chem. Phys. **48**, 4590 (1968).
[17] B. H. Mahan and R. Mandal, J. Chem. Phys. **37**, 307 (1962).
[18] G. Herzberg, *Molecular Spectra and Molecular Structure III* (Van Nostrand, New York, 1966), p. 584.
[19] H. G. Gale, G. S. Monk, and K. O. Lee, Astrophys. J. **67**, 89 (1928).

Reprinted from:

THE JOURNAL OF CHEMICAL PHYSICS VOLUME 57, NUMBER 1 1 JULY 1972

Electronic Transition Moments for the $A \rightarrow X$, $B \rightarrow X$, and $B \rightarrow A$ Transitions in CO^+ and the $A \leftarrow X$ and $B \leftarrow X$ Moments for the $CO \rightarrow CO^+$ Systems; Absolute Cross Sections for the Absorption Processes*

D. L. JUDGE AND L. C. LEE

Department of Physics, University of Southern California, Los Angeles, California 90007

(Received 21 January 1972)

The $A \rightarrow X$, $B \rightarrow X$, and $B \rightarrow A$ bands of CO^+ have been excited using monochromatic photons and the band intensities measured. Using such data the variation of the electronic transition moments for these above emission bands as well as for the absorption bands $CO(X\,^1\Sigma^+, v''=0) \rightarrow CO^+$ $(A\,^2\Pi_i, v'=0\text{–}8)$ and CO^+ $(B\,^2\Sigma^+, v'=0, 1)$ have been determined. Further, the specific cross sections for the absorption processes have been determined by measuring the total emission intensity in the band system through which the upper state decays. The band intensity measurements and the derived results are presented in the ensuing discussion.

I. INTRODUCTION

In the present work photon excitation was used to excite ground state CO molecules into various levels of the ion and the resulting emission intensity was measured. This is in contrast with earlier work by Robinson and Nicholls[1] who studied the comet-tail band intensities using 60–100 eV electrons to obtain the excited ions. Both experimental results have been interpreted according to a method proposed by Fraser[2] to establish the variation of the electronic transition moments. The specific cross section measurements have not been previously obtained.

The measured intensity $I_{v'v''}$ of the (v', v'') band of a system may be written[3,4] as

$$I_{v'v''}{}^{\mathrm{em}} = KN_{v'}R_e^2(\bar{r}_{v'v''})q_{v'v''}/\lambda_{v'v''}{}^4,$$

where K is a constant, $N_{v'}$ is the population of molecules in the level v' of the upper electronic state of the system of interest, $R_e(\bar{r}_{v'v''})$ is the electronic transition moment for the emission bands, and $\bar{r}_{v'v''}$, $q_{v'v''}$, and $\lambda_{v'v''}$ are the r-centroid, Franck–Condon factor, and wavelength of the (v', v'') band, respectively.

The Franck–Condon factors and the r centroids for the band systems of CO^+ have been computed by Nicholls[5] using Morse potentials and by Jain and Sahni[6] using Rydberg–Klein–Rees (RKR) potential energy curves. We have adopted the latter data for our analysis of the emission band transition moments. The precise wavelengths $\lambda_{v'v''}$ for the transitions of interest have been collected and published by Krupenie.[7] Thus, with the intensity measurements we can plot $N_{v'}R_e^2(\bar{r}_{v'v''}) = I_{v'v''}\lambda_{v'v''}{}^4/Kq_{v'v''}$ against $\bar{r}_{v'v''}$. Such a plot consists of a number of segments, one for each v'' progression (v' = constant). Normalizing the data $(N_{v'}R_e^2)$ for each segment as in Robinson and Nicholls[1] work, i.e., making the area under the overlapped segments equal, permits the relative number of molecules in the upper state to be determined and a plot of $R_e(\bar{r}_{v'v''})$ for the emission bands can then be given.

The absorption intensity from the neutral ground state to the ionization state of interest is given by

$$I_{v'0}{}^{\mathrm{abs}} = K'R_e^2(\bar{r}_{v'0})q_{v'0}/\lambda_{v'0} = K''N_{v'}/\lambda_{v'0},$$

where K' and K'' are constants. The second equality holds since, in the present experiment, the decay rate of the upper level, $N_{v'}$, is integrated for a time long compared to the lifetime of the states of interest so that the actual average population of the upper state is obtained. Thus, $R_e(\bar{r}_{v'0}) = K''(N_{v'}/q_{v'0})^{1/2}$ and the relative variation of the electronic transition moment $R_e(\bar{r})$ for the transition from the neutral ground state to the ionized state, can be displayed by plotting the relative values of $(N_{v'}/q_{v'0})^{1/2}$ against $\bar{r}_{v'0}$. The Franck–Condon factors $q_{v'0}$ for transitions from the neutral ground state $(X\,^1\Sigma^+, v''=0)$ to the ionization states $B\,^2\Sigma^+$ and $A\,^2\Pi_i$ have been computed by Wacks,[8] Halmann and Laulicht,[9] and Nicholls[10] using Morse potentials. The calculations of Wacks are used although no significant differences appear in the results of the different authors.

II. EXPERIMENTAL

The apparatus employed in the fluorescence investigations is shown in Fig. 1. Here, vacuum ultraviolet light[11] was obtained from a condensed spark discharge through a boron nitride capillary containing either air, nitrogen, or argon at a pressure of about 20×10^{-3} torr. The source was operated at 40 pulses/sec with a pulse duration of approximately 5 μsec. The emission lines of interest were isolated by a 1-m normal incidence monochromator (McPherson 225). The selected "lines" used for this investigation were 462, 555, 587, 610, 617, 630, 686, 703, 718, and 746 Å. Typical fluxes at the exit slit of the monochromator for each of the above lines were of the order of 10^{11} photons/sec. Differential pumping at the entrance and exit slits of the monochromator permitted the main chamber to be maintained at an average pressure of 7×10^{-5} torr.

The sample cell was 1.75 in. long and attached to the

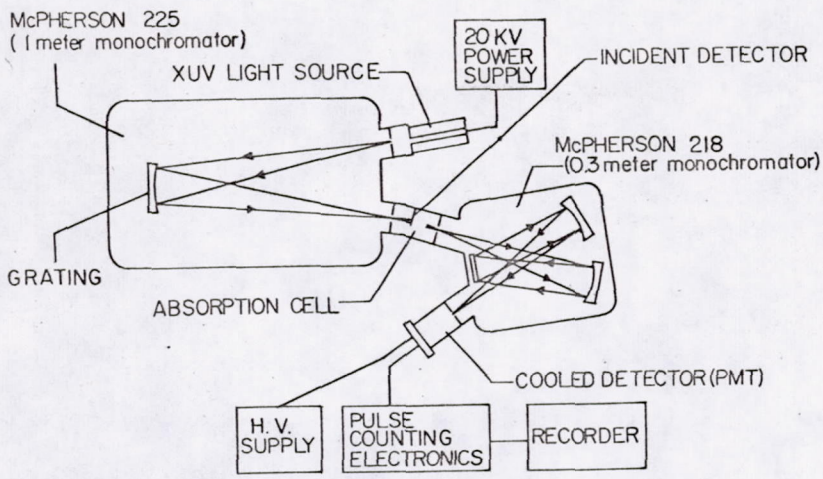

FIG. 1. Schematic diagram of the experimental apparatus.

exit port of the McPherson 225. CO gas, supplied by Airco with a purity of 99.5%, was admitted into the cell and maintained at a pressure of about 10×10^{-3} torr at room temperature for all fluorescence investigations except where the pressure dependence was measured.

The CO^+ fluorescence was dispersed with a normal incidence 0.3-m monochromator (McPherson 218). In order to avoid direct light from the primary light source the entrance optic axis of the McPherson 218 was set 5° off the exit optic axis of the McPherson 225. The monochromator used to disperse the fluorescence light was not evacuated and the fluorescence was viewed through a synthetic quartz (suprasil) window. The slits of this monochromator were set for a bandwidth of 6 Å in the first order for the comet-tail system ($A\rightarrow X$), 4.5 Å for the first negative system ($B\rightarrow X$), and 7.5 Å for the Baldet–Johnson system ($B\rightarrow A$).

The dispersed fluorescence radiation was synchronously detected[12] with a cooled EMI 9558QB photomultiplier. The wavelength response of the 0.3-m monochromator and the associated photomultiplier system was calibrated with a Natl. Bur. Std. standard lamp in 3000–6500 Å region, and with the CO bands between 2500 and 3200 Å. The CO line intensities were measured by using a sodium salicylate wavelength converter and a photomultiplier tube. Over the 2500–3200 Å region sodium salicylate is known to have a constant quantum efficiency.[13] The region between 1800 and 2700 Å could be observed directly with the 9558QB phototube which has a constant quantum efficiency in this range. The experimental errors arise from fluctuation of the light source intensity, optical calibration, and noise of the electronic equipment. The resulting experimental error is less than 15%.

III. EXPERIMENTAL RESULTS

A. The Fluorescence Spectrum

A typical fluorescence spectrum resulting from 555 Å (22.4 eV) photon impact on CO is shown in Fig. 2. The bandhead data given by Krupenie[7] have been used to identify this spectrum which is characteristic of all spectra resulting from incident photons with sufficient energy (20.2 eV) to excite CO molecules up to the $v'=2$ level of the $CO^+(B\,^2\Sigma^+)$ state. For lower incident energies only successively lower states of excitation are

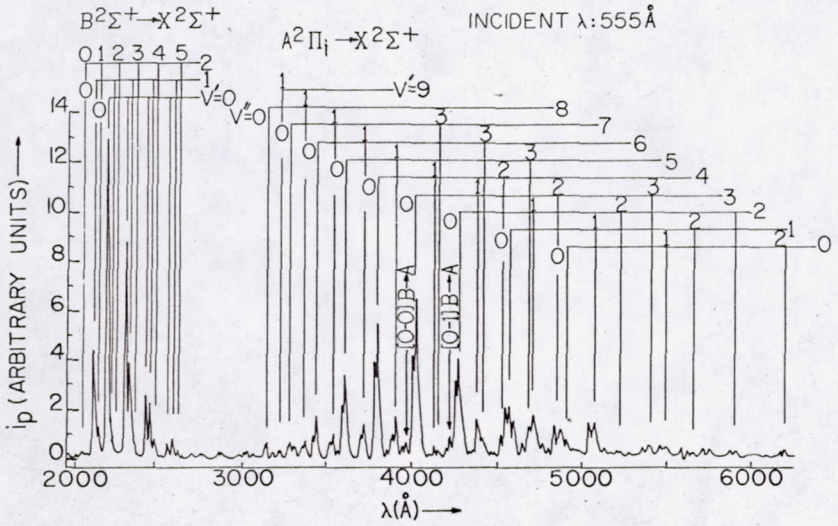

FIG. 2. Dispersed fluorescence of CO for 22.4 eV (555 Å) photon excitation for the $A\,^2\Pi_i\rightarrow X\,^2\Sigma^+$, $B\,^2\Sigma^+\rightarrow X\,^2\Sigma^+$, and $B\,^2\Sigma^+\rightarrow A\,^2\Pi_i$ systems. The bandhead positions collected by Krupenie are indicated. The ordinate indicates the current output from an EMI9558QB photomultiplier and the abscissa indicates the wavelength of the dispersed fluorescence.

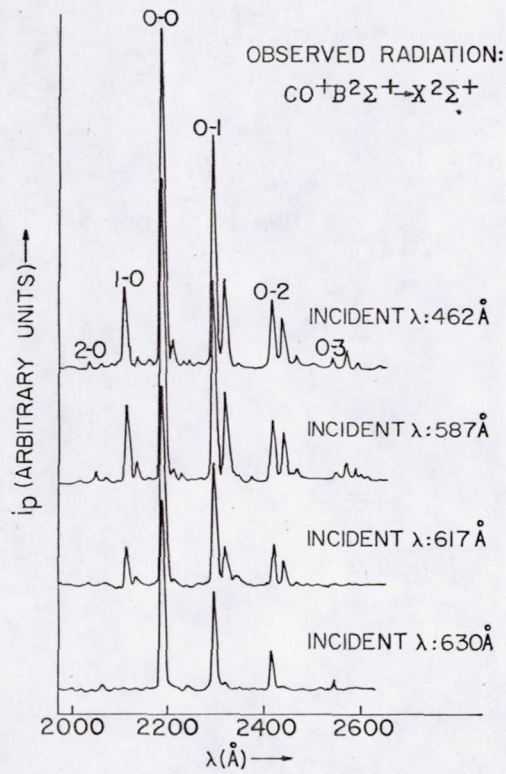

FIG. 3. Dispersed fluorescence of the $CO^+(B\,^2\Sigma^+ \rightarrow X\,^2\Sigma^+)$ system excited by photons of various wavelengths as indicated.

energetically possible as is illustrated in Figs. 3 and 4. Figure 3 shows the $B \rightarrow X$ spectrum of CO^+ for various incident energies while Fig. 4 shows the $A \rightarrow X$ and $B \rightarrow A$ spectra, again for various incident energies. The highest vibrational levels which could be excited with the various photon energies are as follows: $CO^+(B\,^2\Sigma^+, v'=1)$ for incident photons of 617 Å, $CO^+(B\,^2\Sigma^+, v'=0)$ for 630 Å, $CO^+(A\,^2\Pi_i, v'=8)$ for 686 Å, $CO^+(A\,^2\Pi_i, v'=6)$ for 703 Å, and $CO^+(A\,^2\Pi_i, v'=4)$ for 718 Å.

TABLE I. Relative band strengths for the $CO(^1\Sigma^+, v''=0) \rightarrow CO^+(A\,^2\Pi_i, v'=0\text{–}8)$ system.

	v'								
v''	0	1	2	3	4	5	6	7	8
0	0.47	0.91	1.0	0.83	0.61	0.39	0.23	0.12	0.06

The features which appear at 3914, 4390, and 4610 Å are spurious, and correspond to the 0–0 transition of $N_2^+(B \rightarrow X)$ and the second order transitions of the 0–0 and 0–1 bands of $B \rightarrow X$ of CO^+, respectively. These have been deleted from the data on R_e and $N_{v'}$. The band intensities used throughout have been determined by measuring the area under the curve associated with each band.

The results obtained in the analysis of the various band systems are presented in the following sections.

B. $A\,^2\Pi_i \rightarrow X\,^2\Sigma^+$ Bands

The plot of $N_{v'}R_e^2(\bar{r}_{v'v''})$ vs $\bar{r}_{v'v''}$, the r centroid, for the $A\,^2\Pi_i \rightarrow X\,^2\Sigma^+$ transition excited by photons of 686 Å is shown in Fig. 5, where it may be noted that the $N_{v'}R_e^2(\bar{r}_{v'v''})$ segments for each v'' progression are constant within 10%. The constancy of $R_e(\bar{r}_{v'v''})$ derived from different photon-excitation data is shown in Fig. 6. Here, $R_e(\bar{r}_{v'v''})$ for all $(v', 0)$ bands is shown normalized. It is clear from the plot that no statistically significant deviations from constant R_e occur.

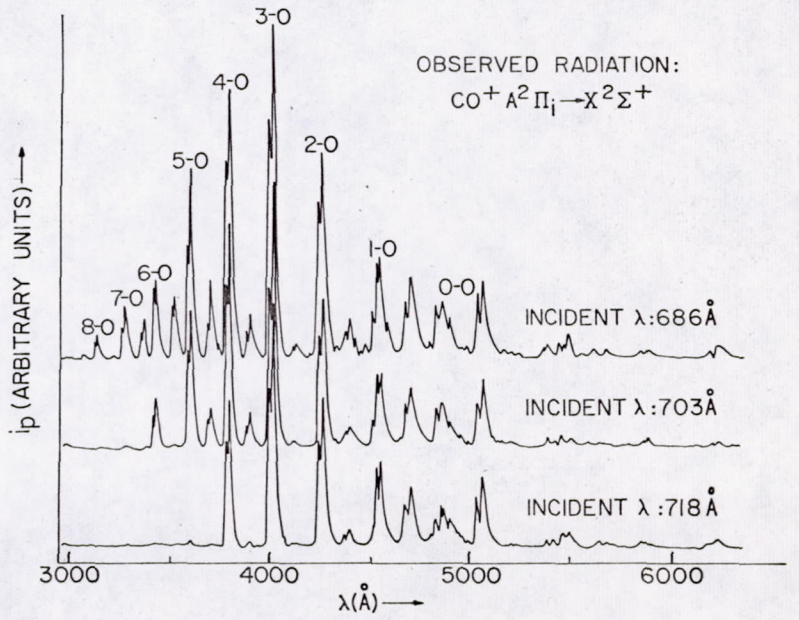

FIG. 4. Dispersed fluorescence of the $CO^+(A\,^2\Pi_i \rightarrow X\,^2\Sigma^+)$ system excited by photons of various wavelengths as indicated.

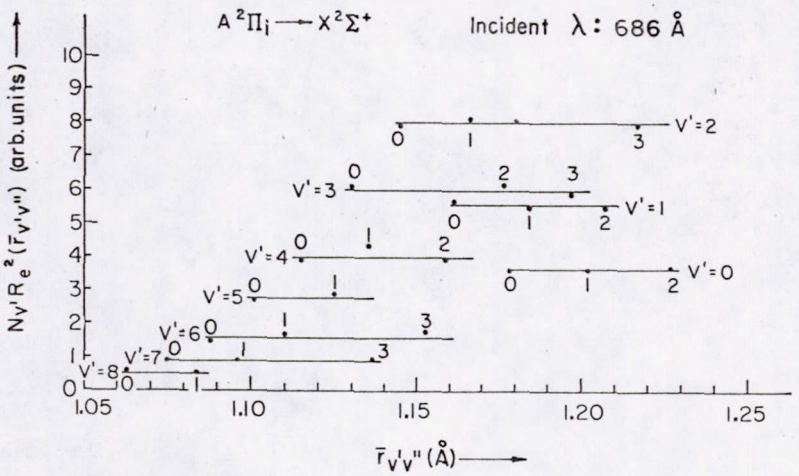

FIG. 5. A plot of $N_{v'}R_e^2(\bar{r}_{v'v''})$ vs $\bar{r}_{v'v''}$ in arbitrary units for the vibrational bands of the $CO^+(A\ ^2\Pi_i \rightarrow X\ ^2\Sigma^+)$ system excited by photons of wavelength 686 Å. The values of $\bar{r}_{v'v''}$ were calculated by Jain and Sahni.

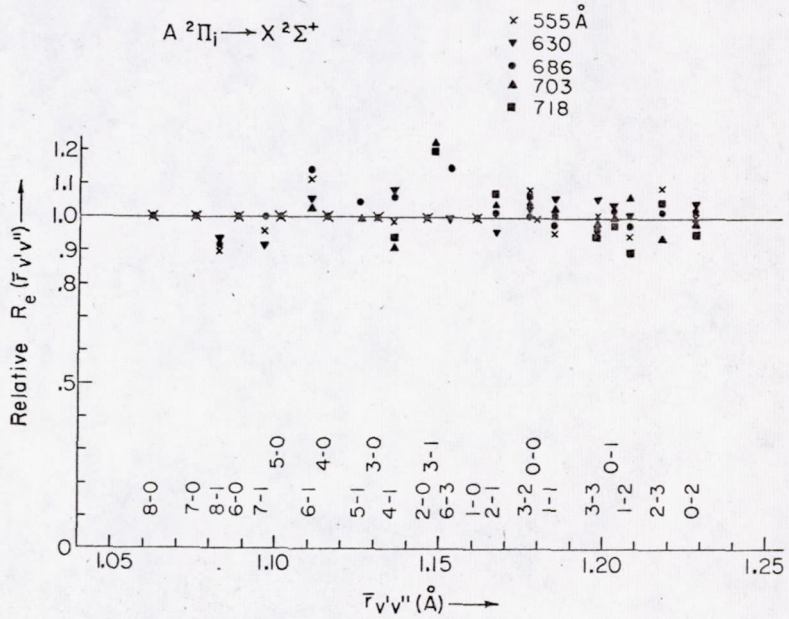

FIG. 6. A plot of the relative electronic transition moment R_e vs the r centroid for the vibrational bands of the $CO^+(A\ ^2\Pi_i \rightarrow X\ ^2\Sigma^+)$ system. The data shown are for incident photons of wavelengths 555, 630, 686, 703, and 718 Å.

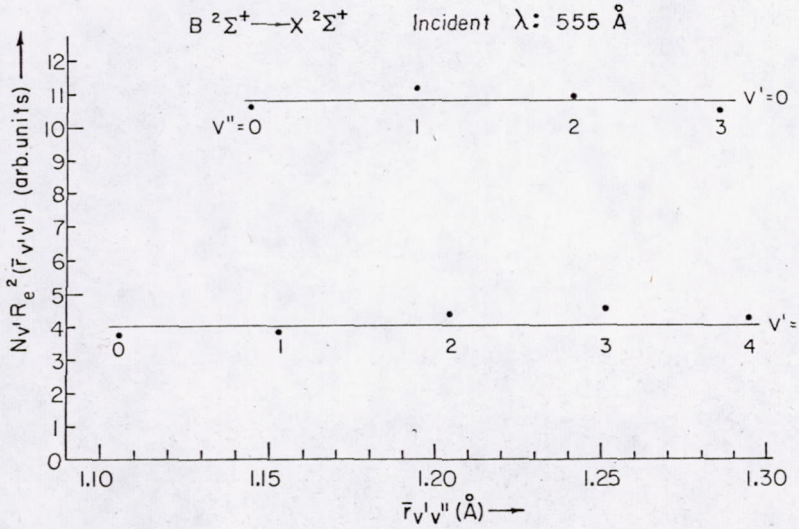

FIG. 7. A plot of $N_{v'}R_e^2(\bar{r}_{v'v''})$ vs $\bar{r}_{v'v2''}$ in arbitrary units for the vibrational bands of the $CO^+(B\ ^2\Sigma^+ \rightarrow X\ ^2\Sigma^+)$ system excited by photons of wavelength 555 Å.

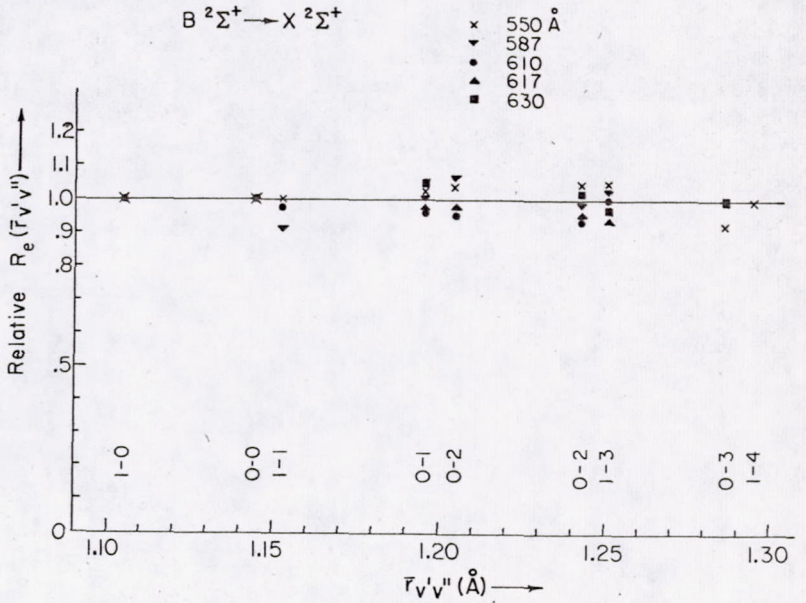

FIG. 8. A plot of the relative electronic transition moment R_e vs the r centroid for the vibrational bands of the $CO^+(B\ ^2\Sigma^+ \rightarrow X\ ^2\Sigma^+)$ system.

C. $B\ ^2\Sigma^+ \rightarrow X\ ^2\Sigma^+$ Bands

In Fig. 7, $N_{v'}R_e^2(\bar{r}_{v'v''})$ vs $\bar{r}_{v'v''}$ for the $B\ ^2\Sigma^+ \rightarrow X\ ^2\Sigma^+$ transitions has been plotted for the case of photon excitation at 555 Å. From the plot it is seen that $N_{v'}R_e^2(\bar{r}_{v'v''})$ is constant for each v'' progression within 10% and $R_e(\bar{r})$ is therefore constant. A plot of $R_e(\bar{r}_{v'v''})$ vs $\bar{r}_{v'v''}$ is given for various incident photon energies in Fig. 8.

D. $B\ ^2\Sigma^+ \rightarrow A\ ^2\Pi_i$ Bands

Only the (0–0) and (0–1) bands were observed for the $B\ ^2\Sigma^+ \rightarrow A\ ^2\Pi_i$ transitions when CO was excited by photons which had an energy higher than 19.7 eV, the energy required to reach the second vibrational level. Since only two data points exist for the measurement of $R_e(\bar{r})$ it has not been plotted but it is constant as found for the other emission systems.

E. $CO(X\ ^1\Sigma^+, v''=0) \rightarrow CO^+(A\ ^2\Pi_i, v'=0\text{–}8)$ Bands

The square of the electronic transition moment is proportional to the band strength for the band of interest, the proportionality constant being the appropriate Franck–Condon factor. The band strengths $p_{v'v''}$ for the absorption transitions are proportional to $N_{v'}$, the relative values of which are obtained from the intensity ratios of the v' progressions, i.e., the normaliza-

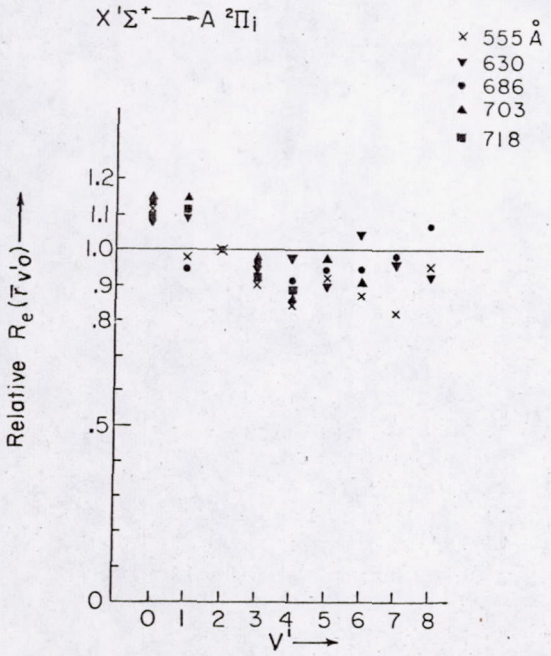

FIG. 9. A plot of the relative transition moment $R_{e\,v'0}$ vs the vibrational level v' for the vibrational bands of the $CO(X\ ^1\Sigma^+, v''=0) \rightarrow CO^+(A\ ^2\Pi_i, v'=0\text{–}8)$ system.

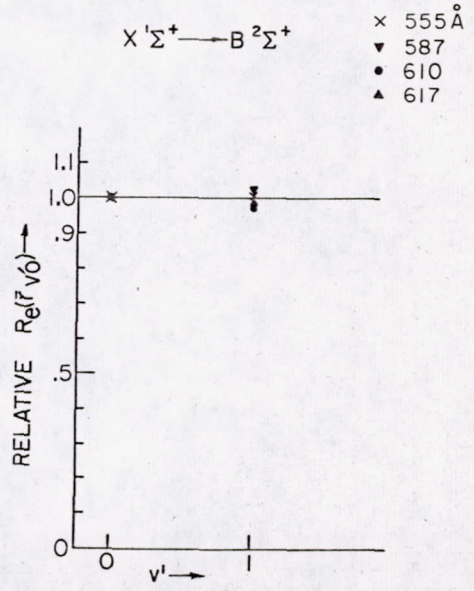

FIG. 10. A plot of the electronic transition moment $R_{e\,v'0}$ vs vibrational level v' for the vibrational bands of the $CO(X\ ^1\Sigma^+, v''=0) \rightarrow CO^+(B\ ^2\Sigma^+, v'=0, 1)$ system.

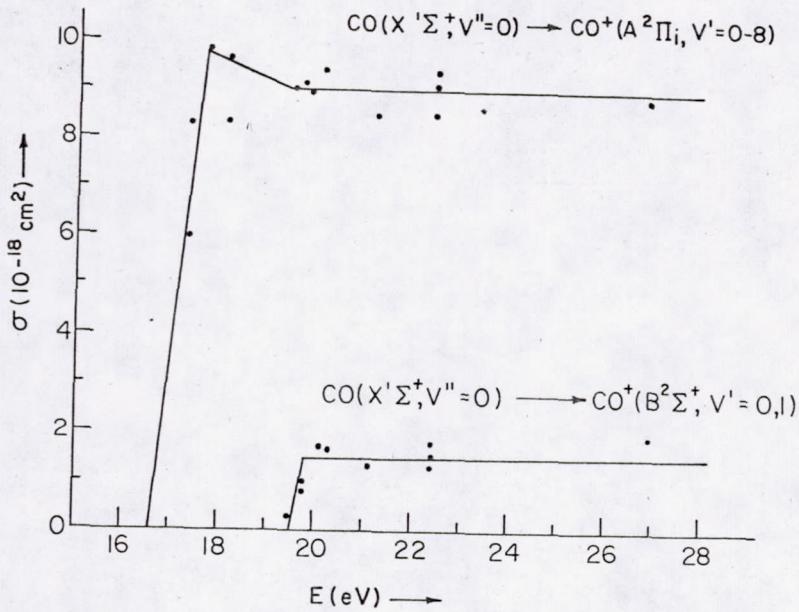

FIG. 11. The cross sections of the $CO(X\,^1\Sigma^+,\ v''=0)\rightarrow CO^+(A\,^2\Pi_i,\ v'=0\text{–}8)$ and $CO(X\,^1\Sigma^+,\ v''=0)\rightarrow CO^+(B\,^2\Sigma^+,\ v'=0,\ 1)$ systems for various incident photon energies.

tion factors used earlier in normalizing the $R_e(\bar{r})$ for the $A\rightarrow X$ system of CO^+. The band strength is related to the band intensity in absorption according to

$$I_{v'v''}{}^{\text{abs}}=K_1R_{e\,v'v''}{}^2q_{v'v''}\nu_{v'v''}=K_1\nu_{v'v''}p_{v'v''},$$

and

$$I_{v'v''}{}^{\text{abs}}=K_2N_{v'}\nu_{v'v''}.$$

Combining the results of the above two equations, the band strength is thus seen to be

$$p_{v'v''}=K_3N_{v'},$$

as stated above.

The measured average band strengths for the $CO(X\,^1\Sigma^+,\ v''=0)\rightarrow CO^+(A\,^2\Pi_i,\ v'=0\text{–}8)$ system are given in Table I.

The variation of $R_{e\,v'v''}$ with v' then is just

$$R_{e\,v'v''}=(p_{v'v''}/q_{v'v''})^{1/2}$$

and the results for the incident wavelengths of 555, 630, 686, 703, and 718 Å are plotted in Fig. 9.

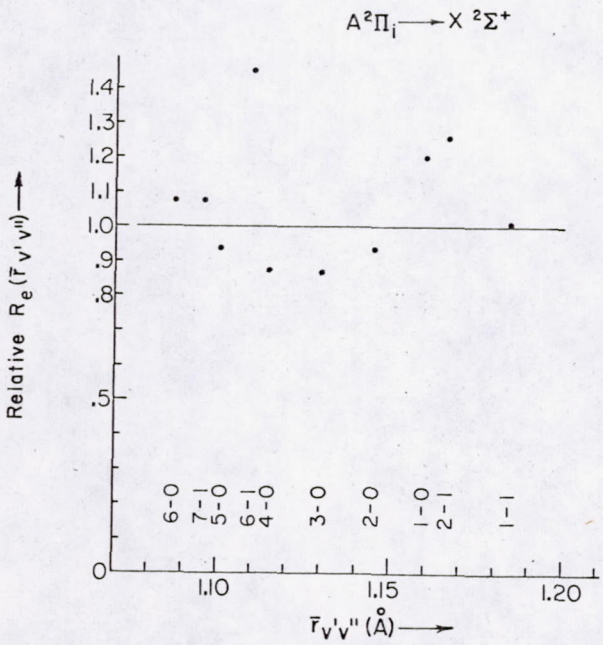

FIG. 12. A plot of the relative electronic transition moment R_e vs the r-centroid bands of the $CO^+(S\,^2\Pi_i\rightarrow X\,^2\Sigma^+)$ system. $R_e(\bar{r}_{v'v''})$ is calculated from the lifetime data published by Fink and Welge.

F. $CO(X\,^1\Sigma^+,\ v''=0)\rightarrow CO^+(B\,^2\Sigma^+,\ v'=0,\ 1)$ Bands

The band strength and the variation of the electronic transition moment for these bands have been determined in the same manner as for the $CO(X\,^1\Sigma^+,\ v''=0)\rightarrow CO^+(A\,^2\Pi_i,\ v'=0\text{–}8)$ bands. The relative band strengths are $p_{0,0}:p_{1,0}=1.0:0.36$. R_e vs v' is given in Fig. 10.

G. Cross Section for the $CO(X\,^1\Sigma^+,\ v''=0)\rightarrow CO^+(A\,^2\Pi_i$ $v'=0\text{–}8)$ and $CO(X\,^1\Sigma^+,\ v''=0)\rightarrow$ $CO^+(B\,^2\Sigma^+,\ v'=0\text{–}1)$ Bands

The absolute cross sections for the above systems were determined by measuring the photon production rate of these bands relative to nitrogen, for which the cross section for the $N_2(X\,^1\Sigma^+,\ v''=0)\rightarrow N_2{}^+(B\,^2\Sigma^+,\ v'=0)$ band is known[14] to be 2.2×10^{-18} cm^2. The cross sections are equal to the photon production rate $\sum_{v'}\dot{n}_{v'}$ multiplied by a normalization constant, i.e.,

$$\sigma=K\sum_{v'}\dot{n}_{v'},$$

where the normalization constant is determined

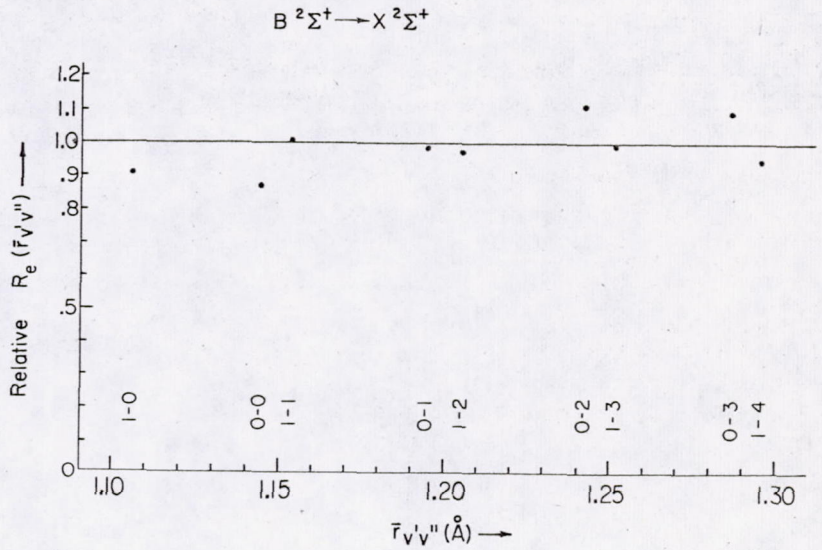

FIG. 13. A plot of the relative electronic transition moment R_e vs the r centroid for the vibrational bands of the $CO^+(B\,^2\Sigma^+ \rightarrow X\,^2\Sigma^+)$ system. $R_e(\bar{r}_{v'v''})$ is calculated from the data of transition probabilities published by Lawrence.

through comparison with the nitrogen fluorescence measurements. Figure 11 shows the cross sections as a function of incident photon energy. For incident photon energies beyond threshold, the cross section for the $CO(X\,^1\Sigma^+, v''=0) \rightarrow CO^+(A\,^2\Pi_i, v'=0\text{–}8)$ bands is about 9×10^{-18} cm^2 and for the $CO(X\,^1\Sigma^+, v''=0) \rightarrow CO^+(B\,^2\Sigma^+, v'=0, 1)$ bands is about 1.5×10^{-18} cm^2. The sum of the band strengths of the $CO^+(B\,^2\Sigma^+, v'=0) \rightarrow CO^+(A\,^2\Pi_i, v''=0, 1)$ transition is about 8% of that of the $CO^+(B\,^2\Sigma^+, v'=0, 1) \rightarrow CO^+(X\,^2\Sigma^+, v''=0\text{–}4)$ bands.

H. Fluorescence Pressure Dependence

In order to ensure that the emission process was only through radiation, the pressure dependence of the fluorescence intensity was studied. The fact that at low pressure the fluorescence intensity is proportional to the number of photons absorbed confirms that the emission process is only through radiation. It has been noted that the fluorescence intensity from the $v'=0$ level of $CO^+(A\,^2\Pi_i)$ state continues to increase up to a pressure of about 50×10^{-3} torr, whereas the fluorescence intensities from most of the levels only increase up to approximately 30×10^{-3} torr. This intensity enhancement of the $v'=0$ level of $CO^+(A\,^2\Pi_i)$ is attributed to "dumping" of the higher vibrational levels through collisional relaxation into the lowest level of the state.

IV. DISCUSSION OF RESULTS

It has been shown that all of the electronic transition moments measured here are independent of the internuclear separation r. This result is in disagreement with the work of Robinson and Nicholls[1] who found a systematic variation of $R_e(r)$ for the comet-tail system but is in agreement with the semiempirical results of Spindler and Wentink[15] and is further confirmed by the lifetime measurements of Fink and Welge[16] and Bennett and Dalby.[17] To compute R_e from the lifetime data recall that the electronic moment is related to the lifetime of the mth electronic level $\tau_{v'v''}{}^{mn}$ according to

$$1/\tau_{v'v''}{}^{mn} = \alpha d_n \nu_{v'v''}{}^3 \mid R_e{}^{mn} \mid^2 q_{v'v''},$$

where m and n represent the initial and final electronic states, respectively. α is a constant and d_n is the degeneracy of the final state. A plot of R_e vs $\bar{r}$ for each of the vibrational levels for which the lifetime was measured is given in Fig. 12 where it may be noted that there is no systematic variation of $R_e(r)$, in agreement with the present work.

The electronic transition moment for the $B \rightarrow X$ bands of CO^+ can also be obtained from lifetime measurements. Lawrence[18] has measured several of the band lifetimes and a plot of R_e on $\bar{r}$ is shown in Fig. 13 using his data.

The constancy of the cross sections of both the $A \rightarrow X$ and $B \rightarrow X$ systems for excitation energies well beyond threshold is consistent with the photoelectron spectroscopy data given by Schoen.[19]

The ratio of specific cross sections for formation of the $B\,^2\Sigma^+$ and $A\,^2\Pi_i$ states is equal to 17% and agrees with Schoen's result. Taking Schoen's data that the $A\,^2\Pi_i$ state contributes 60 ± 18% of the excitation of CO to the three CO^+ states, we find that the maximum total ionization cross section is 15 ± 5 Mb. This value is consistent with that of 17 Mb given by Cook *et al.*,[20] but is lower than that of 22 Mb given by Cairns *et al.*[21] Finally, the branching ratio for the $B \rightarrow A$ to $B \rightarrow X$ system is 8% and agrees well with Lawrence[11] who gives a value of 10% within a factor of 2.

ACKNOWLEDGMENTS

The authors wish to thank Professor M. Ogawa for his encouraging discussions and Professor R. W. Nicholls for his helpful suggestions.

This may be due to a pressure effect, since their measurements were obtained at 61 mtorr whereas the lower values found here were obtained at a pressure of 35 mtorr. The experimental error of the relative values for the cross sections is less than 10%.

D. Absolute $CO_2^+[A\,^2\Pi_u, B\,^2\Sigma_u^+ \rightarrow X\,^2\Pi_g]$ Fluorescence Cross Sections

At low pressure the observed fluorescence radiation rate described by Eq. (1) can be reduced to

$$\dot{n}_f(\lambda, \lambda_f) = \sigma_f(\lambda, \lambda_f) F(\lambda_f) I_0(\lambda) \gamma(\lambda) p, \qquad (2)$$

where $\gamma(\lambda) \equiv \beta(\lambda)/\sigma_T(\lambda)$ is a pressure independent factor which characterizes the density distribution.

The absolute fluorescence cross section for an electronic state, $\sum_f \sigma_f(\lambda, \lambda_f)$, can be obtained from Eq. (2), if we compare the total fluorescence rate $\sum_f \dot{n}_f(\lambda, \lambda_f)/F(\lambda_f)$ for the CO_2^+ electronic state with that of the $N_2^+(B\,^2\Pi_u^+,\ v'=0) \rightarrow N_2^+(X\,^2\Sigma_g^+, v''=0)$ band, for which the absolute cross section is known.[13] The factor $\gamma(\lambda)$ can be assumed to be the same for both CO_2 and N_2.[12] The spatial distribution of the CO_2^+ radiation is isotropic as measured by Wauchop and Broida,[6] and that of N_2^+ is presumed isotropic since the photoionization electron distribution is isotropic.[14]

The CO_2^+ fluorescence cross sections are shown in Fig. 4. The cross sections at the wavelengths between 555 and 686 Å are about 7 Mb for the $B\,^2\Sigma_u^+ \rightarrow X\,^2\Pi_g$ band system and 19 Mb for the $A\,^2\Pi_u \rightarrow X\,^2\Pi_g$ system.

The experimental error for these absolute cross sections is estimated to be less than 20%.

IV. CONCLUDING REMARKS

The present $CO_2^+[A\,^2\Pi_u, B\,^2\Sigma_u^+ \rightarrow X\,^2\Pi_g]$ fluorescence cross sections of 19 and 7 Mb, respectively, are lower than those of Wauchop and Broida,[6] although they are in qualitative agreement with their corresponding measurements of 25 and 17 Mb. Thus both sets of fluorescence cross section data are just the reverse of Bahr's result[5] on the specific ionization cross sections.

Due to the resolution limitation of Bahr's photoelectron spectrometer, the relative cross sections for producing the $CO_2^+(A\,^2\Pi_u)$ and $CO_2^+(B\,^2\Sigma_u^+)$ states given by Bahr *et al.*[5] may be in error, although there is probably no error in the relative cross sections for forming $CO_2^+(X\,^2\Pi_g)$ and $CO_2^+(C\,^2\Sigma_g^+)$ since they are well separated. Bahr's data that excitation to the $CO_2^+(X\,^2\Pi_g)$ state contributes about 25% to the total ionization cross section, combined with the present

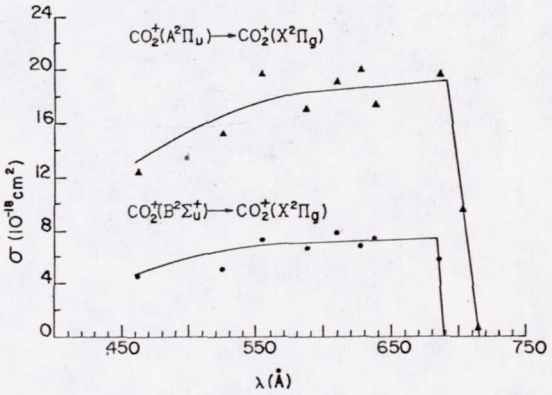

FIG. 4. Fluorescence cross sections for the production of the $CO_2^+[A\,^2\Pi_u, B\,^2\Sigma_u^+ \rightarrow X\,^2\Pi_g]$ band systems.

cross section, yields a total cross section for the production of $CO_2^+(X\,^2\Pi_g, A\,^2\Pi_u,$ and $B\,^2\Sigma_u^+)$ of about 35 Mb from 640 to 686 Å, in agreement with Cairns' and Samson's data.[1] At shorter wavelengths the formation of $CO_2^+(C\,^2\Sigma_g^+)$ also contributes to the total cross section. Again, by combining Bahr's data with the present data, reasonable agreement is found with Cairns' and Samson's results.

The possibility of radiation from $CO_2^+(C\,^2\Sigma_g^+ \rightarrow A\,^2\Pi_u)$ was also investigated, but none was observed, perhaps due to predissociation of the upper state.

* This research was supported by NASA Contract #NGR 05-018-138.

[1] R. B. Cairns and J. A. R. Samson, J. Opt. Soc. Am. **56**, 526 (1966), and J. Geophys. Res. **70**, 99 (1965).
[2] H. Sun and G. L. Weissler, J. Chem. Phys. **23**, 1625 (1966).
[3] R. S. Nakata, K. Watanabe, and F. M. Matsunaga, Sci. Light **14**, 54 (1965).
[4] G. R. Cook, P. H. Metzger, and M. Ogawa, J. Chem. Phys. **44**, 2935 (1966).
[5] J. L. Bahr, A. J. Blake, J. H. Carver, and V. Kumar, J. Quant. Spectry. Radiative Transfer **9**, 1359 (1969).
[6] T. S. Wauchop and H. P. Broida, J. Geophys. Res. **76**, 21 (1971).
[7] J. B. Pearce, K. A. Gause, E. F. Mackey, K. K. Kelly, W. G. Fastie, and C. A. Barth, Appl. Optics, **10**, 805 (1971).
[8] M. Shimizu, Rept. Ion. Space Res. Japan **20**, 271 (1966).
[9] D. L. Judge and L. C. Lee, J. Chem. Phys. **57**, 455 (1972); A. R. Welch and D. L. Judge, *ibid.* **57**, 286 (1972).
[10] W. C. Walker, N. Wainfan, and G. L. Weissler, J. Appl. Phys. **26**, 1366 (1955).
[11] Trade name of a capacitance monometer manufactured by MKS Instruments, Inc.
[12] D. L. Judge and L. C. Lee, "Cross Section for the Production of $CO(a'\,^3\Sigma^+, d\,^3\Delta_i, e\,^3\Sigma^-)$ Triplet States by Photodissociation of CO_2," J. Chem. Phys. (to be published).
[13] D. L. Judge and G. L. Weissler, J. Chem. Phys. **48**, 4590 (1968).
[14] J. Berkowitz, H. Ehrhardt, and T. Tekaat., Z. Physik **200**, 69 (1967).

Reprinted from:
THE JOURNAL OF CHEMICAL PHYSICS VOLUME 58, NUMBER 1 1 JANUARY 1973

Cross sections for the production of CO($a'\,^3\Sigma^+$, $d\,^3\Delta_i$, and $e\,^3\Sigma^- \rightarrow a\,^3\Pi$) fluorescence through photodissociation of CO_2†

D. L. Judge and L. C. Lee
Department of Physics, University of Southern California, Los Angeles, California 90007
(Received 5 April 1972)

Cross sections for the production of CO($a'\,^3\Sigma^+$, $d\,^3\Delta_i$, and $e\,^3\Sigma^- \rightarrow a\,^3\Pi$) fluorescence through photodissociation of CO_2 have been measured from 764 to 923 Å using a line emission source. The CO fluorescence spectra produced in the photodissociation are presented and identified. The cross sections for the production of fluorescence from various vibrational levels of CO* using incident photons of 901 and 923 Å are also presented.

I. INTRODUCTION

When a CO_2 molecule absorbs a high energy photon (<1080 Å) it is possible for the following reactions to occur:

$$CO_2 + h\nu \rightarrow CO_2^*$$
$$\rightarrow CO(a'\,^3\Sigma^+, d\,^3\Delta_i, e\,^3\Sigma^-, \text{or } a\,^3\Pi) + O(^3p).$$

The excited CO molecules formed in those states above the metastable $a\,^3\Pi$ state will then cascade into the $a\,^3\Pi$ state through radiative decay, i.e.,

$$CO(a'\,^3\Sigma^+, d\,^3\Delta_i, \text{or } e\,^3\Sigma^-) \rightarrow CO(a\,^3\Pi) + h\nu'.$$

The production of CO($a\,^3\Pi$) by this process has been studied by Welge and Gilpin[1] using a time-of-flight spectroscopy technique. It has also been directly observed by Lawrence[2] from the "phosphorescence" of the CO($a\,^3\Pi - X\,^1\Sigma$) Cameron bands.

The fluorescence from CO($a'\,^3\Sigma^+$, $d\,^3\Delta_i$, or $e\,^3\Sigma^-$) to CO($a\,^3\Pi$) has been observed by Cook *et al.*[3] and Judge and Carlson[4] although there have been no absolute measurements of the cross section for formation of these states, nor has the pressure dependence been adequately investigated. These measurements and their implications are presented in the present paper.

II. EXPERIMENT

The experimental setup has been described in a previous paper.[5] The nominal vacuum uv emission lines selected for this investigation were 764, 789, 835, 879, 901, and 923 Å. The bandwidth of the 1-m normal incidence monochromator (McPherson 225) used for isolation of those lines was set at 4 Å. The bandwidth of the 0.3-m normal incidence monochromator (McPherson 218) used for dispersing the fluorescence was set at 12.5 Å or less.

The scattered source light of wavelength shorter than 715 Å produces an intense CO_2^+ fluorescence[6] from 2883 to 5000 Å, of which the second order would interfere with the measured CO triplet bands. Thus, a sharp cutoff filter (Corning 3–75) was placed in front of the cooled EMI 9558QB photomultiplier to remove the fluorescence of wavelength shorter than 3800 Å. The detecting system was calibrated with a NBS standard quartz iodine lamp. The relative system response (photons/second) is shown in Fig. 1. The intensity of the light source was measured with a nickel film for which the quantum efficiency was known.[7]

CO_2 gas supplied by Airco with a purity of 99.99% was used for this investigation without further purification. The pressure measurements indicated throughout the text were obtained with a Baratron capacitance monometer (MKS Instruments, Inc.), which was remote from the absorption cell and on the high pressure side of the flow system.

III. RESULTS

A. Fluorescence Spectra

The CO fluorescence spectra produced by photodissociation of CO_2 with incident light of 901 and 923 Å are shown in Fig. 2 and with 764 Å in Fig. 3. The bandhead positions given by Krupenie[8] were used to identify the Asundi ($a'\,^3\Sigma^+ \rightarrow a\,^3\Pi$) and the Herman ($e\,^3\Sigma^- \rightarrow a\,^3\Pi$) bands while the Triplet ($d\,^3\Delta_i \rightarrow a\,^3\Pi$) bandheads were identified using the calculated values of Albritton *et al.*[9] If we adopt the CO_2 dissociation energy as 5.45 eV,[10] the highest energetically possible levels are CO($a'\,^3\Sigma^+$, $v'=11$) for an incident energy of 13.77 eV (901 Å), and CO($a'\,^3\Sigma^+$, $v'=8$) for 13.45 eV (923 Å). All possible bands were experimentally observed. The fluorescence bands produced with higher incident energies are difficult to identify because several bands are mixed together (see, for example, Fig. 3, Curve a). The spectrum shown in Fig. 3, Curve b, includes a part of the CO_2^+ fluorescence spectrum produced by scattered source light of energy higher than 17.36 eV (715 Å), the threshold for excitation of the first excited state of CO_2^+.

B. Pressure Dependence of the Fluorescence Intensity

The pressure dependence of the CO($d\,^3\Delta_i$, $v'=3$) $\rightarrow$ CO($a\,^3\Pi$, $v''=0$) fluorescence band intensity produced by photodissociation of CO_2 with 923 Å photons incident is shown in Fig. 4; that of the $N_2^+(B\,^2\Sigma_u^+, v'=0) \rightarrow N_2^+(X\,^2\Sigma_g^+, v''=0)$ band intensity with 555 Å photons incident is also shown in Fig. 4 for comparison.

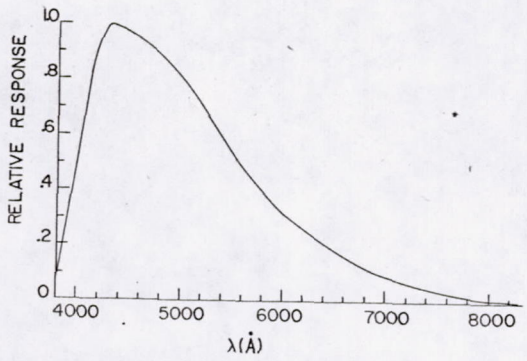

FIG. 1. Relative response (per photon/second) of the fluorescence detection system as a function of wavelength.

If the pressure is low enough such that the fluorescence intensity is linearly dependent on the CO_2 pressure, the observed average fluorescence radiation rate of the CO bands may be described[11] by

$$\dot{n}_f(\lambda, \lambda_f) = I_0(\lambda)\ \exp\left(-\sigma_T(\lambda)\int_0^L n'(x)\,dx\right).$$

$$\times\int_0^l n(x)\sigma_f(\lambda, \lambda_f)\ \exp\left(-\sigma_T(\lambda)\int_0^x n(x)\,dx\right) F(\lambda_f)\,dx,$$

where λ and λ_f are the incident and the fluorescence wavelengths, $I_0(\lambda)$ is the incident vacuum uv radiation intensity (in units of photons per second), $\sigma_T(\lambda)$ is the total absorption cross section at the incident wavelength λ, $n'(x)$ and L are the gas concentration and the light path over which fluorescence radiation is not detected, $n(x)$ and l are the detectable gas concentration and light path, $\sigma_f(\lambda, \lambda_f)$ is the cross section for production of the fluorescing state, and $F(\lambda_f)$ is the efficiency of the detection system as shown in Fig. 1.

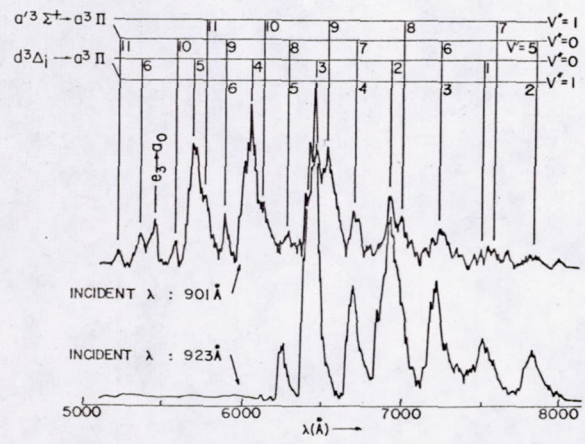

FIG. 2. The CO fluorescence spectra produced by the photodissociation of CO_2 with incident photons having wavelengths of 901 and 923 Å. The bandhead positions given by Krupenie and by Albritton *et al.* are indicated.

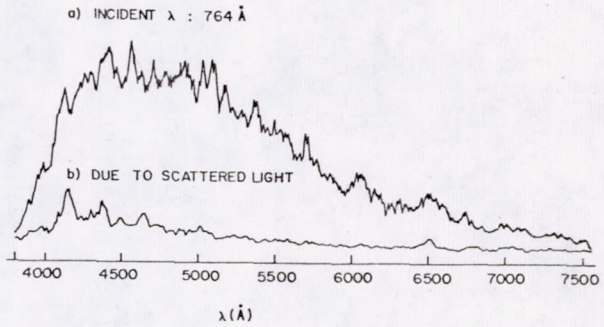

FIG. 3. a: The CO fluorescence spectrum produced by photodissociation of CO_2 with incident photons having a wavelength of 764 Å. b: The CO_2^+ spectrum due to scattered light at wavelengths shorter than 715 Å. This contribution to the total signal can be determined by taking off-line data and thereby be removed from it.

Both $n'(x)$ and $n(x)$ are proportional to the local pressure and in a steady state the local pressure will be proportional to the pressure monitored by the pressure meter. Thus, the observed fluorescence radiation rate can be expressed by

$$\dot{n}_f(\lambda, \lambda_f) = \sigma_f(\lambda, \lambda_f) F(\lambda_f) I_0(\lambda)\ \exp[-\alpha(\lambda)p]$$
$$\times\{1-\exp[-\beta(\lambda)p]\}/\sigma_T(\lambda), \quad (1)$$

or

$$\dot{n}_f(\lambda, \lambda_f) = a(\lambda, \lambda_f)\ \exp[-\alpha(\lambda)p]\{1-\exp[-\beta(\lambda)p]\}, \quad (2)$$

where

$$\alpha(\lambda) \equiv \sigma_T(\lambda)\left(\int_0^L n'(x)\,dx\right) \Big/ p$$

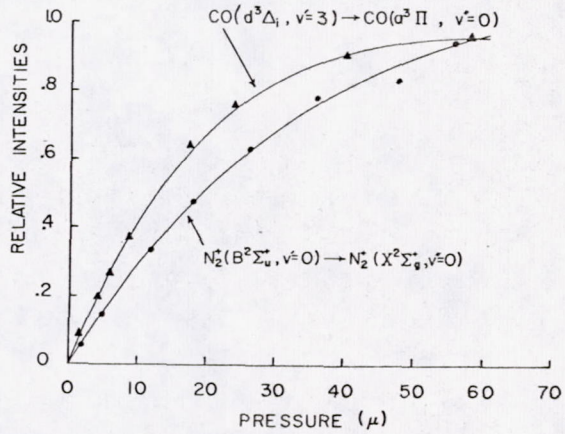

FIG. 4. The pressure dependence of the relative intensities of the $CO(d\,^3\Delta_i, v'=3)\rightarrow CO(a\,^3\Pi, v''=0)$ and $N_2^+(B\,^2\Sigma_u^+, v'=0)\rightarrow N_2^+(X\,^2\Sigma_g^+, v''=0)$ bands. The curves are fit by Eq. (2) with $a=1.4$, $\alpha=0.004$, and $\beta=0.04$ for the CO band, and $a=1.55$, $\alpha=0.0023$, and $\beta=0.023$ for the N_2^+ band. The pressure indicated in the figure was measured on the high pressure side of the gas handling system and is an upper limit to the actual but unknown lower pressure in the absorption cell.

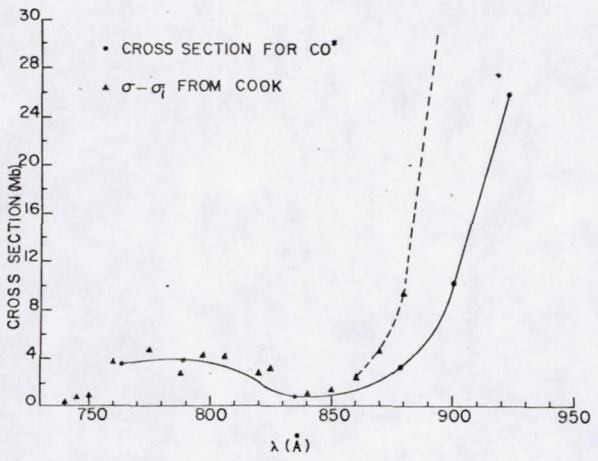

FIG. 5. Cross section for the production of the detected CO triplet states for various incident photon wavelengths. The data for the continuum photodissociation cross section, $\sigma-\sigma_i$, published by Cook *et al.* is also indicated.

and

$$\beta(\lambda)\equiv\sigma_T(\lambda)\left[\int_0^l n(x)\,dx\right]\Big/ p$$

are pressure independent factors which characterize the density distribution, $a(\lambda, \lambda_f)\equiv\sigma_f(\lambda, \lambda_f)F(\lambda_f)I_0(\lambda)/\sigma_T$, and p is the measured pressure.

As shown in Fig. 4, the pressure dependence curve for the CO band ($d\,^3\Delta_i$, $v'=3\rightarrow a\,^3\Pi$, $v''=0$) is fit with $a=1.4$, $\alpha=0.004$, and $\beta=0.04$, and the N_2^+ band with $a=1.55$, $\alpha=0.0023$, and $\beta=0.023$. The analysis thus shows that the radiation rate is proportional to the incident photon flux and it also ensures that the observed radiation rate is linearly dependent on the CO_2 pressure.

C. Cross Sections

When the pressure $p\rightarrow 0$ the observed radiation rate from Eq. (1) will reduce to

$$\dot{n}_f(\lambda, \lambda_f)=\sigma_f(\lambda, \lambda_f)F(\lambda_f)I_0(\lambda)\gamma(\lambda)p,$$

where

$$\gamma(\lambda)\equiv\beta(\lambda)/\sigma_T(\lambda)=\int_0^l n(x)\,dx/p.$$

The total measured cross section for an incident photon of wavelength λ will thus be

$$\sum_f \sigma_f(\lambda, \lambda_f)=\sum_f[\dot{n}_f(\lambda, \lambda_f)/F(\lambda_f)]/I_0(\lambda)\gamma(\lambda)p,$$

where the sum is carried out over all observed emission bands.

The absolute cross section can be obtained if we compare the fluorescence rate for the CO bands with that of the N_2^+ bands for which the cross section for the production of the $N_2^+(B\,^2\Sigma_u^+,\ v'=0)$ state is known.[12]

The factor $\gamma(\lambda)$ may be assumed to be the same for both CO_2 and N_2 since pumping efficiency was similar for these gases, and may be verified by noting that the ratios $\alpha/\sigma_T=9\times10^{-5}$ and $\beta/\sigma_T=9\times10^{-4}$ are independent of the gas. The cross section values used to compute the above ratios were 46 Mb for CO_2 at $\lambda=923$ Å[3] and 26 Mb for N_2 at $\lambda=555$ Å.[13] The angular distribution of the fluorescence is assumed to be the same for both gases.

The measured cross sections, which represent the fluorescence from all vibrational levels of the a', d, and e states higher than $a'\,^3\Sigma^+(v'=4)$ or $d\,^3\Delta_i(v'=0)$, for incident light of wavelengths 764, 789, 835, 879, 901, and 923 Å, are shown in Fig. 5. The continuum photodissociation cross section, $\sigma-\sigma_i$, of Cook *et al.*[3] is also shown in Fig. 5 for comparison. The difference between the two sets of data at the longer wavelengths and the reasonableness of the agreement at shorter wavelengths is discussed in Sec. IV. The estimated experimental error is within 10% for the relative values and within 20% for the absolute values.

D. Cross Sections for the Production of Fluorescence from Specific Vibrational Levels

As shown in Fig. 2, the vibrational bands excited by the incident photons of wavelengths 901 and 923 Å are separable. The radiation rates for the $a'_{v'}\rightarrow a_1$ and $d_{v'}\rightarrow a_1$ bands, which are overlapped with other bands, can be calculated[14] in terms of the well separated $a'_{v'}\rightarrow a_0$ and $d_{v'}\rightarrow a_0$ bands, respectively, by using known Franck–Condon factors.[9,15] The radiation rate for each band can thus be obtained, and accordingly the cross sections for the production of the fluorescing levels can be found. The results, which are the average values of several similar spectra, are shown in Table I, where the cross sections are in units of megabarns. The cross sections for the a_6, a_5, and d_1 bands are only the lower limits. Since the $v'\rightarrow v''=1$ bands which, according to the Franck–Condon factors,[9,15] may contribute significantly to these levels and are not observable with the present detecting system.

The branching ratio of the detected Asundi bands ($a'\rightarrow a$) to the triplet bands ($d\rightarrow a$) is 0.50 for incident photons of wavelength 901 Å and 0.58 for 923 Å.

IV. CONCLUDING REMARKS

In the present investigation we have confirmed the production of CO molecules in the $a'\,^3\Sigma^+$, $d\,^3\Delta_i$, or $e\,^3\Sigma^-$ states, produced through photodissociation of CO_2. Also the cross section for the production of those states which radiate photons with wavelengths between 3800–8000 Å was measured.

A minimum cross section is observed at 835 Å in this investigation and by Cook *et al.*[3] in their measure-

TABLE I. Cross sections, in units of megabarns, for the production of the fluorescing vibrational levels of the CO($a'\,^3\Sigma^+$, $d\,^3\Delta_i$, and $e\,^3\Sigma^-$) states for incident photons of 901 and 923 Å.

	a_{11}'	a_{10}'	a_9'	a_8'	a_7'	a_6'	a_5'	d_6	d_5	d_4	d_3	d_2	d_1	e_3
901 Å	0.06	0.16	0.44	0.58	1.02	0.58	0.66	0.04	0.53	1.09	2.20	2.52	0.55	0.07
923 Å	0	0	0	0.79	2.89	3.00	3.61	0	0	0	4.07	8.19	3.13	0

ments of both the total fluorescence yield and the continuum photodissociation cross section. If we adopt Cook's data, we find that the yield for the production of the observed CO a', d, and e states is more than 85% at the incident wavelengths of 764, 789, and 835 Å. The high fluorescence yield at these incident wavelengths implies that the yield for any undetected fluorescence is relatively small. With photons of such high incident energies, the yield for the undetected lower levels, $d\,^3\Delta_i(v'=0)$ and $a'\,^3\Sigma^+(v'\leq 4)$, should be rather small if most of the excited CO molecules are in the observable high vibrational levels, as would be expected if the vibrational population follows the Poisson distribution of the quasidiatomic model.[14] The primary yield for production of the $a\,^3\Pi$ state should also be small since the high vibrational levels, which should be preferentially populated at high incident photon energies according to the quasidiatomic model, simply are not observed in the CO_2^+ dissociative recombination experiment of Wauchop and Broida.[16] The cross section for excitation to the $A\,^1\Pi$ state in this wavelength region is about 1 Mb.[17] From these considerations, we conclude that the continuum photodissociation cross section, $\sigma-\sigma_i$, is essentially determined by excitation to the detected vibrational levels.

Since all the CO molecules in the triplet states will finally cascade into the metastable $a\,^3\Pi$, the cross section measured by observing the "phosphorescence" of the CO($a\,^3\Pi\rightarrow X\,^1\Sigma$) Cameron bands should yield the total cross section for the total production of all CO triplet states ($a'\,^3\Sigma^+$, $d\,^3\Delta_i$, $e\,^3\Sigma^-$, and $a\,^3\Pi$) from the photodissociation of CO_2. The cross section measured in the present investigation is only a part of this total cross section which has been measured by Lawrence.[2] Lawrence's cross section is higher than ours by about a factor of 2 for incident photons of wavelength longer than 850 Å. This difference in the cross sections is larger than would be expected, particularly at the short wavelength limit of Lawrence's work (850 Å) where the probability of any direct excitation of the $a\,^3\Pi$ state is probably small. The difference is perhaps attributable to the different techniques used to establish the absolute cross sections.

† This research was supported by NASA Grant No. NGR 05-018-138.

[1] K. H. Welge and R. Gilpin, J. Chem. Phys. 54, 4224 (1971).
[2] G. M. Lawrence, J. Chem. Phys. 56, 3435 (1972).
[3] G. R. Cook, P. H. Metzger, and M. Ogawa, J. Chem. Phys. 44, 2935 (1966).
[4] D. L. Judge, "A Wavelength Analysis of the Visible Fluorescence of Excited CO Produced by VUV Photodissociation of CO_2," Gaseous Electronis Conference, Atlanta, Ga., October 1966; also, D. L. Judge and R. W. Carlson, Trans. Amer. Geophys. Union 50, 261 (1969).
[5] D. L. Judge and L. C. Lee, J. Chem. Phys. 57, 455 (1972).
[6] L. C. Lee and D. L. Judge, J. Chem. Phys. 57, 4443 (1972).
[7] W. C. Walker, N. Wainfan, and G. L. Weissler, J. Appl. Phys. 26, 1366 (1955).
[8] P. H. Krupenie (editor), Natl. Std. Ref. Data Ser., Natl. Bur. Std. 5 (1966).
[9] D. L. Albritton, A. L. Schmeltekopf, and R. N. Zare, *Diatomic Intensity Factors* (Harper and Row, New York, to be published). The $d\rightarrow a$ Franck–Condon factors were calculated using RKR potentials and were adopted in this paper.
[10] G. Herzberg, *Electronic Spectra and Electronic Structure of Polyatomic Molecules* (Van Nostrand, New York, 1966), p. 597.
[11] R. I. Schoen, Can. J. Chem. 47, 1879 (1969). In the present paper, however, the molecular number densities n' and n are assumed to depend on x where Schoen assumed the densities to be independent of x.
[12] D. L. Judge and G. L. Weissler, J. Chem. Phys. 48, 4590 (1968).
[13] J. A. R. Samson and R. B. Cairns, J. Geophys. Res. 69, 4583 (1964).
[14] L. C. Lee and D. L. Judge, "The Population Distribution of Triplet Vibrational Levels of CO Molecules Produced by Photodissociation of CO_2," Can. J. Phys. (to be published).
[15] T. Wentink, Jr., E. P. Marram, L. Isaacson, and R. J. Spindler, Air Force Weapons Lab., Tech. Report No. AFWL-TR-67-30, Vol. 1, 1967; also W. R. Jarmain, P. A. Fraser, and R. W. Nicholls, Astrophys. J. 122, 55 (1955).
[16] T. S. Wauchop and H. P. Broida, J. Chem. Phys. 56, 339 (1972).
[17] J. E. Mentall (private communication).

Population Distribution of Triplet Vibrational Levels of CO Produced by Photodissociation of CO_2 [1]

L. C. Lee and D. L. Judge

Department of Physics, University of Southern California, Los Angeles, California 90007

Received October 4, 1972

The CO fluorescence of the $a'\,^3\Sigma^+$, $d\,^3\Delta_i$, and $e\,^3\Sigma^- \rightarrow a\,^3\Pi$ systems, produced by photodissociation of CO_2, is identified and analyzed and the population distributions of the vibrational levels of the $a'\,^3\Sigma^+$ and $d\,^3\Delta_i$ states are obtained. The data are found to be reasonably represented by a Poisson distribution.

La fluorescence CO des systèmes $a'\,^3\Sigma^+$, $d\,^3\Delta_i$, et $e\,^3\Sigma^- \rightarrow a\,^3\Pi$, produite par la photodissociation du CO_2, a été identifiée et analysée. On a aussi obtenu les distributions de population des niveaux vibrationels des états $a'\,^3\Sigma^+$ et $d\,^3\Delta_i$. Les valeurs se trouvent raisonnablement représentées par une distribution de Poisson. [Traduit par le journal]

Can. J. Phys., **51**, 378 (1973)

Several authors (Judge 1966; Cook *et al.* 1966; Judge and Carlson 1969) have reported that the photodissociation of CO_2 in the vacuum ultraviolet spectral region produces CO triplet band fluorescence, yet there have been few quantitative measurements. Here, we have identified the fluorescence bands and measured the vibrational population distribution of the excited CO states formed in the photodissociation of CO_2. These data are the first available on the primary population distribution in a molecular fragment formed through photodissociation and thus provide a basis for further study of the photodissociation mechanism.

The experimental setup was described in a previous paper (Judge and Lee 1972). The fluorescence spectra of the CO band systems produced by photodissociation of CO_2 with monochromatic light of wavelengths 901 Å and 923 Å are shown in Fig. 1. The band head data given by Krupenie (1966) and by Albritton *et al.* (1972) have been used to identify the observed bands. The relative radiation rates (defined as the number of photons per second) for the $a'\,^3\Sigma^+ \rightarrow a\,^3\Pi$, $d\,^3\Delta_i \rightarrow a\,^3\Pi$, and $e\,^3\Sigma^- \rightarrow a\,^3\Pi$ bands are displayed in Table 1 for the two different incident photon energies. The data represent averages of several similar spectra and were measured relative to the sum of the radiation rates of the $d_3 \rightarrow a_0$ and $a_9' \rightarrow a_1$ bands. The distribution of the measurements from the average is shown in Fig. 2.

[1]This work was supported by NASA grant NGR-05-018-138.

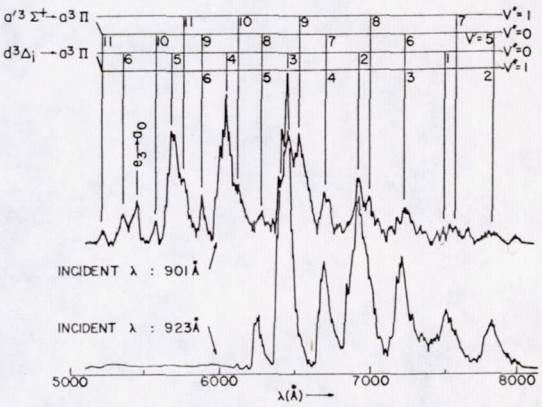

FIG. 1. The CO fluorescence spectra of the Asundi ($a'\,^3\Sigma^+ \rightarrow a^3\Pi$), Triplet ($d\,^3\Delta_i \rightarrow a\,^3\Pi$), and Herman ($e\,^3\Sigma^- \rightarrow a\,^3\Pi$) bands. The resolution for the fluorescence spectra was 12.5 Å for the incident wavelength of 901 Å and 8 Å for 923 Å. The band head positions given by Krupenie and by Albritton *et al.* are indicated.

The $a'_{v'} \rightarrow a_1$ and $d_{v'} \rightarrow a_1$ transitions which are overlapped with several other transitions can be separated by calculation using the known Franck–Condon factors (Jarmain *et al.* 1966; Wentink *et al.* 1967, Albritton *et al.* 1972) as follows. The radiation rate from a vibrational state v' to a vibrational state v'', of a lower electronic state (Nicholls 1962) is

$$[1] \qquad \dot{n}_{v'v''} = KN_{v'}Re^2{}_{v'v''}/\lambda^3{}_{v'v''}$$

where K is a constant, $Re_{v'v''}$ is the electronic transition moment, $q_{v'v''}$ is the Franck–Condon factor, $\lambda_{v'v''}$ is the transition wavelength, and $N_{v'}$ is the population of the upper level, v'. Assuming that $Re_{v'v''}$ is a constant, which may

TABLE 1. Relative radiation rates $\dot{n}_{v'v''}$ of the observed CO triplet systems

Bands / λ (Å)	$a'_{11} \to a_0$	$d_6 \to a_0$	$e_3 \to a_0$	$a'_{10} \to a_0$	$d_5 \to a_0$	$a'_9 \to a_0$	$d_4 \to a_0$	$a'_8 \to a_0$	$d_3 \to a_0$	$a'_7 \to a_0$	$d_2 \to a_0$	$a'_6 \to a_0$	$d_1 \to a_0$	$a'_5 \to a_0$
					$a'_{11} \to a_1$	$d_6 \to a_1$	$a'_{10} \to a_1$	$d_5 \to a_1$	$a'_9 \to a_1$	$d_4 \to a_1$	$a'_8 \to a_1$	$d_3 \to a_1$	$a'_7 \to a_1$	$d_2 \to a_1$
901	0.007	0.018	0.033	0.023	0.29	0.064	0.58	0.11	1.0	0.26	0.87	0.56	0.55	0.47
923	0	0	0	0	0	0	0	0.10	1.0	0.46	1.60	1.28	1.49	2.38

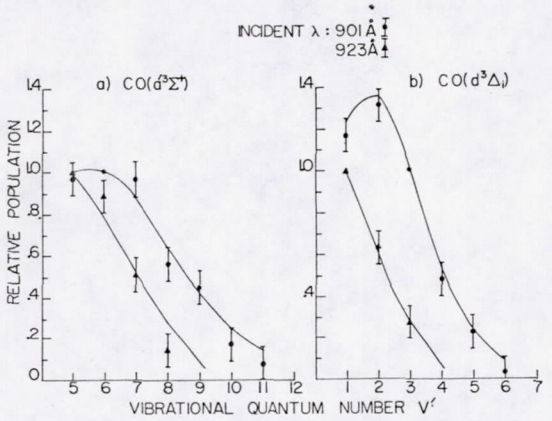

FIG. 2. The relative vibrational population distribution of the CO($a'\,^3\Sigma^+$) and CO($d\,^3\Delta_i$) states produced by photodissociation of CO_2 with incident photon energies of 13.77 eV (901 Å) and 13.45 eV (923 Å). The a'_6 and d_3 population shave been normalized to 1 for the incident energy of 13.77 eV, and a'_5 and d_1 for 13.45 eV. The data have been fit by a Poisson distribution.

be justified by the data of Wentink *et al.* (1967), the radiation rate for $v' \rightarrow v'' = 1$, in terms of the radiation rate for $v' \rightarrow v'' = 0$, will be

$$\dot{n}_{v'1} = \dot{n}_{v'0}(q_{v'1}\lambda^3{}_{v'0}/q_{v'0}\lambda^3{}_{v'1})$$

From this expression it is possible to separate the contributions of each band to the total radiation rate of the mixed bands indicated in Table 1. The CO $d \rightarrow a$ Franck–Condon factors given by Albritton *et al.* (1972) were adopted in this calibration.

The population of vibrational states v' relative to that of states α can be derived from eq. 1 and is given by

$$N_{v'}/N_\alpha = (q_{\alpha 0}\lambda^3{}_{v'0}/q_{v'0}\lambda^3{}_{\alpha 0})(\dot{n}_{v'0}/\dot{n}_{\alpha 0})$$

From this expression the calculated population distributions for incident monochromatic light of wavelengths 901 Å and 923 Å are shown in Fig. 2.

For all pressure values below 10 mTorr, the population distributions are essentially pressure independent which implies that the deactivation of CO* by CO_2 is not significant at these pressures. The CO($a'\,^3\Sigma^+$, $d\,^3\Delta_i$)–CO_2 quenching rate coefficients are, however, not available. If they are assumed to be approximately equal to the CO($a\,^3\Pi$)–CO_2 quenching rate coefficient, which is given by Lawrence (1971) and Slanger and Black (1971) as about 1.2×10^{-11} cm^3 molecule^{-1} s^{-1}, the deactivation time is 240 μs at a CO_2 pressure of 10 mTorr. This is much longer than the radiation time for the triplet bands, which is less than 11 μs (Wentink *et al.* 1967). The deactivation due to CO or O is completely negligible as the partial pressure for these constituents is less than 10^{-6} mTorr.

To interpret the observations we note that a direct photodissociation process for linear symmetric molecules has been previously proposed (Herzberg 1966). The process $CO_2 + h\nu \rightarrow CO(a'\,^3\Sigma^+, d\,^3\Delta_i) + O(^3P)$ thus may correspond to a direct dissociation or a fast predissociation, where the photon absorption is localized to break a C–O bond. Using the forced harmonic oscillator model derived by Kerner (1958), which is also applied by Holdy *et al.* (1970) in the quasi-diatomic model for ICN, we tentatively propose the following simple mechanism for the photodissociation of CO_2: When a ground state CO_2 molecule absorbs a high energy photon, it will be excited directly to a dissociating electronic state and the excited molecule will then separate into CO and O fragments. During the separation period, the fragments have "half collisions" (Shuler *et al.* 1965) with each other, and the available energy, which is equal to the difference between the incident photon energy and the dissociation energy, will be partially transferred to the CO by the collision. We tentatively assume that the CO fragment will be first excited to an electronic state with no vibrational quanta, and then forced to a vibrational state during the "half collision". The electronic transition probability, p_e, for an excitation of the CO molecule to a specific electronic state with no vibrational quanta depends on the parameters of that state, while the probability for a forced excitation from a zero vibrational level to a v' vibrational level obeys a Poisson distribution (Kerner 1958) and is given by

$$p_{v'0} = (\Delta E)^{v'} \exp(-\Delta E)/v'!$$

where ΔE is the classical phase-average energy transferred to the forced oscillator and is in units of vibrational energy quanta $\hbar\omega_0$. The population of the vibrational state is thus proportional to the total probability $p_e p_{v'0}$.

All the triplet electronic states of the CO molecule are well defined (Krupenie 1966) and each can be approximately treated as independent states. They may accordingly be expected to have the same kind of population distribution. The data of our experiment are fit by the Poisson dis-

tribution as shown in Fig. 2 for both the a' and d states. The ΔE for the $a'\,^3\Sigma^+$ and $d\,^3\Delta_i$ states are 6.0 and 2.2 for the incident wavelength of 901 Å and 4.6 and 1.26 for 923 Å, respectively. The ΔE are about one half of the quantum number of the highest excited vibrational level. Although the CO potential well becomes somewhat anharmonic for high vibrational levels and the Poisson distribution is thus only an approximation, such a distribution is found to fit the present data reasonably well.

Acknowledgment

The authors wish to thank Professor M. Ogawa for his encouraging discussions.

ALBRITTON, D. L., SCHMELTEKOPF, A. L., and ZARE, R. N. 1972. Diatomic intensity factors, in preparation for Harper and Row Publisher.

COOK, G. R., METZGER, P. H.,and OGAWA, M. 1966. J. Chem. Phys. **44**, 2935.

HERZBERG, G. (Editor). 1966. Electronic spectra and electronic structure of polyatomic molecules (Van Nostrand Reinhold Co., N.Y.), pp. 429–451.

HOLDY, K. E., KLOTZ, L. C., and WILSON, K. R. 1970. J. Chem. Phys. **52**, 4588.

JARMAIN, W. R., FRASER, P. A., and NICHOLLS, R. W. 1966. Astrophys. J. **122**, 55.

JUDGE, D. L. 1966. Gaseous Electronics Conference, Atlanta, Ga.

JUDGE, D. L. and CARLSON, R. W. 1969. Trans. Am. Geophys. Union, **50**, 261.

JUDGE, D. L. and LEE, L. C. 1972. J. Chem. Phys. **57**, 455.

KERNER, E. H. 1958. Can. J. Phys. **36**, 371.

KRUPENIE, P. H. (Editor). 1966. The band spectrum of carbon monoxide, NSRDS-NBS 5 (U.S. Government Printing Office, Wash. D.C.).

LAWRENCE, G. M. 1971. Chem. Phys. Lett. **9**, 575.

NICHOLLS, R. W. 1962. J. Quant. Spectrosc. Radiat. **2**, 433.

SHULER, K. E., CARRINGTON, T., and LIGHT, J. C. 1965. Appl. Opt. Suppl. **2**, 81.

SLANGER, T. G. and BLACK, G. 1971. J. Chem. Phys. **55**, 2164.

WENTINK, T., JR., MARRAM, E. P., ISAACSON, L., and SPINDLER, R. J. 1967. Air Force Weapons Lab., Tech. Report No. AFWL-TR-67-30, Vol. 1.

* This research was supported by NASA Contract No. NGR 05-018-138.

[1] D. Robinson and R. W. Nicholls, Proc. Phys. Soc. (London) A75, 817 (1960).
[2] P. A. Fraser, Can. J. Phys. 32, 515 (1954).
[3] R. W. Nicholls, J. Quant. Spectry. Radiative Transfer 2, 433 (1962).
[4] G. Herzberg, *Molecular Spectra and Molecular Structure* (Van Nostrand, New York, 1967), p. 200.
[5] R. W. Nicholls, Can. J. Phys. 40, 1772 (1962).
[6] D. C. Jain and R. C. Sahni, J. Quant. Spectry. Radiative Transfer 6, 705 (1966).
[7] P. H. Krupenie (Ed.), Natl. Std. Ref. Data Ser., Natl. Bur. Std. (U.S.) 5 (1966).
[8] M. E. Wacks, J. Chem. Phys. 41, 930 (1964).
[9] M. Halmann and I. Laulicht, J. Chem. Phys. 43, 1503 (1965).
[10] R. W. Nicholls, J. Phys. B 1, 1192 (1968).
[11] G. L. Weissler, J. Appl. Phys. (Japan) Suppl. I 4, 486 (1965).
[12] J. A. R. Samson, *Techniques of Vacuum Ultraviolet Spectroscopy* (Wiley, New York, 1967), p. 174.
[13] W. Slavin, R. W. Mooney, and D. T. Palumbo, J. Opt. Soc. Am. 51, 93 (1961).
[14] D. L. Judge and G. L. Weissler, J. Chem. Phys. 48, 4590 (1968).
[15] R. J. Spindler and T. Wentink, Jr., Research and Advanced Development Division, AVCO Corp., Wilmington, Mass., Technical Memorandum RAD-TM-63-55, 1963.
[16] E. H. Fink and K. H. Welge, Z. Naturforsch. 23a, 358 (1968).
[17] R. G. Bennett and E. W. Dalby, J. Chem. Phys. 32, 1111 (1960).
[18] G. M. Lawrence, J. Quant. Spectry. Radiative Transfer 5, 359 (1965).
[19] R. I. Schoen, J. Chem. Phys. 40, 1830 (1964).
[20] G. R. Cook, P. H. Metzger, and M. Ogawa, Can. J. Phys. 43, 1706 (1965).
[21] R. B. Cairns and James A. R. Samson, J. Opt. Soc. Am. 56, 526 (1966).

Reprinted from:

THE JOURNAL OF CHEMICAL PHYSICS VOLUME 57, NUMBER 10 15 NOVEMBER 1972

Cross Sections for the Production of $CO_2^+[A\ ^2\Pi_u, B\ ^2\Sigma_u^+ \rightarrow X\ ^2\Pi_g]$ Fluorescence by Vacuum Ultraviolet Radiation*

L. C. Lee and D. L. Judge

Department of Physics, University of Southern California, Los Angeles, California 90007

(Received 7 April 1972)

Fluorescence cross sections for the production of the $CO_2^+[A\ ^2\Pi_u, B\ ^2\Sigma_u^+ \rightarrow X\ ^2\Pi_g]$ bands are presented at several vacuum ultraviolet (vuv) wavelengths between 462 and 715 Å. The cross sections, for incident vuv photons from 600 to 680 Å, are 19 Mb for the production of $CO_2^+(A\ ^2\Pi_u)$ and 7 Mb for $CO_2^+(B\ ^2\Sigma_u^+)$ and decrease monotonically toward the shorter wavelength region. The relative fluorescence cross sections of the observed sequences are also given for the various incident photon energies.

I. INTRODUCTION

The photoionization cross section of CO_2 has been measured by several authors,[1–6] yet there is little agreement among the various sets of data. The results given by Cairns and Samson[1] and Sun and Weissler[2] are about 50% higher than those given by Nakata *et al.*[3] and Cook *et al.*[4] The specific cross sections published by Bahr *et al.*[5] provide no information on the absolute cross section since they were normalized to Cook's results. The specific ionization cross section for the formation of $CO_2^+(B\ ^2\Sigma_u^+)$ measured by Bahr *et al.*[5] was higher than that for $CO_2^+(A\ ^2\Pi_u)$, while just the opposite is true for Wauchop and Broida's[6] fluorescence cross section at 584 Å for the band systems having the same upper states. Differences between the ionization and fluorescence cross sections are important to an understanding of the absorption processes and hence, for example, to an understanding of the Martian[7] and Venusian[8] atmospheres. Extended fluorescence cross section measurements thus seemed desirable and are presented below.

II. EXPERIMENT

The experimental setup has been described in previous papers.[9] The source lines used in this investigation were 462, 525, 555, 587, 610, 629, 637, 686, 703, and 715 Å. The bandwidth of the 1-m normal incident monochromator (McPherson 225) used to isolate these lines was set at 4 Å or less. The absolute line intensities were measured with a nickel film photoelectric detector for which the quantum efficiency was known.[10] The bandwidth of the 0.3-m normal incident monochromator (McPherson 218) used to disperse the fluorescence was set at 4 Å.

The response of the combination of a grating blazed at 5000 Å and a cooled photomultiplier (EMI 9558 QB) was calibrated with a NBS quartz iodine standard lamp. The detection system response (per photon/sec) as a function of wavelength is shown in Fig. 1.

CO_2 gas supplied by Airco with a purity of 99.99% was used for this investigation without further purification. The pressure inside the sample cell was monitored with a Baratron[11] capacitance monometer.

III. RESULTS

A. Fluorescence Spectra

The CO_2^+ fluorescence spectra are shown in Figs. 2 and 3. The bandhead positions used by Wauchop and Broida[6] are indicated in Fig. 2 to identify the observed bands. This spectrum produced by incident photons of 19.7 eV (629 Å), is characteristic of all spectra produced with incident photon energies higher than 18.1 eV (686 Å). For lower incident photon energies the spectrum is limited by the excitation energy available. For example, the highest possible excited level for the

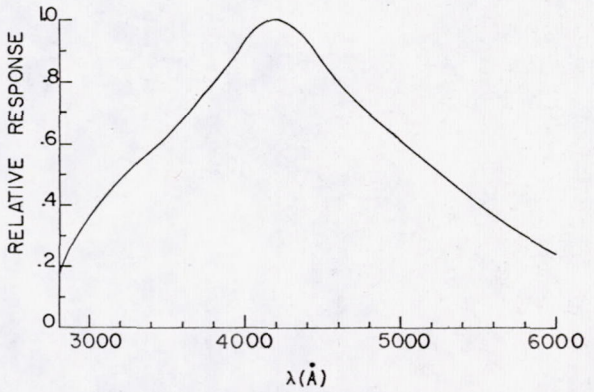

FIG. 1. Relative response (per photon/second) of the fluorescence detection system as a function of wavelength.

incident photon energy of 17.6 eV (703 Å) is $CO_2^+(A\ ^2\Pi_u, 2, 0, 0)$ and is accordingly the highest emission level shown in Fig. 3. The spectrum for an incident photon energy of 22.4 eV (555 Å) is also shown in Fig. 3 for comparison.

B. Pressure Dependence

For the present system the dependence of the observed fluorescence radiation rate, $\dot{n}_f(\lambda, \lambda_f)$, on gas pressure can be described by[12]

$$\dot{n}_f(\lambda, \lambda_f) = \sigma_f(\lambda, \lambda_f) F(\lambda_f) I_0(\lambda) \exp[-\alpha(\lambda) p] \times \{1 - \exp[-\beta(\lambda) p]\}/\sigma_T(\lambda), \quad (1)$$

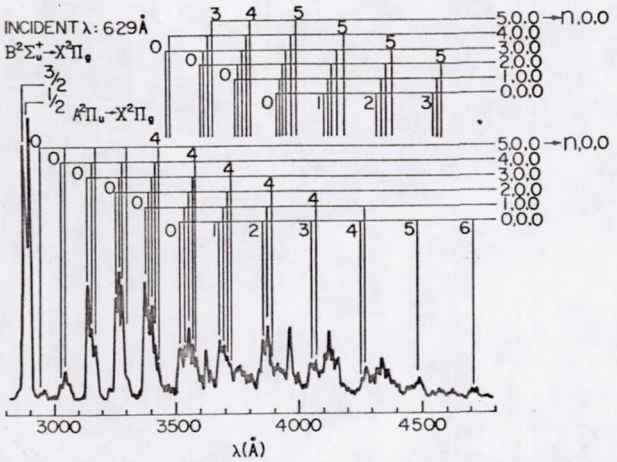

FIG. 2. The fluorescence spectrum of CO_2^+ produced by incident photons of 629 Å. The bandhead data used by Wauchop and Broida are indicated.

where $\sigma_f(\lambda, \lambda_f)$ is the specific fluorescence cross section of CO_2^+ at the incident wavelength λ and the fluorescence wavelength λ_f, $F(\lambda_f)$ is the response as shown in Fig. 1, $I_0(\lambda)$ is the incident vacuum ultraviolet radiation flux, p is the pressure, $\alpha(\lambda)$ and $\beta(\lambda)$, which characterize the pressure distribution, are pressure independent and are proportional to the total absorption cross section $\sigma_T(\lambda)$.

TABLE I. Relative fluorescence cross sections for the observed sequences of the CO_2^+ $(A\ ^2\Pi_u)$–CO_2^+ $(X\ ^2\Pi_g)$ system for various incident photon wavelengths.

		Incident λ (Å)				
Sequence bandhead	λ (Å)	462	525 555 587 610	629 637 686	703	584[a]
(5, 0, 0)–(0, 0, 0)	2960	0.23	0.20	0.09	0	
(4, 0, 0)–(0, 0, 0)	3048	0.58	0.31	0.22	0	0.30
(3, 0, 0)–(0, 0, 0)	3137	0.68	0.82	0.81	0	0.89
(2, 0, 0)–(0, 0, 0)	3254	1.00	1.00	1.00	1.00	1.00
(1, 0, 0)–(0, 0, 0)	3378	0.69	0.93	0.89	1.38	1.00
(3, 0, 0)–(0, 0, 2)	3467	0.05	0.07	0.07	0.08	0.03
(0, 0, 0)–(0, 0, 0)	3513	0.38	0.66	0.71	0.98	0.87
(2, 0, 0)–(0, 0, 2)	3600	0.10	0.19	0.17	0.04	0.24
(0, 0, 0)–(1, 0, 0)	3675	0.25	0.39	0.41	0.81	0.71
(1, 0, 0)–(0, 0, 2)	3749	0.17	0.32	0.46	0.29	0.28
(0, 0, 0)–(2, 0, 0)	3856	0.20	0.34	0.30	0.72	0.55
(0, 0, 0)–(0, 0, 2)	3914	0.22	0.41	0.43	0.46	0.56
(0, 0, 0)–(3, 0, 0)	4051	0.09	0.13	0.14	0.33	0.27
(0, 0, 0)–(1, 0, 2)	4110	0.31	0.47	0.44	0.72	0.62
(0, 0, 0)–(4, 0, 0)	4268	0.06	0.08	0.07	0.09	0.09
(0, 0, 0)–(2, 0, 2)	4308	0.19	0.30	0.30	0.37	0.35
(0, 0, 0)–(5, 0, 0)	4450	0.07	0.12	0.12	0.13	0.16
(0, 0, 0)–(3, 0, 2)	4544	0.11	0.12	0.10	0.12	0.16
(0, 0, 0)–(6, 0, 0)	4745	0.07	0.08	0.07	0.13	

[a] Measured by Wauchop and Broida, Ref. 6.

It should be noted that Eq. (1) applies strictly only when vibrational relaxation is negligible. At the low pressures at which the cross sections were measured, this equation is applicable; however, we did observe that, when the pressure increases, the fluorescence rates of higher vibrational levels decrease faster than those of lower vibrational levels.[6,9] This may be attributable to the relaxation of the higher vibrational levels to the lower vibrational levels by collisions.

C. Relative Fluorescence Cross Sections for Various Sequences

According to Eq. (1), the relative cross section for the emission bands can be measured by comparing their radiation rates at a fixed low pressure and a fixed incident photon flux. The results that were measured for various incident photon wavelengths at a pressure of 35 μ are shown in Table I. Each band given identifies

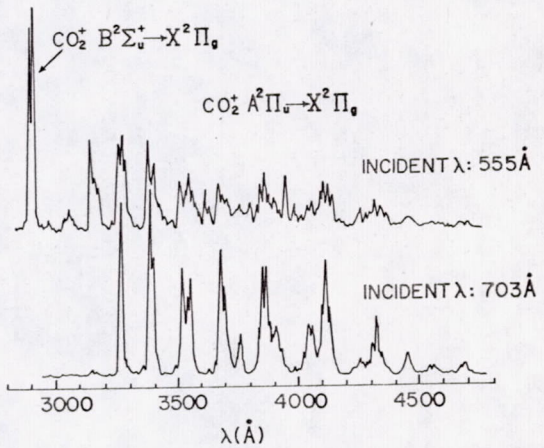

FIG. 3. Dispersed fluorescence spectra of the $CO_2^+(B\ ^2\Sigma_u^+ \rightarrow X\ ^2\Pi_g)$ and $CO_2^+(A\ ^2\Pi_u \rightarrow X\ ^2\Pi_g)$ systems produced by incident photons of 555 and 703 Å.

the corresponding sequence, for which the cross section data are given. For example, the (2, 0, 0)–(0, 0, 0) band at 3254 Å also includes the (3, 0, 0)–(1, 0, 0), (4, 0, 0)–(2, 0, 0), and the (5, 0, 0)–(3, 0, 0) bands.

The variation of the relative cross sections for the incident wavelengths from 525 to 686 Å is not appreciable. The data listed under the middle two columns are thus given as averages of data at the incident wavelengths indicated. However, for the incident photons of 462 Å the fluorescence cross section increases for the shorter wavelength bands, while for the incident photons of 703 Å, the fluorescence cross section for the longer wavelength bands increases.

The data measured by Wauchop and Broida[6] are listed in the last column for comparison. Except for the (0, 0, 0)–(n, 0, m) bands, their results agree with ours within 20% or better. The cross sections for the (0, 0, 0)–(n, 0, m) bands measured by Wauchop and Broida are consistently higher than the present measurements.